

**MONO- AND BINUCLEAR TRANSITION METAL COMPLEXES OF
N(4)-SUBSTITUTED THIOSEMICARBAZONES DERIVED FROM
SALICYLALDEHYDE AND 2-HYDROXYACETOPHENONE :
SYNTHESIS, SPECTRAL AND STRUCTURAL STUDIES**

Thesis submitted to the

COCHIN UNIVERSITY OF SCIENCE AND TECHNOLOGY

*in partial fulfillment of the requirements
for the degree of*

DOCTOR OF PHILOSOPHY

in

CHEMISTRY

by

SEENA E.B.



DEPARTMENT OF APPLIED CHEMISTRY

COCHIN UNIVERSITY OF SCIENCE AND TECHNOLOGY

KOCHI-22

AUGUST 2006

*To
my family*

DECLARATION

I hereby declare that the work presented in this thesis entitled "MONO- AND BINUCLEAR TRANSITION METAL COMPLEXES OF *N*(4)-SUBSTITUTED THIOSEMICARBAZONES DERIVED FROM SALICYLALDEHYDE AND 2-HYDROXYACETOPHENONE : SYNTHESIS, SPECTRAL AND STRUCTURAL STUDIES" is based on the original work done by me under the guidance of Dr. M. R. Prathapachandra Kurup, Professor and Head, Department of Applied Chemistry, Cochin University of Science and Technology, Kochi - 682 022 and has not been included in any other thesis submitted previously for the award of any degree.



SEENA E.B.

Kochi-22

16th August 2006

**DEPARTMENT OF APPLIED CHEMISTRY
COCHIN UNIVERSITY OF SCIENCE AND TECHNOLOGY
KOCHI - 682 022, INDIA**

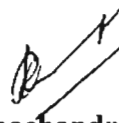
**Dr. M.R. PRATHAPACHANDRA KURUP
PROFESSOR & HEAD**



Off. : 0484-25758
Res. : 0484-25769
Fax : 0484-25775

CERTIFICATE

This is to certify that the thesis entitled "MONO- AND BINUCLEAR TRANSITION METAL COMPLEXES OF *N*(4)-SUBSTITUTED THIOSEMICARBAZONES DERIVED FROM SALICYLALDEHYDE AND 2-HYDROXYACETOPHENONE SYNTHESIS, SPECTRAL AND STRUCTURAL STUDIES" submitted by Mrs. SEENA E.B is an authentic and bonafied record of the original research work carried out by her under my guidance and supervision in the Department of Applied Chemistry, Cochin University of Science and Technology, in partial fulfillment of the requirements for the degree of Doctor of Philosophy and has not been included in any other thesis or submitted previously for the award of any other degree.



M. R. Prathapachandra Kurup

(Supervising Guide)

Kochi-22
16th August 2006

ACKNOWLEDGEMENT

I am grateful to all those who inspired me during this research work and I wish to express my deep feeling of gratitude towards them, without whose valuable suggestions and encouragement, the accomplishment of this thesis would have been impossible.

It is my immense pleasure and a great privilege to express my sincere gratitude and obligation to Dr. M.R. Prathapachandra Kurup, Professor and Head, Department of Applied Chemistry, for his valuable guidance and endless support, which helped me complete my thesis effectively and satisfactorily.

My earnest thanks to Prof. Dr. K.K. Mohammed Yusuff, Prof. Dr. S. Sugunan, Dr. K. Girish Kumar and all other teaching, non-teaching and technical staff of this department for providing necessary facilities for carrying out these investigations.

I extend my gratitude to Dr. N. Chandramohana Kumar, Head of the Department of Chemical Oceanography, CUSAT, for assisting me with their instrumental facilities and also I am thankful to Mr Renjith, Research Scholar of the same department, who helped me to record the Electronic spectral data.

I acknowledge Dr. E. Suresh, Analytical Science Division, Bhavnagar, Gujarat and Prof. Dr. P Mathur, National Single Crystal X-Ray Diffraction Facility, IIT, Bombay, for single crystal X-ray diffraction studies.

I take this opportunity to express my thanks to the authorities of Regional Sophisticated Instrumentation centres (RSICs) IIT Bombay and IIT Roorkee, Sophisticated Instrumentation Facility (SAIF) - Cochin and IISc Bangalore.

I am grateful to my seniors Dr. Rohit P. John, Dr. Chandini R. Nayar, Dr. S. Sivakumar, Dr. A. Sreekanth, Dr. P.B. Sreeja, Dr. Varughese Philip, Dr. Marthakutty Joseph and Dr. V. Suni for their timely help whenever I needed it most.

I remember each and everyone of my labmates Rapheal sir, Mini, Bessy, Manoj, Sreasha, Leji, Suja, Sheeja, Renjusha, Prem, Laly teacher and Jessy teacher, whose whole-hearted support during this period. I am also thankful to Reshmi R. of Physical Chemistry Lab, who helped me to scan most of the spectra.

I also express my feeling of gratitude to my beloved father, brothers and in laws for imparting love and confidence with their earnest prayers and sustained support. The loving memory of my mother leads me in all my ways.

Finally, I place on record the assistance from my husband, Nandakumar who has all along been an endearing source of encouragement and I express my deep sense of love to my son, Athul who missed lot of my care and attention during the course of this investigation.

SEENA E.B.

Preface

The work embodied in this thesis was carried out by the author in the Department of Applied Chemistry during 2003-2006. The primary aim of these investigations was to probe the spectroscopic and single crystal X-ray diffraction studies of some selected transition metal complexes of *N*(4)-substituted thiosemicarbazones.

The chemistry of thiosemicarbazones has received considerable attention due to their proliferate applications. The transition metal complexes of them found applications in biology, medicine and industry. The present investigation is confined to the spectral and structural studies of Cu(II), Ni(II), Mn(II), Zn(II), oxovanadium(IV) and dioxomolybdenum(VI) complexes of dianionic tridentate thiosemicarbazones with ONS donor atoms.

The work embodied in the thesis is divided into eight chapters. Chapter 1 gives a brief introduction about metal complexes of thiosemicarbazones, including their structural and bonding properties. Chapter 2 deals with the synthesis and single crystal X-ray diffraction studies of various thiosemicarbazones used up for the present investigations and various characterization techniques. Chapter 3 deals with synthesis, spectral and structural studies of Cu(II) complexes with ONS donor thiosemicarbazones. Chapter 4 deals with synthesis and spectral studies of Ni(II) complexes with 2-hydroxyacetophenone *N*(4)-cyclohexyl thiosemicarbazone as the ligand. Chapter 5 includes synthesis and spectral studies of Mn(II) complexes. Chapter 6 deals with synthesis, spectral and structural studies of Zn(II) complexes. Chapter 7 includes synthesis and spectral studies of oxovanadium(IV) complexes. Chapter 8 deals with synthesis, spectral and single crystal X-ray diffraction studies of dioxomolybdenum(VI) complexes.

CONTENTS

CHAPTER 1	A BRIEF INTRODUCTION OF THIOSEMICARBAZONES AND THEIR TRANSITION METAL COMPLEXES	1-18
1.1	General introduction	1
1.2	Bonding in thiosemicarbazone complexes	2
1.3	Stereochemistries and oxidation states of thiosemicarbazone complexes	3
1.4	Structural characterization techniques	7
1.4.1	Estimation of carbon, hydrogen and nitrogen	7
1.4.2	Magnetic susceptibility measurements	7
1.4.3	Infrared spectroscopy	9
1.4.4	Electronic spectroscopy	9
1.4.5	EPR spectroscopy	10
1.4.6	NMR spectroscopy	11
1.4.7	X-Ray crystallography	11
1.5	Significance of thiosemicarbazones and their metal complexes	11
1.6	Objective and scope of the present work	13
	References	15
CHAPTER 2	SYNTHESIS, SPECTRAL AND STRUCTURAL STUDIES OF THIOSEMICARBAZONE LIGANDS	19-47
2.1	Introduction	19
2.2	Synthesis of thiosemicarbazone ligands	21
2.2.1	Materials	21
2.2.2	Synthesis of the ligands H_2L^1 and H_2L^2	21
2.2.3	Synthesis of the ligands H_2L^3 and H_2L^4	22
2.3	Characterization techniques	23
2.3.1	X-Ray crystallography	23
2.4	Results and discussion	26
2.4.1	Synthesis	26
2.4.2	Crystal structure of H_2L^2	26
2.4.3	Crystal structure of H_2L^3	30
2.4.4	Crystal structure of H_2L^4	34

2.4.5	Spectral studies	38
2.5	Unusual isolation of the compound 2-[5-(cyclohexylamino)-1,3,4-thiadiazol-2-yl]phenol	41
	References	45
CHAPTER 3	SYNTHESIS, SPECTRAL AND STRUCTURAL STUDIES OF Cu(II) COMPLEXES OF N(4)-SUBSTITUTED THIOSEMICARBAZONES OF SALICYLALDEHYDE AND 2-HYDROXYACETOPHENONE	48-80
3.1	Introduction	48
3.2	Experimental	48
3.2.1	Materials	48
3.2.2	Synthesis of the complexes	49
3.2.3	X-Ray crystallography	51
3.3	Results and discussion	53
3.3.1	Physical measurements	53
3.3.2	Crystal structure of the compound [CuL ¹ dmbipy]	55
3.3.3	Crystal structure of the compound [(CuL ²) ₂]	59
3.3.4	Infrared spectra	64
3.3.5	Electronic spectra	69
3.3.6	EPR spectra	71
	References	78
CHAPTER 4	SYNTHESIS AND SPECTRAL STUDIES OF Ni(II) COMPLEXES OF 2-HYDROXYACETOPHENONE N(4)-CYCLOHEXYL THIOSEMICARBAZONE	81-91
4.1	Introduction	81
4.2	Experimental	81
4.2.1	Materials	81
4.2.2	Synthesis of the complexes	82
4.3	Results and discussion	83
4.3.1	Physical measurements	83
4.3.2	Infrared spectra	84
4.3.3	Electronic spectra	88
	References	90

CHAPTER 5	SYNTHESIS AND SPECTRAL STUDIES OF Mn(II) COMPLEXES OF N(4)-SUBSTITUTED THIOSEMICARBAZONES	92-103
5.1	Introduction	92
5.2	Experimental	93
5.2.1	Materials	93
5.2.2	Synthesis of the complexes	93
5.3	Results and discussion	93
5.3.1	Physical measurements	93
5.3.2	Infrared spectra	94
5.3.3	Electronic spectra	97
5.3.4	EPR spectra	99
	References	102
CHAPTER 6	SYNTHESIS, SPECTRAL AND STRUCTURAL STUDIES OF Zn(II) COMPLEXES OF SALICYLALDEHYDE N(4)-PHENYL THIOSEMICARBAZONE	104-121
6.1	Introduction	104
6.2	Experimental	105
6.2.1	Materials	105
6.2.2	Synthesis of the complexes	105
6.2.3	X-Ray crystallography	106
6.3	Results and discussion	107
6.3.1	Physical measurements	107
6.3.2	Crystal structure of the compound [ZnL ³ bipy]	108
6.3.3	Infrared spectra	113
6.3.4	Electronic spectra	116
6.3.5	¹ H NMR spectra	118
	References	120
CHAPTER 7	SYNTHESIS AND SPECTRAL STUDIES OF OXOVANADIUM(IV) COMPLEXES OF N(4)-SUBSTITUTED THIOSEMICARBAZONES	122-136
7.1	Introduction	122
7.2	Experimental	123
7.2.1	Materials	123

7.2.2	Synthesis of the complexes	123
7.3	Results and discussion	125
7.3.1	Physical measurements	125
7.3.2	Infrared spectra	126
7.3.3	Electronic spectra	130
7.3.4	EPR spectra	132
	References	135
CHAPTER 8	SYNTHESIS, SPECTRAL AND STRUCTURAL STUDIES OF DIOXOMOLYBDENUM(VI) COMPLEXES OF 2-HYDROXYACETOPHENONE N(4)-SUBSTITUTED THIOSEMICARBAZONES	137-153
8.1	Introduction	137
8.2	Experimental	138
8.2.1	Materials	138
8.2.2	Synthesis of the complexes	138
8.3	Results and discussion	139
8.3.1	Synthesis	139
8.3.2	Spectral studies	140
8.3.3	Description of the crystal structure of the compounds $[(\text{MoO}_2\text{L}^2)_2]$, $[\text{MoO}_2\text{L}^2\text{py}]$ and $[\text{MoO}_2\text{L}^4\text{py}]$	144
	References	152
	SUMMARY AND CONCLUSION	

CHAPTER 1

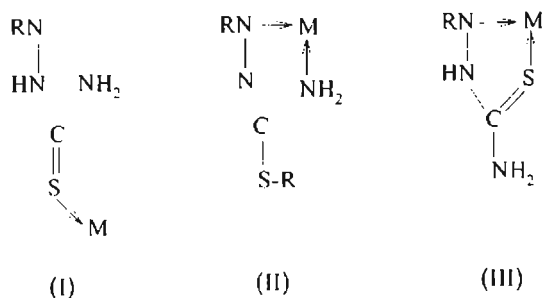
A BRIEF INTRODUCTION OF THIOSEMICARBAZONES AND THEIR TRANSITION METAL COMPLEXES

1.1. General introduction

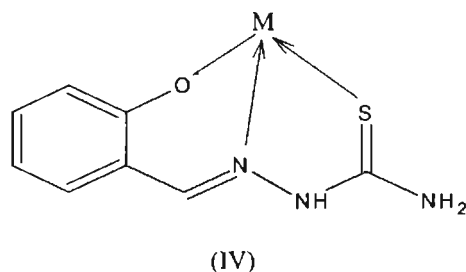
Thiosemicarbazones are a class of compounds possessing a broad spectrum of biological activity including antitumour, antibacterial, antimalarial and antifungal activities [1]. Moreover, metal complexes of thiosemicarbazones often display enhanced activities when compared to the uncomplexed thiosemicarbazones. Thiosemicarbazones are prepared by the condensation of thiosemicarbazides with aldehydes or ketones in the presence of a few drops of glacial acetic acid [2].

According to the IUPAC recommendations for the nomenclature of organic compounds [3], derivatives of semicarbazides of the types $R-CH=N-NH-C(X)-NH_2$ and $R^1R^2C=N-NH-C(X)-NH_2$ which are usually obtained by condensation of semicarbazide with suitable aldehydes and ketones, may be named by adding the class name 'semicarbazone' ($X=O$) or 'thiosemicarbazone' ($X=S$) after the name of the condensed aldehyde $RCHO$ or ketone $R^1R^2C=O$. It is also usual to include in this class derivatives with substituents on the amide or thioamide nitrogen, $R^1R^2C=N-NH-C(X)-NR^3R^4$; on the X atom, $R^1R^2C=N-N=CXR^3-NH_2$; or on the 'hydrazinic' nitrogen, $R^1R^2C=N-NR^3-C(X)-NH_2$. These classes of compounds usually react with metallic cations giving complexes in which the semicarbazones (SCs) and thiosemicarbazones (TSCs) behave as chelating ligands.

Thiosemicarbazones are versatile ligands which can coordinate as neutral ligands or in their deprotonated form. They are extensively delocalized systems, especially when aromatic radicals are bound to the azomethine carbon atom. Ligands with additional donor groups at the substituent R^1 or R^2 are of special interest since they can coordinate in a tridentate fashion which results in a significant increase of



When an additional coordinating functionality is present in the proximity of the SN donating centres, the ligands are found to act as tridentate species (IV).



1.3. Stereochemistries and oxidation states of metal complexes

The stereochemistries adopted by thiosemicarbazone ligands while interacting with transition metal ions depend essentially upon the presence of an additional coordination center in the ligand moiety and the charge on the ligand, which in turn, is influenced by the thione \leftrightarrow thiol equilibrium. Besides the dentacity variation, consideration of the charge distribution is complicated in thiosemicarbazones due to the existence of thione and thiol tautomers. Although the thione form predominates in the solid state, solutions of thiosemicarbazone molecules show a mixture of both tautomers. As a result depending upon preparative conditions (particularly solvent and pH), the metal complexes can be cationic, neutral or anionic. For example,

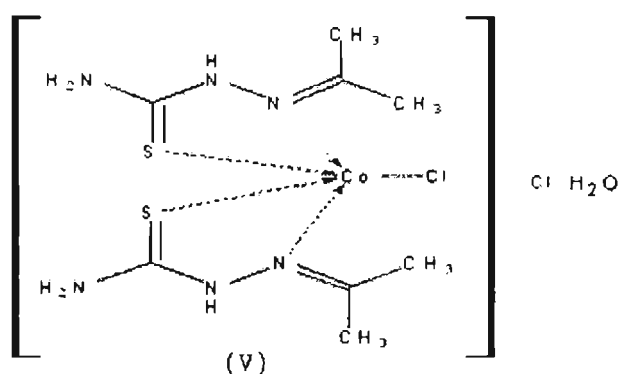
benzaldehyde thiosemicarbazone is generally found to act as a neutral bidentate ligand, yielding complexes of the type $[ML_2X_2]$ (where $M = Co(II), Ni(II), Cu(II)$ and $Fe(II)$, $L =$ ligand in the thione form and $X =$ monoanionic ligand), whereas salicylaldehyde thiosemicarbazone is found to act as a tridentate uninegative ligand yielding compounds of the type ML_2 , which may be spin-free or spin paired.

Most of the earlier investigations of metal complexes of thiosemicarbazones have involved ligands in the uncharged thione form, but a number of recent reports have featured complexes in which the 2N -hydrogen is lost, and bonding within the thiosemicarbazone moiety is closer to that of the thiol form. Furthermore, it is possible to isolate complexes containing both the neutral and anionic forms of the ligand bonded to the same metal ion [8]. Ablov and Gerbeleu suggested that the formation of these mixed "tautomer" complexes is promoted by trivalent central metal ions like $Cr(III)$, $Fe(III)$ and $Co(III)$ [9].

The structural studies on $Fe(III)$ complexes of substituted salicylaldehyde thiosemicarbazone ligands have shown that the ligands are tridentate and the iron atoms are octahedrally coordinated with S, O and trans N atoms. Although no substantial differences are observed between bond lengths and bond angles in the ligands of high-spin and low-spin compounds, the high-spin complexes have a highly distorted octahedral configuration [10]. Octahedral complexes are reported in the case of manganese(II) ions with thiosemicarbazide and acetone thiosemicarbazone ligands [11]. Reaction $MnCl_2$ with 2-acetylpyridine $N(4)$ -phenylthiosemicarbazone also gives a bis(ligand) complex possessing an octahedral structure [12].

The influence of the parent ligand moiety on the final geometry of the coordination complex derived from the interaction of metal salt with potentially bidentate or tridentate thiosemicarbazone ligands of the type $R^1R^2C=N-NH-C(S)-NH_2$. The complex $[Co(AcTSc)_2Cl]Cl \cdot H_2O$ (V), where

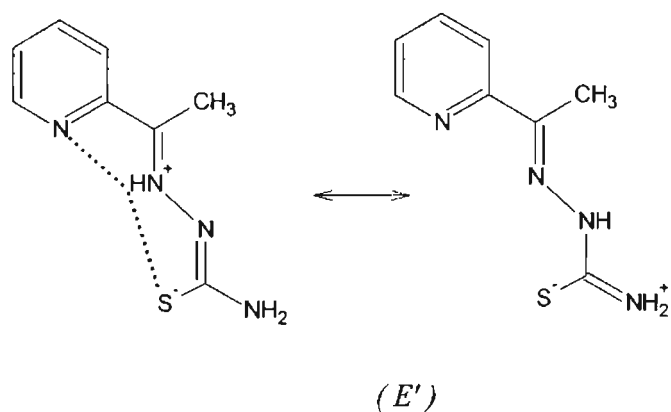
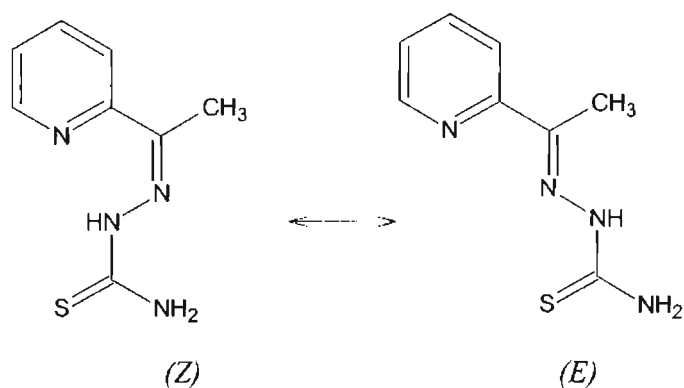
(AcTSc = acetone thiosemicarbazone) was found to possess a trigonal bipyramidal configuration with two sulfur atoms and one of the chlorine atoms lying approximately in a plane, while the azomethine nitrogen atoms are situated trans to each other [13]. The transition metal complexes of 2-heterocyclic thiosemicarbazones suggest that stereochemistry adopted by these complexes often depend upon the anion of the metal salt used and nature of the N(4)-substituents [14].



The most common stereochemistries encountered with 2-heterocyclic thiosemicarbazones are six coordinated having the general formula ML_2^{n+} where M is Fe(III), Co(III) and Ni(II), L is tridentate anionic ligand and $n = 0, 1$ and planar with the stereochemistry of MLX , where $M = Ni(II)$ or $Cu(II)$, L = tridentate anionic ligand and X is generally a halo or pseudohalo ligand. In addition to this, there are reports on the mixed ligand complexes of Mn(II), Cu(II), Ni(II) etc and even homo and hetero bimetallic complexes [15]. Moreover it is also possible to isolate complexes containing two nonequivalent ligands – one protonated and the other deprotonated within the same coordination sphere. Recently there are reports on complexes with tetra and pentadentate N_2S_2 , N_2SO and N_3S_2 donor ligand in the monoanionic or dianionic states [16].

As a result of the above considerations, the most common stereochemistries encountered in metal complexes of thiosemicarbazones are octahedral and square planar. On rare occasions five coordinate structures are also obtained, as in the case of Co(II), Fe(II) and Ni(II) complexes of acetone thiosemicarbazone [17-19] and the Fe(III) complex of 2-acetylpyridine thiosemicarbazone [20].

The tautomeric forms *Z* and *E* and the resonance polar forms of 2-acetylpyridine thiosemicarbazone [21] are as follows :



HSAB considerations dictate that the oxidation state of a metal affects the degree of its “softness” character, and it is found to be stronger for transition metals in low oxidation states. Thus the low spin d^8 ions Pd(II), Pt(II) and Au(III) and d^{10} ions Cu(I), Ag(I), Au(I) and Hg(II) exhibit higher stability constants with this class of sulfur ligands because of the formation of strong σ bonds as well as $d_{\pi}-d_{\pi}$ bonds by donation of a pair of electrons to ligands [22]. Thiols but not thioethers cause spin-pairing of Co and Ni. Thiosemicarbazones are not capable of spin-pairing of Fe(III) ions, unlike other soft bases such as CN^- , diarsine and certain charged sulfur ligands [23]. Consequently, intermediate spin states are found to be stabilized [24]. This potential of the class of thiosemicarbazone ligands has not been recognized to the extent as for diethyldithiocarbamate ligands.

1.4. Structural characterization techniques

1.4.1. Estimation of carbon, hydrogen and nitrogen

Elemental analyses of C, H and N were done on a Vario EL III elemental analyzer at SAIF, Cochin University of Science and Technology, Kochi 22, India.

1.4.2. Magnetic susceptibility measurements

Magnetic susceptibility measurements were carried out at IIT, Roorkee, in the polycrystalline state at room temperature on a Par model 155 Vibrating Sample Magnetometer at 5 k Oersted field strength. Diamagnetic corrections were made using Pascal's constants.

The effective magnetic moment of a compound (μ_{eff}) is related to the corrected paramagnetic molar susceptibility ($\chi_{\text{m}}^{\text{corr}}$). The quantity that is most frequently obtained from experimental measurements of magnetism is the gram susceptibility (χ_{g}). It is obtained by dividing the experimental magnetic moment value to the

weight of the sample. By multiplying the gram susceptibility of a compound by its molecular weight (MW), we can obtain the molar susceptibility, χ_M .

$$\chi_M = \chi_g \cdot \text{MW}$$

Once the experimental value of χ_M has been obtained for a paramagnetic substance, it can be used to determine how many unpaired electrons are there per molecule or ion. In order to translate the experimental result into the number of unpaired spins, it must first be recognized that a measured susceptibility will include contributions from both paramagnetism and diamagnetism in the sample. The common procedure is to correct a measured susceptibility for the diamagnetic contribution. The diamagnetic susceptibility for a particular substance can be obtained as a sum of contributions from its constituent units: atoms, ions, bonds etc. To obtain the exact value of the paramagnetic susceptibility, the value of diamagnetic susceptibility must be subtracted from the susceptibility calculated from the observed results [25].

$$\chi_M^{\text{corr.}} = \chi_M - (\text{Diamagnetic corrections})$$

The next step is to connect the macroscopic susceptibility to individual molecular moments and finally to the number of unpaired electrons. From classical theory, the corrected paramagnetic molar susceptibility is related to the permanent paramagnetic moment of a molecule, μ_{eff} , by :

$$\chi_M^{\text{corr.}} = \frac{N^2 \mu_{\text{eff}}^2}{3RT}$$

where, N is Avogadro's number, R is the ideal gas constant, T is the absolute temperature and μ_{eff} is the effective magnetic moment and is expressed in

Bohr magnetons (B.M.). Solving the above expression, the effective magnetic moment is given by

$$\mu_{\text{eff}} = \sqrt{\frac{3RT}{N} \chi_M^{\text{Orr}}} = 2.828 \sqrt{\chi_M^{\text{Orr}} T}$$

But, the field strength (H) produced by the Vibrating sample magnetometer is 5 k Oersted. Then,

$$\mu_{\text{eff}} = 2.828 \sqrt{\frac{\chi_M^{\text{Orr}} T}{5 \times 10^3}}$$

1.4.3. Infrared spectroscopy

FT-IR spectra were recorded on a Thermo Nicolet AVATAR 370 DTGS FT-IR spectrophotometer instrument using KBr pellets, in 4000-400 cm^{-1} region at SAIF, Cochin University of Science and Technology, Kochi 22, India. The infrared radiation involves the class of electromagnetic (EM) radiation with frequencies between 4000 and 400 cm^{-1} (wavenumbers). The interpretation of infrared spectra involves the correlation of absorption bands in the spectrum of an unknown compound with the known absorption frequencies for types of bonds.

1.4.4. Electronic spectroscopy

Electronic spectra in solutions were recorded on a GENESYSTM 10 series spectrophotometer at the Department of Chemical Oceanography, CUSAT, Kochi-16 and Spectro UV-VIS Double Beam UVD-3500 spectrophotometer at Department of Applied Chemistry, CUSAT, Kochi-22 in the 200-900 nm range. Electronic spectra mainly involves ultraviolet region and visible region. The ultraviolet (UV) region scanned is normally from 200 to 400 nm, and the visible portion is from 400 to 800 nm. It works in the following procedure: A beam of light from a visible and / or UV

light source (colored red) is separated into its component wavelengths by a prism or diffraction grating. Each monochromatic (single wavelength) beam in turn is split into two equal intensity beams by a half-mirrored device. One beam, the sample beam (colored magenta), passes through a small transparent container (cuvette) containing a solution of the compound being studied in a transparent solvent. The other beam, the reference (colored blue), passes through an identical cuvette containing only the solvent. The intensities of these light beams are then measured by electronic detectors and compared. The intensity of the reference beam is defined as I_0 and the intensity of the sample beam is defined as I .

1.4.5. EPR spectroscopy

EPR spectral measurements were carried out on a Varian E-112 X-band spectrometer using TCNE as standard. One of the fundamental roles of any spectroscopic technique is identification of the chemical species being studied. EPR is a spectroscopic technique that detects chemical species that have unpaired electrons. EPR spectroscopy is capable of providing molecular structural details inaccessible by any other analytical tool. It worked as follows: By application of a strong magnetic field 'B' to material containing paramagnetic species, the individual magnetic moment arising via the electron "spin" of the unpaired electron can be oriented either parallel or anti-parallel to the applied field. This creates distinct energy levels for the unpaired electrons, making it possible for net absorption of electromagnetic radiation (in the form of microwaves) to occur. The situation referred to as the resonance condition takes place when the magnetic field and the microwave frequency are "just right" (*i.e.*, the energy of the microwaves corresponds to the energy difference ΔE of the pair of involved spin states). The equation describing the absorption (or emission) of microwave energy between two spin states is $\Delta E = h\nu = g\beta H$, where :

ΔE is the energy difference between the two spin states

h is Planck's constant

ν is the microwave frequency

g is the Zeeman splitting factor

β is the Bohr magneton

H is the applied magnetic field.

1.4.6. NMR spectroscopy

For diamagnetic complexes, NMR spectroscopy is an essential tool for establishing their structural characterizations. There are several NMR techniques like ^1H NMR, ^{13}C NMR, HMQC and COSY. The ^1H NMR spectra were recorded on a Bruker DRX 500 instrument using CDCl_3 as the solvent and TMS as the internal reference at Sophisticated instruments facility, Indian Institute of Science, Bangalore.

1.4.7. X-Ray crystallography

Single crystal X-ray crystallographic analysis of the compounds were carried out using a Siemens SMART CCD area-detector diffractometer at Analytical Science Division, Bhavnagar, Gujarat, India and the Argus (Nonius, MACH3 software) at Single Crystal X-Ray Diffraction Facility, IIT, Bombay. The structures were solved by direct methods and refined by least-square on F_0^2 using the SHELXTL software package [26]. The collected data were reduced using SAINT program [27]. Graphics quality plots were made by using the package Diamond Version 3.0 and PLATON [28, 29].

1.5. Significance of thiosemicarbazones and their metal complexes

Thiosemicarbazones are a large group of organic molecules whose biological activity was first reported in 1946 [30]. The biological properties of thiosemicarbazones are often related to metal ion coordination. The metal complex

can be more active than the free ligand, and some side effects may decrease upon complexation. In addition, the complex can exhibit bioactivities which are not shown by the free ligand. The mechanism of action can involve binding to a metal *in vivo* or the metal complex may be a vehicle for activation of the ligand as the cytotoxic agent. Moreover, coordination may lead to significant reduction of drug-resistance [1].

Thiosemicarbazones and their metal complexes exhibit wide spectrum of antimicrobial activity. The antibacterial activity of a variety of 2-acetylpyridine thiosemicarbazones was determined in clinical isolates of bacteria. The compounds tested were able to inhibit *Neisseria gonorrhoeae*, *Neisseria meningitides*, *Staphylococcus faecalis*, *Streptococcus faecalis* and *D Enterococcus*. Poor antibacterial activity was shown toward the Gram-negative bacilli, *ie*, *Pseudomonas*, *Klebsiella-Enterobacter*, *Shigella*, *Escherichia Coli* and *Proteus* [31].

Base adducts of Cu(II) complexes have been prepared with N(4)-phenyl salicylaldehyde thiosemicarbazone. The thiosemicarbazone and its complexes showed growth inhibitory activity against the human pathogenic bacteria *Salmonella typhi*, *Shigella dysenteriae*, *Non-coagulace staphylococcus*, *Photobacterium sp.* and *S. aureus* and the complexes against plant pathogenic fungi [32].

Many other thiosemicarbazones and metal complexes were screened for antibacterial and antifungal activity. For example, 2-formylpyridine thiosemicarbazones and their oxovanadium(IV) complexes exhibited powerful *in vitro* antibacterial activities towards *E Coli* [33], and aryl thiosemicarbazones showed good activity against *Aeromonas hydrophilia* and *Salmonella typhimurium* [34].

Collins *et al* reported a study of structure antimicrobial activity in a series of N(4)-substituted 2-acetylpyridine thiosemicarbazones [35]. The work reveals that antimicrobial activity occurs for compounds having partition coefficients (log P)

between 3.0 and 4.0, which suggests that the activity of these compounds depends on their possessing an optimum hydrophobicity, which in turn controls their rate of entry into the bacterial cell.

The antitumor properties of many thiosemicarbazones and their metal complexes have been investigated. The antitumor activity of bis(thiosemicarbazones) was widely investigated after the discovery of the strong antineoplastic activity of 3-ethoxy-2-oxobutyraldehyde bis(thiosemicarbazone) in solid animal tumors [36]. 5-Hydroxy-2-formylpyridine thiosemicarbazone (5-HP) was the only member of the α (N)-heterocyclic thiosemicarbazone series to be clinically evaluated in man [37].

The antiviral activity of thiosemicarbazones was first reported in 1950 by Hamre *et al* [38]. They found that benzaldehyde thiosemicarbazone derivatives were active against neurovaccinial infection in mice. The isatin-thiosemicarbazones were found to be very active and a clinical trial of N-methyl-isatin- β -thiosemicarbazone (methisazone) against small pox was carried out in India [39-41]. The drug has also been used to treat patients with herpes simplex virus (HSV) [42]. Its 4',4'-diethyl derivatives have shown to inhibit Moloney leukemia virus [43] and human immunodeficiency virus (HIV) [44].

1.6. Objective and scope of the present work

Thiosemicarbazones and their metal complexes have been subject of interest in numerous studies because of their chemical and biological properties [45,46]. The coordination chemistry of tridentate ONS donor ligands is a highly interesting field. Their importance increased markedly after the presence of ONS donor environment was detected at the active sites of some metalloenzymes [47].

Thiosemicarbazones obtained by condensation of N(4)-substituted thiosemicarbazides with salicylaldehyde [48-50] or with 2-hydroxyacetophenone

[51,52] form a class of versatile NS / NSO chelating ligands and are known to exhibit diverse biological activities. They also stabilize uncommon oxidation states [53]. A number of studies dealing with the complex formation properties of this class of compounds exist [54,55]. Transition metal ions like Cu(II), Ni(II), Mn(II), Zn(II), oxovanadium(IV) and dioxomolybdenum(VI) were used for the synthesis of complexes. We have undertaken the work along the following lines

To synthesize interesting N(4)-substituted ONS donor ligands

Salicylaldehyde N(4)-cyclohexylthiosemicarbazone (H_2L^1)

2-Hydroxyacetophenone N(4)-cyclohexylthiosemicarbazone (H_2L^2)

Salicylaldehyde N(4)-phenylthiosemicarbazone (H_2L^3)

2-Hydroxyacetophenone N(4)-phenylthiosemicarbazone (H_2L^4)

To characterize these ligands using elemental analyses, IR, electronic and 1H NMR spectral studies.

To synthesize Cu(II), Ni(II), Mn(II), Zn(II), oxovanadium(IV) and dioxomolybdenum(VI) complexes and characterize these complexes using elemental analyses, magnetic susceptibility measurements, IR, electronic, EPR and 1H NMR spectral studies.

To carry out single crystal X-ray diffraction studies of the ligands H_2L^2 , H_2L^3 and H_2L^4 and some of their Cu(II), Zn(II), dioxomolybdenum(VI) complexes.

To find out the EPR parameters of Cu(II), Mn(II) and oxovanadium(IV) complexes of thiosemicarbazone.

To carry out single crystal X-ray diffraction study of an unusual compound 2-[5-(cyclohexylamino)-1,3,4-thiadiazol-2-yl]phenol (TDZ).

References

1. D.X. West, S.B. Padhye, P.B. Sonawane, Structure and Bonding (Berlin) 76 (1971) 1.
2. R.B. Singh, B.S. Garg, R.P. Singh, Talanta 25 (1978) 619.
3. J.S. Casas, M.S. Garcia-Tasende, J. Sordo, Coord. Chem. Rev. 209 (2000) 197.
4. S. Padhye, G.B. Kauman, Coord. Chem. Rev. 63 (1985) 127.
5. P. Domiano, G. Gasparri Fava, M. Nardelli, P. Sgarabotto, Acta Cryst. B26 (1970) 1005.
6. N.V. Gerbeleu, M.D. Revenko, V.M. Leovats, Russ. J. Inorg. Chem. 22 (1977) 1009.
7. L. Coghi, A.M. Lanfredi, A. Tiripicchio, J. Chem. Soc., Perkin Trans. 2 (1976) 1808.
8. D.X. West, R.M. Makeever, J.P. Scovill, D.L. Klayman, Polyhedron 3 (1984) 947.
9. A.V. Ablov, N.V. Gerbeleu, Russ. J. Inorg. Chem. 9 (1964) 1260.
10. N.A. Ryabova, V.I. Ponomarev, L.O. Atomyan, V.V. Zelentsov, V.I. Shipilov, Sov. J. Coord. Chem. 4 (1976) 95.
11. B. Pradhan, D.V. Ramana Rao, J. Ind. Chem. Soc. 54 (1977) 136.
12. A. Usman, I.A. Razak, S. Chantrapromma, A. Sreekanth, S. Sivakumar, M.R.P. Kurup, Acta Cryst. C58 (2002) m461.
13. G. Dessy, V. Fares, L. Scarmuzza, Cryst. Struct. Commun. 5 (1976) 605.
14. S.B. Padhye, P.B. Sonawane, R.C. Chikate, D.X. West, Asian J. Chem. Rev. 2 (1980) 125.
15. S. Sivakumar, Ph.D thesis, CUSAT, 2003.

16. W. Kaminsky, D.R. Kelman, J.M. Giesen, K.I. Goldberg, K.A. Claborn, D.X. West, *J. Mol. Struct.* 616 (2002) 79.
17. N.V. Gerbeleu, K.I. Turta, J.T. Kashkaval, F. Tui, *Russ. J. Inorg. Chem.* 26 (1981) 1154.
18. M. Mathew, G.J. Palenik, G.R. Clark, *Inorg. Chem.* 12 (1973) 446.
19. U.N. Pandey, *J. Ind. Chem. Soc.* 55 (1978) 645.
20. Y.K. Bhoon, S. Mitra, J.P. Scovill, D.L. Klayman, *Trans. Met. Chem.* 7 (1982) 264.
21. D.K. Demertzi, A. Domopouleu, M. Demertzis, *Polyhedron* 13 (1994) 1917.
22. M. A. Ali, S.E. Livingstone, *Coord. Chem. Rev.* 13 (1974) 101.
23. R.K.Y. Ho, S.E. Livingstone, T.N. Lockyer, *Aust. J. Chem.* 19 (1966) 1179.
24. Y.K. Bhoon, S. Mitra, J.P. Scovill, D.L. Klayman, *Trans. Met. Chem.* 7 (1982) 264.
25. J.E. Huheey, E.A. Keiter, R.L. Keiter, *Inorganic Chemistry*, 4th edn, Addison-Wesley publishing company, India, 1993.
26. G.M. Sheldrick, *SHELXTL Version 5.1, Software Reference Manual*, Bruker AXS Inc., Madison, Wisconsin, USA, 1997.
27. Siemens, *SMART and SAINT, Area Detector Control and Integration software*, Siemens Analytical X-ray Instruments Inc., Madison, Wisconsin, USA, 1996.
28. K. Brandenburg, *Diamond Version 3.0, Crystal Impact GbR, Bonn, Germany*, 1997-2004.
29. A. L. Spek, *ORTEP-III and PLATON, a Multipurpose Crystallographic Tool*, Utrecht University, Utrecht, The Netherlands, 1999.
30. G. Domagk, R. Behnich, F. Mietzsch, H. Schmidt, *Naturwiss* 1946, 315.

31. A.S. Dobek, D.L. Klayman, E.T. Dickson Jr, J.P. Scovill, E.C. Tramont, *Antimicrob Agents Chemother.* 18 (1980) 27.
32. P. Bindu, M.R.P. Kurup, T.R. Satyakeerty, *Polyhedron* 18 (1999) 321.
33. A. Maiti, A.K. Guha, S. Ghosh, *J. Inorg. Biochem.* 33(1988) 57.
34. S.K. Singh, S.N. Pandeya, *Boll. Chim. Farm.* 140(4) (2001) 238.
35. F.M. Collins, D.L. Klayman, N.E. Morrison, *J. General Microbiology* 128 (1982) 1349.
36. D.A. Winkelmann, Y. Bermke, D.H. Petering, *Bioinorg. Chem.* 3 (1974) 261 and references therein.
37. R.C. DeConti, B.R. Toftness, K.C. Agrawal, R. Tomchick, J.A.R. Mead, J.R. Bertino, A.C. Sartorelli, W. Creasey, *Cancer Res.* 32 (1972) 1455.
38. D. Hamre, J. Bernstein, R. Donovan, *Proc. Soc. Exp. Biol. Med.* 73 (1950) 275.
39. D.J. Bauer, *N.Y. Ann, Acad. Sci.* 130 (1965) 110.
40. D.J. Bauer, St. L. Vincent., C.H. Kempe, A.W. Downie, *Lancet* 494 (1963) 494.
41. D.J. Bauer, St. L. Vincent, C.H. Kempe, P.A. Young, A.W. Downie, *Am. J. Epidemiol.* 90 (1969) 130.
42. C. Shipman, S.H. Smith, J.C. Drach, D.L. Klayman, *Antiviral Research* 6 (1986) 197.
43. D. Ronen, E. Nir, Y. Teitz, *Antiviral Research* 5 (1985) 249.
44. Y. Teitz, D. Ronen, A. Vansover, T. Stematsky, J.L. Riggs, *Antiviral Research* 24 (1994) 305.
45. D.L. Klayman, J.P. Scovill, J.F. Bartosevich, J. Bruce, *J. Med. Chem.* 26 (1983) 35, and references therein.

46. A.G. Quiroga, J.M. Perez, E.I. Montero, D.X. West, C. Alonso, C.N. Ranninger, *J. Inorg. Biochem.* 75 (1999) 293.
47. J. Christiansen, R.C. Tittsworth, B.J. Hales, S.P. Cramer, *J. Am. Chem. Soc.* 117 (1995) 1017.
48. V.M. Leovac, A.F. Petrovic, *Trans. Met. Chem.* 8 (1983) 337.
49. S. Purohit, A.P. Koley, L.S. Prasad, P.T. Manoharan, S. Ghosh, *Inorg. Chem.* 28 (1989) 3735.
50. A.P. Koley, S. Purohit, L.S. Prasad, P.T. Manoharan, S. Ghosh, *J. Chem. Soc., Dalton Trans.* (1988) 2607.
51. S.I. Mostafa, A.A. El-Asmy, *Trans. Met. Chem.* 25 (2000) 470.
52. D.K. Demertzi, N. Kourkoumelis, D.X. West, J.V. Martinez, S.H. Ortega, *Eur. J. Inorg. Chem.* (1998) 861.
53. A.P. Koley, R. Nirmala, L.S. Prasad, S. Ghosh, P.T. Manoharan, *Inorg. Chem.* 31(1992) 1764.
54. A.F. Petrovic, M.L. Vukadin, B. Riber, *Trans. Met. Chem.* 11 (1986) 207.
55. R.P. John, A. Sreckanth, M.R.P. Kurup, A. Usman, A.R. Ibrahim, H.-K. Fun, *Spectrochim. Acta A59* (2003) 1349.

CHAPTER 2

SYNTHESIS, SPECTRAL AND STRUCTURAL STUDIES OF THIOSEMICARBAZONE LIGANDS

2.1. Introduction

Thiosemicarbazones of aromatic o-hydroxyaldehydes and ketones have recently attracted considerable attention because of their potential biological properties [1] and catalytic activity [2]. Recent studies of thiosemicarbazone complexes have centered on tridentate ligands containing an oxygen atom besides the thiosemicarbazone moiety *ie*, nitrogen and sulfur atom. The later two atoms are considered the sites of coordination in both neutral and anionic thiosemicarbazone ligands [3]. These aromatic thiosemicarbazones most often coordinate as the dianion on loss of the phenoxy hydrogen and thiosemicarbazone moiety to form mononuclear $[M(ONS)B]$ {ONS represents the dianionic thiosemicarbazone ligand coordinated *via* the phenoxy oxygen, azomethine nitrogen and thiolate sulfur and B represents any neutral heterocyclic base} or dinuclear $[M(ONS)]_2$ have isolated on deprotonation of the ring hydroxy group and loss of the N(2) hydrogen of the thiosemicarbazone moiety [4].

Here, we prepared four tridentate ONS donor ligands and is used for the preparation of metal complexes.

1. Salicylaldehyde N(4)-cyclohexylthiosemicarbazone (H_2L^1)
2. 2-Hydroxyacetophenone N(4)-cyclohexylthiosemicarbazone (H_2L^2)
3. Salicylaldehyde N(4)-phenylthiosemicarbazone (H_2L^3)
4. 2-Hydroxyacetophenone N(4)-phenylthiosemicarbazone (H_2L^4)

This chapter deals with the synthesis and spectral characterization of ligands. It also deals with X-ray diffraction studies of H_2L^2 , H_2L^3 and H_2L^4 . The IUPAC numbering scheme is not very appropriate for describing the structural data of

semicarbazones and thiosemicarbazones because the numbering of C and N atoms on the semicarbazone or thiosemicarbazone chain does not run on into the numbering of substituted groups. This is probably why a variety of different numbering schemes have been used in the literature. In this chapter, the following numbering scheme is used for the above four ligands throughout the entire work, except in X-ray diffraction studies. The structures and the numbering schemes are given in Figure 2.1.

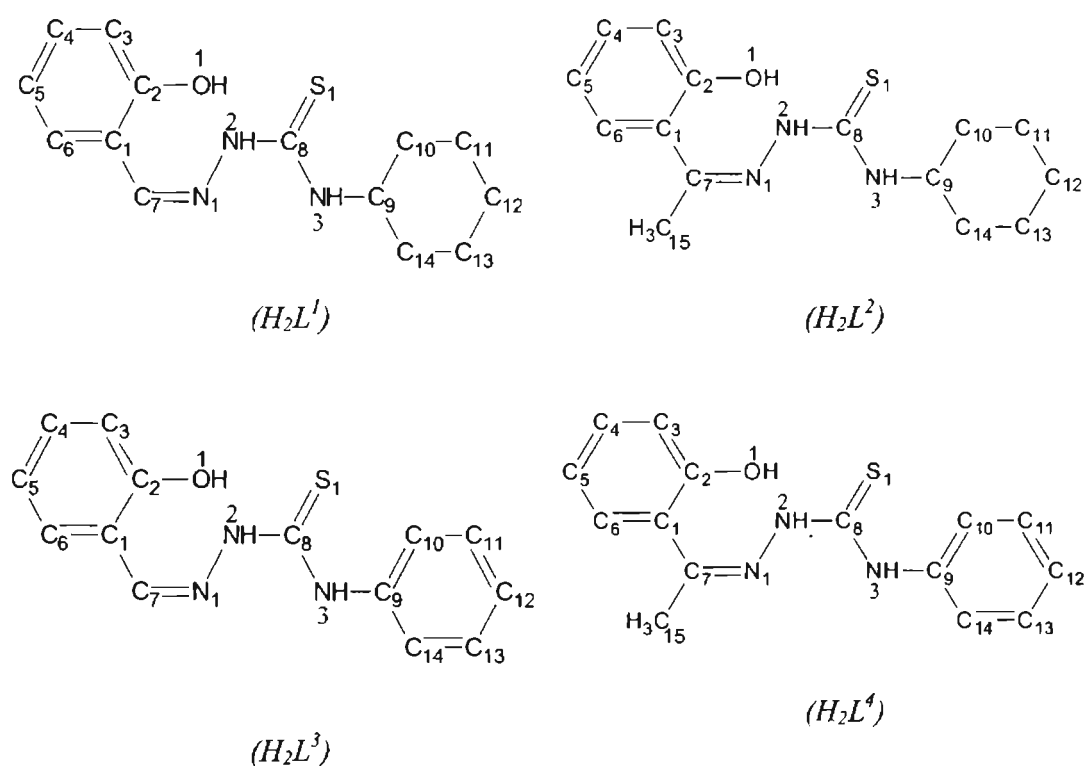


Figure 2.1. Structural formulas of H_2L^1 , H_2L^2 , H_2L^3 and H_2L^4

2.2. Synthesis of thiosemicarbazone ligands

These ligands are prepared by adapting the reported procedure of Klayman *et al* [5] and also others [6,7].

2.2.1. Materials

Cyclohexylisothiocyanate (Fluka), hydrazine hydrate (Lancaster), salicylaldehyde (SRL chemicals), 2-hydroxyacetophenone (SRL chemicals), phenylisothiocyanate (Fluka), ethanol / methanol and glacial acetic acid.

2.2.2. Synthesis of the ligands H_2L^1 and H_2L^2

Step-1

Preparation of N(4)-cyclohexylthiosemicarbazide

Cyclohexylisothiocyanate (15 mmol, 2 ml) in 15 ml ethanol and hydrazine hydrate (90 mmol, 4.3 ml) in 15 ml ethanol were mixed with constant stirring. The resulting solution was kept in a stirred condition for $\frac{1}{2}$ an hour. The white product, N(4)-cyclohexylthiosemicarbazide formed was filtered, washed with ethanol and ether and dried *in vacuo* over P_4O_{10} . m.p. = 140 °C.

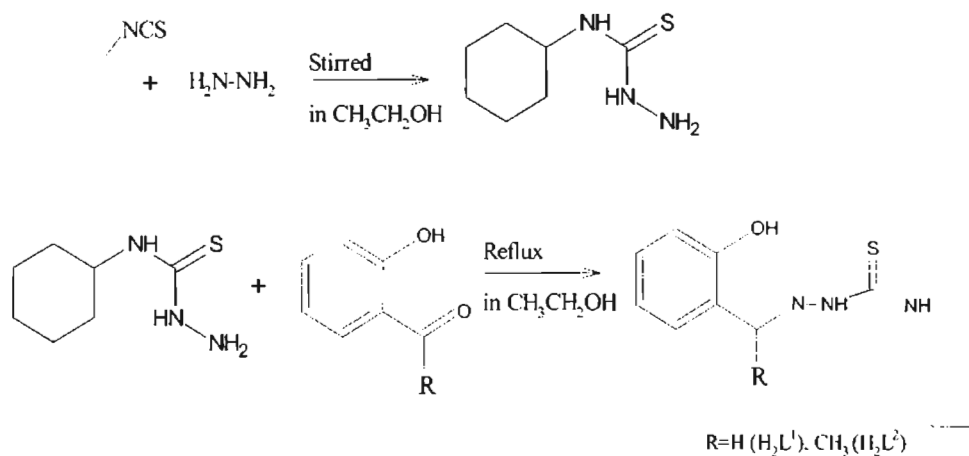
Step-2 :-

Synthesis of salicylaldehyde N(4)-cyclohexylthiosemicarbazone (H_2L^1)

To a hot solution of 0.866 g (5 mmol) of N(4)-cyclohexylthiosemicarbazide in 25 ml of ethanol, added 0.5235 ml (5 mmol) of salicylaldehyde in 25 ml of ethanol with constant stirring. One or two drops of glacial acetic acid was added to the above solution and the mixture was slowly refluxed for 3 h. After cooling, the compound was obtained as white crystalline solids, which was filtered, washed with ethanol and ether and dried *in vacuo* over P_4O_{10} .

Synthesis of 2-hydroxyacetophenone N(4)-cyclohexylthiosemicarbazone (H_2L^2)

H_2L^2 is also prepared according to the above procedure. In the above mentioned procedure, instead of salicylaldehyde, 2-hydroxyacetophenone (5 mmol, 0.6 ml) was used. The compound was obtained as pale yellow parallelepiped crystals.

Scheme for the synthesis of H_2L^1 and H_2L^2

2.2.3. Synthesis of H_2L^3 and H_2L^4

Step-1:-

Preparation of N(4)-phenylthiosemicarbazide

Phenylisothiocyanate (100 mmol, 11.94 ml) in 25 ml ethanol and hydrazine hydrate (100 mmol, 4.86 ml) in 25 ml ethanol were mixed with constant stirring. The resulting solution was kept in a stirred condition for $\frac{1}{2}$ an hour. The white product, N(4)-phenylthiosemicarbazide formed was filtered, washed with ethanol and ether and dried *in vacuo* over P_4O_{10} . m.p. = $135^\circ C$.

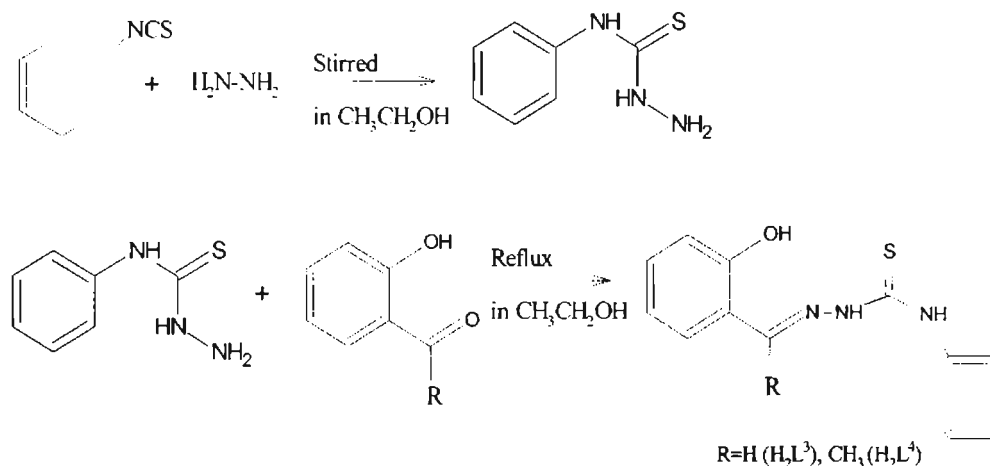
Step-2:-

Synthesis of salicylaldehyde N(4)-phenylthiosemicarbazone (H_2L^3)

To a hot solution of 0.83615 g (5 mmol) of phenylthiosemicarbazide in 25 ml of ethanol, added 0.5235 ml (5 mmol) of salicylaldehyde in 25 ml of ethanol with constant stirring. The above mixture was slowly refluxed for 3 h. After cooling, the compound was obtained as pale yellow crystalline solids, which was filtered, washed with ethanol and ether and dried *in vacuo* over P_4O_{10} .

Synthesis of 2-hydroxyacetophenone N(4)-phenylthiosemicarbazone (H_2L^4)

H_2L^4 is also prepared according to the above procedure. In the above mentioned procedure, instead of salicylaldehyde, 2-hydroxyacetophenone (5 mmol, 0.6 ml) was used. The compound was obtained as yellow solids.



Scheme for the synthesis of H_2L^3 and H_2L^4

2.3. Characterization techniques

Details regarding the analytical measurements and various spectral techniques are given in Chapter 1.

2.3.1. X-Ray crystallography

(i) X-Ray crystallography of H_2L^2 and H_2L^3

The pale yellow parallelepiped crystals of H_2L^2 and pale yellow plates of H_2L^3 suitable for X-ray diffraction studies were obtained by slow evaporation of their solutions in ethanol. The crystal structure data (Table 2.1) collection for these two crystals were done on a BRUKER SMART APEX CCD diffractometer using graphite monochromated MoK α radiation ($\lambda = 0.71073 \text{ \AA}$) at 293(2) and 295(2) K

respectively. Crystals with dimensions 0.42 x 0.31 x 0.28 mm for H_2L^2 and 0.20 x 0.12 x 0.08 mm for H_2L^3 were used. The collected data were reduced by using SAINT [8]. The structure were solved by direct methods with the program SHELXTL-97 [9]. The positions of all the non-hydrogen atoms were included in the full-matrix least-squares refinement using SHELXTL-97 program and all the hydrogen atoms were fixed in calculated positions. The structure of the compound H_2L^2 and H_2L^3 were plotted using the programs Diamond Version 3.0 [10] and PLATON [11].

(ii) X-Ray crystallography of H_2L^4

Yellow block crystals suitable for X-ray analysis were obtained by slow evaporation from its solution in a mixture of methanol-diethylether after one week. A crystal having approximate dimensions 0.30 x 0.25 x 0.20 mm was sealed in a glass capillary. The X-ray diffraction data (Table 2.1) was measured at 293(2) K, data acquisition and cell refinement were done using the Argus (Nonius, MACH3 software) [12]. The Maxus software package (Nonius) was used for data reduction [13]. The structure was solved by direct methods and full-matrix least-squares refinement using SHELXL-97 [14] package. The positions of all the non-hydrogen atoms were included in the full-matrix least-squares refinement using SHELXL-97 program and all the hydrogen atoms were fixed in calculated positions. The structure of the compound H_2L^4 was plotted using the programs Diamond Version 3.0 [10] and PLATON [11].

Table 2.1. Crystal data and structure refinement parameters for H_2L^2 , H_2L^3 and H_2L^4

	(H_2L^2)	(H_2L^3)	(H_2L^4)
Empirical formula	$C_{30}H_{42}N_6O_2S_2$	$C_{14}H_{13}N_3OS$	$C_{15}H_{15}N_3OS$
Formula weight	582.82	271.33	285.36
Temperature	293(2) K	295(2) K	293(2) K
Wavelength	0.71073 Å	0.71073 Å	0.71073 Å
Crystal system	Triclinic	Triclinic	Monoclinic
Space group	$P\bar{1}$	$P\bar{1}$	$C2/c$
Unit cell dimensions	a = 6.9436(8) Å b = 12.4762(15) Å c = 18.588(2) Å $\alpha = 100.187(2)^\circ$ $\beta = 97.069(2)^\circ$ $\gamma = 92.340(2)^\circ$	a = 10.6733(15) Å b = 13.8856(19) Å c = 14.052(2) Å $\alpha = 81.851(2)^\circ$ $\beta = 77.061(2)^\circ$ $\gamma = 83.482(2)^\circ$	a = 16.8636(19) Å b = 7.4520(6) Å c = 23.3228(17) Å $\alpha = 90^\circ$ $\beta = 94.338(7)^\circ$ $\gamma = 90.10^\circ$
Volume	1569.6(3) Å ³	2002.1(5) Å ³	2922.5(5) Å ³
Z	2	6	8
Density (calculated)	1.233 Mg/m ³	1.3503 Mg/m ³	1.297 Mg/m ³
Absorption coefficient	0.206 mm ⁻¹	0.237 mm ⁻¹	0.220 mm ⁻¹
F(000)	624	852	1200
Crystal size	0.42 x 0.31 x 0.28 mm	0.20 x 0.12 x 0.08 mm	0.35 x 0.25 x 0.20 mm
θ range for data collection	1.12 to 28.21 °	1.96 to 28.27 °	1.75 to 24.98 °
Index ranges	-7 < h <= 8, -14 < k <= 16, -23 < l <= 24	-13 < h <= 13, -17 < k <= 18, -18 < l <= 14	-20 < h <= 0, -8 < k <= 0, -27 < l <= 27
Reflections collected	9159	12079	2640
Independent reflections	6801 [R(int) = 0.0178]	5600 [R(int) = 0.0216]	2547 [R(int) = 0.0441]
Refinement method	Full-matrix least-squares on F ²	Full-matrix least-squares on F ²	Full-matrix least-squares on F ²
Data / restraints / parameters	6801 / 0 / 381	8795 / 0 / 653	2547 / 0 / 194
Goodness-of-fit on F ²	1.066	1.019	0.932
Final R indices [$I > 2\sigma(I)$]	R ₁ = 0.0528, wR ₂ = 0.1453	R ₁ = 0.1031, wR ₂ = 0.1886	R ₁ = 0.0576, wR ₂ = 0.0986
R indices (all data)	R ₁ = 0.0718, wR ₂ = 0.1681	R ₁ = 0.0657, wR ₂ = 0.1572	R ₁ = 0.2205, wR ₂ = 0.1313
Largest diff. peak and hole	0.311 and -0.215 e.Å ⁻³	0.025 and 0.001 e.Å ⁻³	0.187 and -0.228 e.Å ⁻³

2.4. Results and discussion

2.4.1. Synthesis

The empirical formulas, melting points and partial elemental analyses of the ligands are presented in Table 2.2. The four ligands H_2L^1 , H_2L^2 , H_2L^3 and H_2L^4 are white, pale yellow, pale yellow and yellow in color respectively. Single crystals of H_2L^2 and H_2L^3 suitable for X-ray diffraction studies were obtained by slow evaporation of their ethanol solutions. Similarly, single crystals of H_2L^4 were obtained from a mixture of methanol-diethylether solution. In spite of many attempts, we were unsuccessful in isolating single crystals of H_2L^1 suitable for single crystal XRD.

Table 2.2. Analytical data

Compound	Empirical formula	Melting point (°C)	Found (Calculated) %		
			C	H	N
H_2L^1	$C_{14}H_{19}N_3OS$	184	59.48 (59.65)	7.06 (6.97)	14.95 (14.91)
H_2L^2	$C_{15}H_{21}N_3OS$	154	61.15 (61.82)	7.56 (7.26)	14.30 (14.42)
H_2L^3	$C_{14}H_{13}N_3OS$	178	62.21 (61.97)	5.13 (4.83)	15.57 (15.49)
H_2L^4	$C_{15}H_{15}N_3OS$	195	62.61 (63.13)	5.35 (5.30)	14.57 (14.73)

2.4.2. Crystal structure of H_2L^2

The molecular structure of H_2L^2 along with the atom numbering scheme, H bonding and its packing in the crystal lattice are given in Figures 2.2, 2.3 and 2.4 respectively. Selected bond lengths and bond angles are listed in Table 2.3. H_2L^2 crystallizes with two molecules per asymmetric unit into triclinic crystal system with a space group of $P\bar{1}$. According to the crystal structure, the compound exists in the thione form with S(1) and N(1) are at *E* configuration with respect to N(2)–C(8) bond. This is confirmed by the torsion angle of $167.13(15)^\circ$ at N(1)–N(2)–C(8)–S(1) moiety [15]. The existence of H_2L^2 in the thione form in the solid state is confirmed

by the observed bond lengths C(8)–S(1) [1.688(2) Å] and C(8)–N(2) [1.351(3) Å]. The C(8)–S(1) bond length [1.688(2) Å] is close to C–S double bond length [1.60 Å] than to C–S single bond [1.81 Å] and C(8)–N(2) bond length [1.351(3) Å] is intermediate between C–N single bond [1.45 Å] and C–N double bond [1.25 Å] [16]. The shorter length of C–N and longer length of C=S points out the extended conjugation in the molecule similar to other thiosemicarbazones.

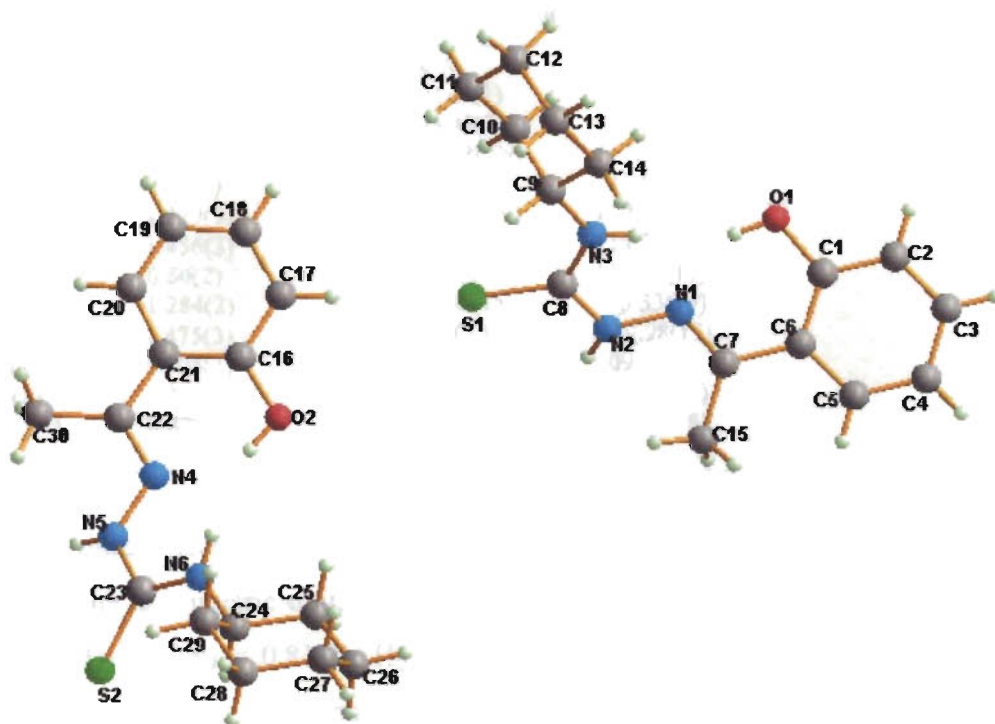


Figure 2.2. Structure and labeling diagram for H_2L^2

The mean plane deviation calculations show that the central thiosemicarbazone bridge C(7)–N(1)–N(2)–C(8)–S(1) itself is nearly planar with a maximum mean plane deviation of 0.1760 Å for S(1) and C(7)–N(1)–N(2)–C(8)–N(3) with a maximum deviation of 0.2807 Å for N(3). The centroid Cg(1) consists of

atoms C(1)–C(2)–C(3)–C(4)–C(5)–C(6) and Cg(2) comprising of the cyclohexyl ring, themselves are puckered, makes a dihedral angle of 74.88° with each other and $27.84(1)^\circ$ and 59.32° respectively with the first bridge C(7)–N(1)–N(2)–C(8)–S(1). The ring puckering analysis and least square calculations show that the cyclohexyl ring is in chair conformation ($Q_T = 0.5828(28) \text{ \AA}$) with the equatorial substitution at C(9) for N(3) [17].

Table 2.3. Selected bond lengths (Å) and bond angles ($^\circ$) for the ligand (H_2L^2).

<i>Bond lengths</i>		<i>Bond angles</i>	
S(1)–C(8)	1.688(2)	C(8)–N(2)–N(1)	119.95(17)
N(2)–C(8)	1.351(3)	C(8)–N(2)–H(2N)	118.3(14)
N(2)–N(1)	1.392(2)	N(1)–N(2)–H(2N)	117.1(15)
N(2)–H(2N)	0.90(2)	C(8)–N(3)–C(9)	123.51(18)
N(3)–C(8)	1.329(3)	C(8)–N(3)–H(3N)	119.6(17)
N(3)–C(9)	1.456(3)	C(9)–N(3)–H(3N)	114.3(17)
N(3)–H(3N)	0.80(2)	N(1)–C(7)–C(6)	116.69(17)
C(7)–N(1)	1.284(2)	N(1)–C(7)–C(15)	123.33(19)
C(7)–C(6)	1.475(3)	C(6)–C(7)–C(15)	119.98(17)
C(7)–C(15)	1.504(3)	C(1)–O(1)–H(1)	109.5
O(1)–C(1)	1.351(3)	C(7)–N(1)–N(2)	117.67(17)
O(1)–H(1A)	0.8200	N(3)–C(8)–N(2)	117.90(18)

Two intramolecular hydrogen bonding interactions are observed within each molecule of the asymmetric unit. One between N(3)–H(3N)...N(1) [N(3)...N(1) = 2.686(3), N(3)---H(3N) = 0.81(3), H(3N)...N(1) = 2.39(2), N(3)---H(3N)...N(1) = $102.9(18)^\circ$] and other between O(1)–H(1)...N(1) [O(1)...N(1) = 2.559(2), O(1)---H(1) = 0.82, H(1)...N(1) = 1.85, O(1)---H(1)...N(1) = 144°]. Similarly in the second molecule of the asymmetric unit also. The first one forces the molecule to exist in such a configuration that S(1) and N(1) are trans to each other with respect to N(2)–C(8) bond.

In the crystal lattice, the two dimensional packing of the molecules is stabilized by intermolecular hydrogen bonding interactions. These interactions

observed are $N(2)-H(2N)\dots S(1)^i$ [(i) = 2-x, 1-y, 1-z; $N(2)\dots S(1) = 3.319(2)$, $N(2)\text{---}H(2N) = 0.90(2)$, $N(2)\text{---}H(2N)\dots S(1) = 163.2(19)^\circ$] and $N(3)-H(3N)\dots O(2)^{ii}$ [(ii) = 1-x, 1-y, 1-z; $N(3)\dots O(2) = 3.175(2)$, $N(3)\text{---}H(3N) = 0.81(3)$, $N(3)\text{---}H(3N)\dots O(2) = 165(2)^\circ$] of another unit. Similarly $N(5)-H(5N)\dots S(2)^{iii}$ [(iii) = 1-x, -y, -z; $N(5)\dots S(2) = 3.414(2)$, $N(5)\text{---}H(5N) = 0.86(3)$, $N(5)\text{---}H(5N)\dots S(2) = 167(2)^\circ$] and $N(6)-H(6N)\dots O(1)^{ii}$ [(ii) = 1-x, 1-y, 1-z; $N(6)\dots O(1) = 3.063(3)$, $N(6)\text{---}H(6N) = 0.83(2)$, $N(6)\text{---}H(6N)\dots O(1) = 150(2)^\circ$] are also observed.

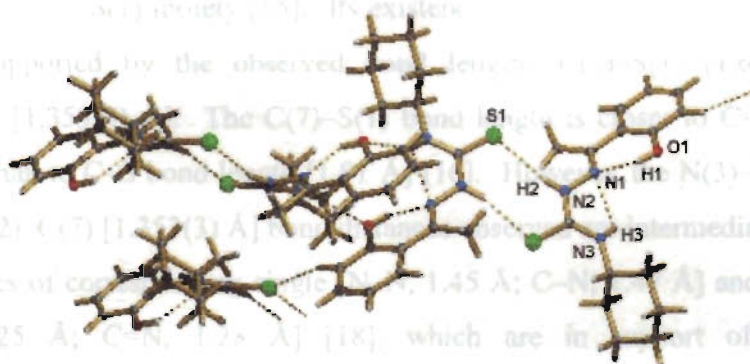


Figure 2.3. Hydrogen bonding interactions for H_2L^2

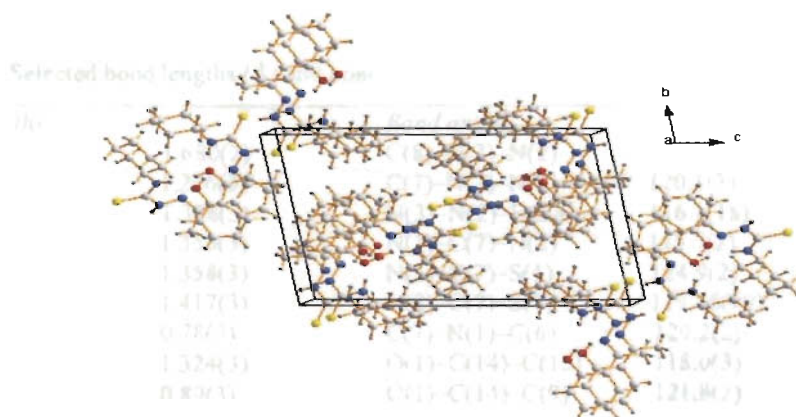


Figure 2.4. Unit cell packing diagram for H_2L^2 viewed along the a axis

2.4.3. Crystal structure of H_2L^3

The molecular structure of H_2L^3 along with atom numbering scheme is given in Figure 2.5 and selected bond lengths and bond angles are given in Table 2.4. The compound crystallizes with three molecules per asymmetric unit into triclinic crystal system with a space group of $P\bar{1}$. From Table 2.4, it is clear that three molecules in the asymmetric unit are almost identical. So the discussion can be limited to one of the molecules. According to the crystal structure, the compound exists in the thione form with S(1) and N(3) in the *E* configuration with respect to the N(2)–C(7) bond as in the case of H_2L^2 . This is confirmed by the torsion angle of 179.49° of the N(3)–N(2)–C(7)–S(1) moiety [15]. Its existence in the thione form in the solid state is also supported by the observed bond lengths C(7)–S(1) [1.680(2) Å] and C(7)–N(2) [1.353(3) Å]. The C(7)–S(1) bond length is closer to C=S bond length [1.60 Å] than to C–S bond length [1.81 Å] [16]. However, the N(3)–N(2) [1.378(3) Å] and N(2)–C(7) [1.353(3) Å] bond distances observed are intermediate between the ideal values of corresponding single [N–N, 1.45 Å; C–N, 1.47 Å] and double bonds [N=N, 1.25 Å; C=N, 1.28 Å] [18], which are in support of an extended π delocalization along the thiosemicarbazone chain. Similar trend is observed in the second and third molecules of the asymmetric unit also.

Table 2.4. Selected bond lengths (Å) and bond angles ($^\circ$) for the ligand (H_2L^3).

<i>Bond lengths</i>		<i>Bond angles</i>	
S(1)–C(7)	1.680(2)	C(8)–N(3)–N(2)	117.4(2)
N(3)–C(8)	1.276(3)	C(7)–N(2)–N(3)	120.1(2)
N(3)–N(2)	1.378(3)	N(3)–N(2)–H(2A)	116.1(18)
N(2)–C(7)	1.353(3)	N(1)–C(7)–N(2)	115.7(2)
O(1)–C(14)	1.358(3)	N(1)–C(7)–S(1)	124.9(2)
N(1)–C(6)	1.417(3)	N(2)–C(7)–S(1)	119.45(19)
N(1)–H(1A)	0.78(3)	C(7)–N(1)–C(6)	129.2(2)
C(7)–N(1)	1.324(3)	O(1)–C(14)–C(13)	118.0(3)
N(2)–H(2A)	0.89(3)	O(1)–C(14)–C(9)	121.8(2)

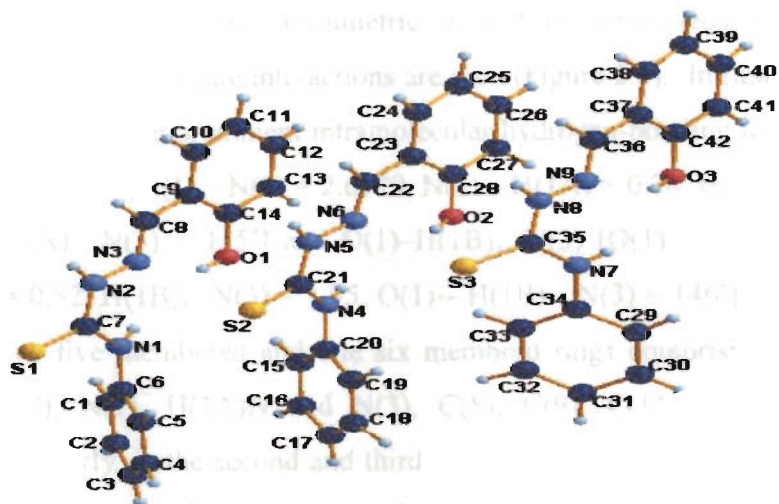


Figure 2.5. Structure and labeling diagram for H_2L^3

The mean plane deviation calculations show that the central thiosemicarbazone moiety C(8)–N(3)–N(2)–C(7)–S(1)–N(1) itself is nearly planar with a maximum mean plane deviation of 0.0140 Å at C(8) and 0.0180 Å at N(2). Ring puckering analysis and least square plane calculations show that the rings Cg(1) comprising of atoms C(1)–C(2)–C(3)–C(4)–C(5)–C(6) and Cg(2) comprising of atoms C(9)–C(10)–C(11)–C(12)–C(13)–C(14), themselves are puckered, makes a dihedral angle of 54.98° with each other and they are deviated from the central thiosemicarbazone moiety C(8)–N(3)–N(2)–C(7)–S(1)–N(1) at angles 55.13° and 0.18° respectively. In the second molecule of the asymmetric unit, the rings Cg(3) comprising of atoms C(15)–C(16)–C(17)–C(18)–C(19)–C(20) and Cg(4) comprising of atoms C(23)–C(24)–C(25)–C(26)–C(27)–C(28), themselves are puckered, makes a dihedral angle of 67.33° with each other and in the third molecule, the rings Cg(5) comprising of atoms C(29)–C(30)–C(31)–C(32)–C(33)–C(34) and Cg(6) comprising of atoms C(37)–C(38)–C(39)–C(40)–C(41)–C(42), both are puckered and makes a

dihedral angle of 68.25° with each other.

In each molecule of the asymmetric unit, two intramolecular and one intermolecular hydrogen-bonding interactions are seen (Figure 2.6). In first molecule of the asymmetric unit, the prominent intramolecular hydrogen-bonding interactions, viz. $N(1)-H(1A)\dots N(3)$ [$N(1)\dots N(3) = 2.6170$, $N(1)\cdots H(1A) = 0.78$, $H(1A)\dots N(3) = 2.19$, $N(1)\cdots H(1A)\dots N(3) = 115^\circ$] and $O(1)-H(1B)\dots N(3)$ [$O(1)\dots N(3) = 2.6656$, $O(1)\cdots H(1B) = 0.82$, $H(1B)\dots N(3) = 1.95$, $O(1)\cdots H(1B)\dots N(3) = 146^\circ$] leads to the formation of one five membered and one six memberd rings comprising of atoms $N(3)$, $N(2)$, $C(7)$, $N(1)$, $H(1A)N$ and $N(3)$, $C(8)$, $C(9)$, $C(14)$, $O(1)$, $H(1B)O$ respectively. Similarly, in the second and third molecules, intramolecular hydrogen-bonding interactions are $N(4)-H(4A)\dots N(6)$ [$N(4)\dots N(6) = 2.6452$, $N(4)\cdots H(4A) = 0.80$, $H(4A)\dots N(6) = 2.29$, $N(4)\cdots H(4A)\dots N(6) = 108^\circ$], $O(2)-H(2B)\dots N(6)$ [$O(2)\dots N(6) = 2.6493$, $O(2)\cdots H(2B) = 0.82$, $H(2B)\dots N(6) = 2.00$, $O(2)\cdots H(2B)\dots N(6) = 136^\circ$] and $N(7)-H(7A)\dots N(9)$ [$N(7)\dots N(9) = 2.6410$, $N(7)\cdots H(7A) = 0.72$, $H(7A)\dots N(9) = 2.29$, $N(7)\cdots H(7A)\dots N(9) = 112^\circ$], $O(3)-H(3B)\dots N(9)$ [$O(3)\dots N(9) = 2.6567$, $O(3)\cdots H(3B) = 0.82$, $H(3B)\dots N(9) = 1.96$, $O(3)\cdots H(3B)\dots N(9) = 143^\circ$] respectively. The short interatomic contact, $N(2)-H(2A)\dots S(3)$ [$N(2)\dots S(3) = 3.4524$, $N(2)\cdots H(2A) = 0.89$, $H(2A)\dots S(3) = 2.57$, $N(2)\cdots H(2A)\dots S(3) = 168^\circ$]; $N(5)-H(5A)\dots S(2)$ [$N(5)\dots S(2) = 3.4155$, $N(5)\cdots H(5A) = 0.85$, $H(5A)\dots S(2) = 2.62$, $N(5)\cdots H(5A)\dots S(2) = 157^\circ$]; $N(8)-H(8A)\dots S(1)$ [$N(8)\dots S(1) = 3.4968$, $N(8)\cdots H(8A) = 0.82$, $H(8A)\dots S(1) = 2.69$, $N(8)\cdots H(8A)\dots S(1) = 170^\circ$] respectively for the three molecules, also help to stabilize the present conformation of the thiosemicarbazone. The packing of the molecules of H_2L^3 is shown in Figure 2.7, where the unit cell is viewed along the c axis. The molecules in the unit cell are arranged in opposite manner, which are the repeating units of the packing in the crystal lattice.

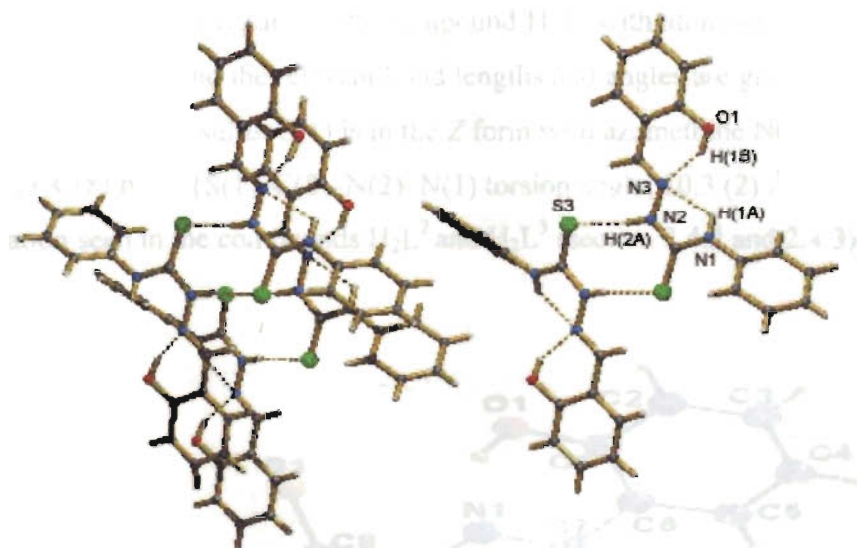


Figure 2.6. Hydrogen bonding interactions for H_2L^3

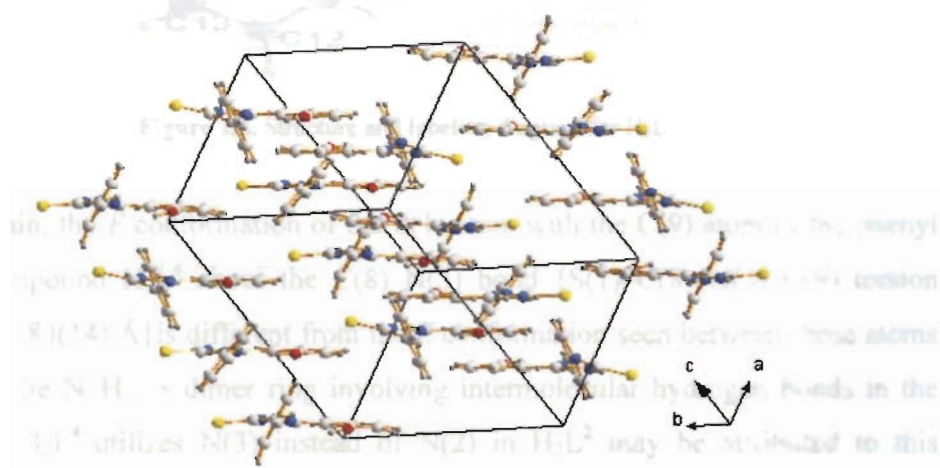


Figure 2.7. Unit cell packing diagram for H_2L^3 viewed along the c axis

2.4.4. Crystal structure of H_2L^4

The molecular structure of the compound H_2L^4 with atom numbering scheme is given in Figure 2.8 and the relevant bond lengths and angles are given in Table 2.5. In the compound H_2L^4 , sulfur S(1) is in the *Z* form with azomethine N(1) with respect to the N(2)–C(8) bond {S(1)–C(8)–N(2)–N(1) torsion angle, $10.3(2)^\circ$ }, unlike the *E* configuration seen in the compounds H_2L^2 and H_2L^3 (section 2.4.2 and 2.4.3).

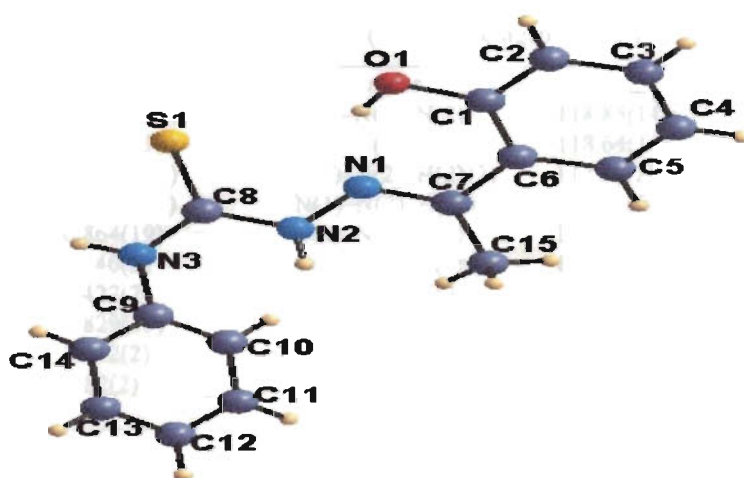


Figure 2.8. Structure and labeling diagram for H_2L^4

Again, the *E* conformation of the S(1) atom with the C(9) atom of the phenyl ring in compound H_2L^4 about the C(8)–N(3) bond {S(1)–C(8)–N(3)–C(9) torsion angle, $-179.83(14)^\circ$ } is different from the *Z* conformation seen between those atoms in H_2L^2 . The N–H...S dimer ring involving intermolecular hydrogen bonds in the compound H_2L^4 utilizes N(3) instead of N(2) in H_2L^2 may be attributed to this conformation changes. The C(8)–S(1) and C(8)–N(2) and C(8)–N(3) bond distances (Table 2.5) are close to a C–S double bond and a C–N single bond in thiosemicarbazones [19,20,21] and suggest the thione form for H_2L^4 . The C(8)–S(1)

bond length of H_2L^4 is in agreement with its di-2-pyridyl [16], 2-acetylpyridine [22] and acetophenone [23] counterparts, but less than the 1.688(2) Å value in H_2L^2 . The decrease of 0.016(3) Å for the C(8)–N(3) bond distance compared to C(8)–N(2) suggests greater double bond to the former and increased electron localization at this substituted end. This is confirmed by the somewhat typical double bond nature of N(1)–C(7) [1.289(2) Å] and considerable decrease from single bond length for N(3)–C(9) [1.422(2) Å].

Table 2.5. Selected bond lengths (Å) and bond angles (°) for the ligand (H_2L^4).

<i>Bond lengths</i>		<i>Bond angles</i>	
S(1)–C(8)	1.6659(16)	C(7)–N(1)–N(2)	118.85(14)
N(1)–C(7)	1.2905(19)	C(8)–N(2)–N(1)	118.64(14)
N(1)–N(2)	1.3736(19)	C(8)–N(2)–H(2N2)	117.2(12)
N(2)–C(8)	1.3631(19)	N(1)–N(2)–H(2N2)	119.6(12)
N(2)–H(2N2)	0.864(19)	C(8)–N(3)–C(9)	128.99(13)
N(3)–C(8)	1.346(2)	C(8)–N(3)–H(3N)	114.4(13)
N(3)–C(9)	1.422(2)	C(9)–N(3)–H(3N)	115.9(13)
N(3)–H(3N)	0.829(19)	C(1)–O(1)–H(101)	108.4(17)
O(1)–C(1)	1.352(2)	O(1)–C(1)–C(2)	116.49(19)
O(1)–H(101)	0.82(2)	O(1)–C(1)–C(6)	123.24(16)

On complexation, the coordination occurs through thiolate form and the C–S bond length increases to 1.734(3) Å and 1.754(8) Å in Sn(IV) complexes [SnMe₂(L)] and [SnBu₂(L)] respectively [7], where L is the doubly deprotonated form of compound H_2L^4 . The enolization on coordination leads to changes in the bond lengths of N(2)–C(8), N(1)–N(2) and N(3)–C(8) though the conformation of the compound H_2L^4 is retained.

The 2-hydroxyacetophenone thiosemicarbazone moiety excluding S(1) and N(3) atoms lies in a plane with a maximum deviation of 0.0726(15) Å for atom N(2). The planarity is associated with the six membered ring O(1), H(101), N(1), C(7), C(6), C(1) formation *via* the intramolecular hydrogen bond O(1)–H(101)...N(1)

[O(1)...N(1) = 2.533(2), O(1)---H(1O1) = 0.84(3), H(1O1)...N(1) = 1.80(3), O(1)---H(1O1)...N(1) = 145 (2)°] [21]. As a result, the exocyclic angles around atom C(1) and angles subtended at C(7) show considerable asymmetry. The core thiosemicarbazone moiety C(7), N(1), N(2), C(8), N(3), C(9) is in a plane, with a maximum deviation of 0.0844(14) Å for N(1) atom from the mean plane, makes a dihedral angle of 15.77(7)° with the plane comprising atoms O(1), C(1) and C(6). The phenyl substituent is twisted away from this thiosemicarbazone plane as evidenced by the C(8)–N(3)–C(9)–C(10) torsion angle of –48.3 (3)°

Two kinds of intermolecular hydrogen bonding are seen in the Figure 2.9. First, the molecules are paired using N(3)–H(1N3)...S(1)ⁱ interactions [(i) = -x, y, ½-z; N(3)...S(1) = 3.4141(18), N(3)---H(1N3) = 0.84(2), H(1N3)...S(1) = 2.60(2), N(3)–(1N3)...S(1) = 165.7(17)°] and a three-dimensional motif is formed using second intermolecular hydrogen bond C(11)–H(11)...O(1)ⁱⁱ [(ii) = x-½, y-½, z; C(11)...O(1) = 3.473(3), C(11)---H(11) = 0.93, H(11)...O(1) = 2.56, C(11)–H(11)...O(1) = 168°] with the help of the C(10)–H(10)...Cg(1)ⁱⁱⁱ interaction with Cg(1) [C(10)...Cg(1) = 3.681(2), C(10)---H(10) = 0.93, H(10)...Cg(1) = 2.83, C(10)–H(10)...Cg(1) = 152°]{Cg(1) = C(1), C(2), C(3), C(4), C(5), C(6) at (iii) ½+x, ½+y, 1+z}. The unit cell packing diagram of the molecules are seen in the Figure 2.10, where the molecules are arranged in a zig-zag manner.

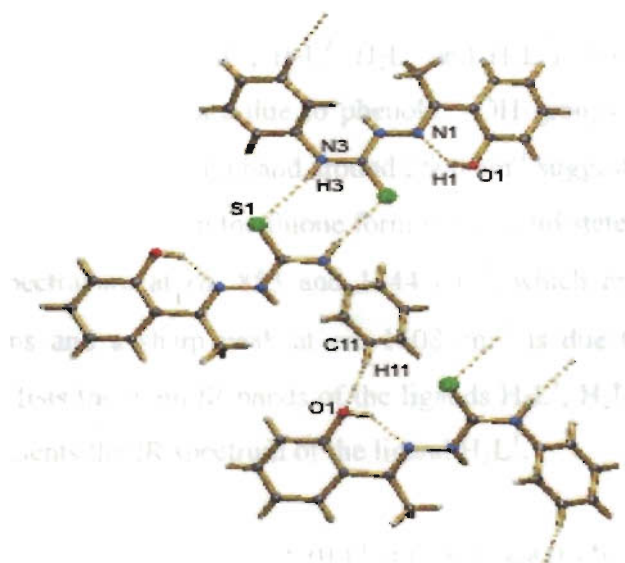


Figure 2.9. Hydrogen bonding interactions for H_2L^4

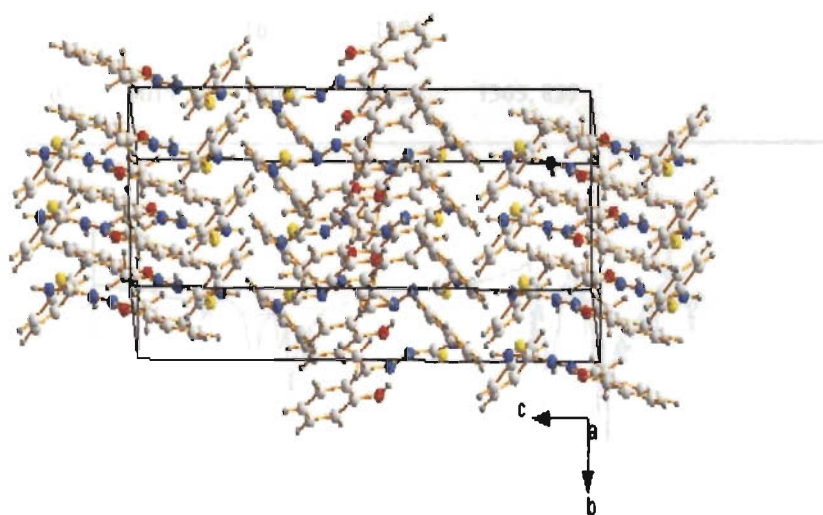


Figure 2.10. Unit cell packing diagram for H_2L^4 viewed along the a axis

2.4.5. Spectral studies

The IR spectra of H_2L (H_2L^1 , H_2L^2 , H_2L^3 and H_2L^4) show broad bands at *ca.* 3371 and 3100 cm^{-1} which are due to phenolic $-OH$ groups and $-NH$ groups respectively. The absence of $\nu(S-H)$ band around 2600 cm^{-1} suggests the existence of these thiosemicarbazone ligands in the thione form in the solid state. The other bands observed in the spectra are at *ca.* 853 and 1344 cm^{-1} , which are due to $\nu(C=S)$ stretching vibrations and a sharp peak at *ca.* 1608 cm^{-1} is due to $\nu(C=N)$ bonds [24,25]. Table 2.6 lists the main IR bands of the ligands H_2L^1 , H_2L^2 , H_2L^3 and H_2L^4 and Figure 2.11 presents the IR spectrum of the ligand H_2L^1

Table 2.6. Selected IR bands (cm^{-1}) of the ligands (H_2L^1 , H_2L^2 , H_2L^3 and H_2L^4)

Ligands	$\nu(O-H)$	$\nu(N-H)$	$\nu(C=N)$	$\nu(N-N)$	$\nu(C=S)$	$\nu(C-O)$	$\nu(C-C-O)$
H_2L^1	3402	3137	1613	1111	1328, 856	1263	1027
H_2L^2	3308	3109	1613	1111	1358, 846	1263	1045
H_2L^3	3336	3146	1613	1149	1328, 874	1255	1027
H_2L^4	3440	3011	1604	1126	1365, 837	1245	1034

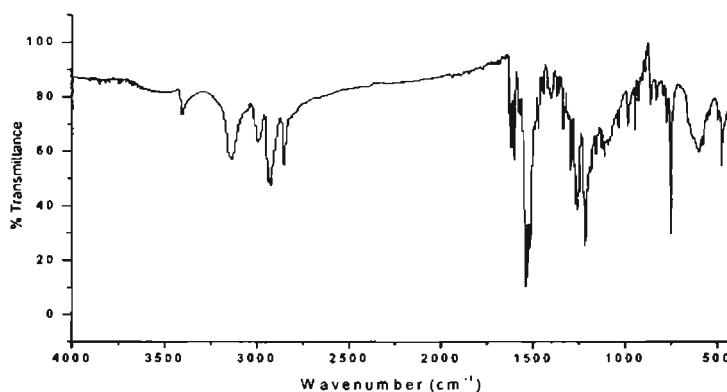
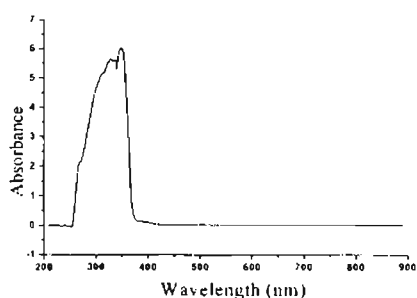


Figure 2.11. IR spectrum of the ligand H_2L^1

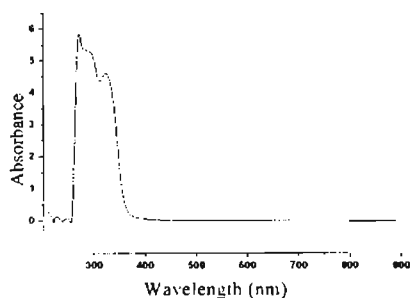
The electronic spectral data of the ligands H_2L^1 , H_2L^2 , H_2L^3 and H_2L^4 in DMF solution are presented in Table 2.7 and their representative spectra are presented in Figure 2.12. Each ligand has a ring $\pi \rightarrow \pi^*$ band of the aromatic ring are observed in the range 32000 - 38000 cm^{-1} and $n \rightarrow \pi^*$ bands associated with the azomethine linkage are observed in the range 28500 - 31500 cm^{-1} respectively [26,27].

Table 2.7. Electronic spectral assignments for the ligands

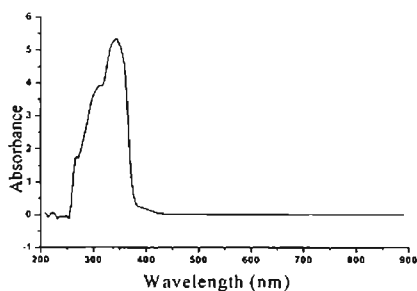
Ligands	$\pi - \pi^*$	$n - \pi^*$
H_2L^1	32150	28730
H_2L^2	36900	30860
H_2L^3	32250	29060
H_2L^4	36490	31250



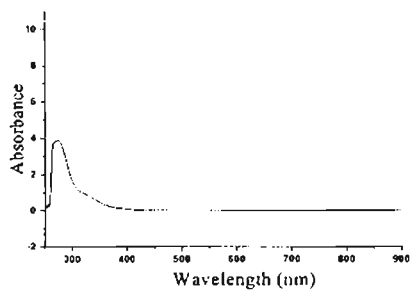
H_2L^1



H_2L^2



H_2L^3



H_2L^4

Figure 2.12. Electronic spectra of the ligands

The ^1H NMR spectrum of the ligand H_2L^3 recorded in CDCl_3 is given in Figure 2.13. This ligand has signals at $\delta = 11.36, 9.54,$ and 8.37 ppm, which are due to $-\text{OH}$, $-\text{NH}^2$ and $-\text{CH}=\text{N}^1$ respectively. The high δ values observed for $-\text{OH}$ and $-\text{NH}^2$ proton for H_2L^3 ligand is assumed to be due to hydrogen bonding interactions. The low field position of $-\text{NH}^4$ ($\delta = 7.26$ ppm) could be attributable to the deshielding caused by the phenyl group and the adjacent $-\text{N}=\text{C}<$ of the system $-\text{N}=\text{C}(\text{SH})-\text{NH}-\text{C}_6\text{H}_5$. The presence of $-\text{NH}^2$ proton signal suggests enolization of $-\text{NH}^2-\text{C}=\text{S}$ group to $-\text{N}=\text{C}-\text{SH}$, but, H_2L^3 does not show any peak attributable to $-\text{SH}$ proton. Aromatic protons appear as multiplet at $\delta = 6.84 - 7.60$ ppm range [28].

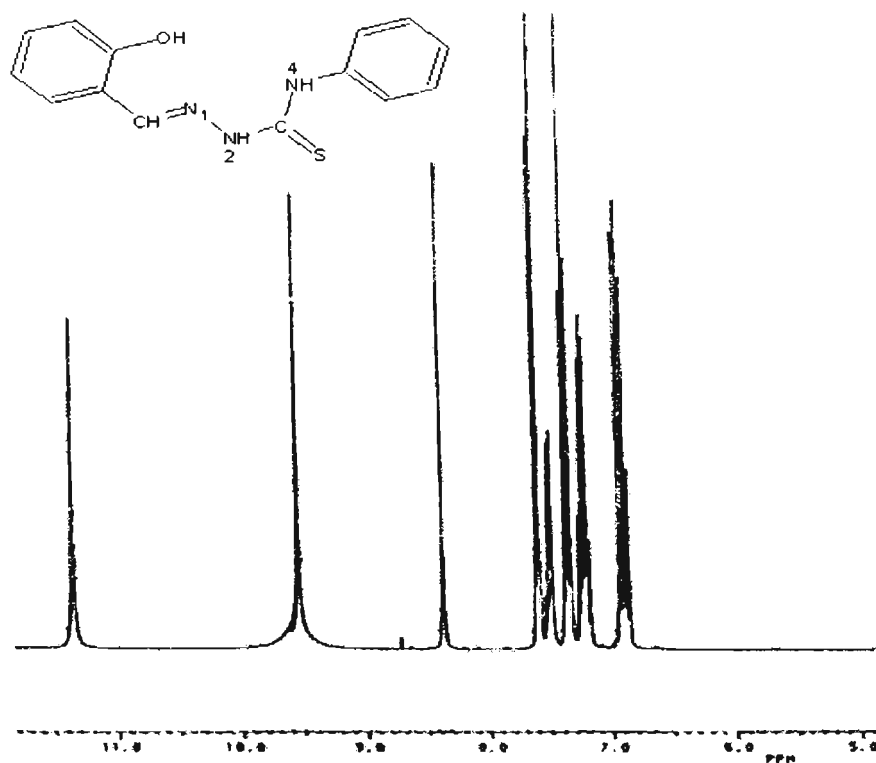
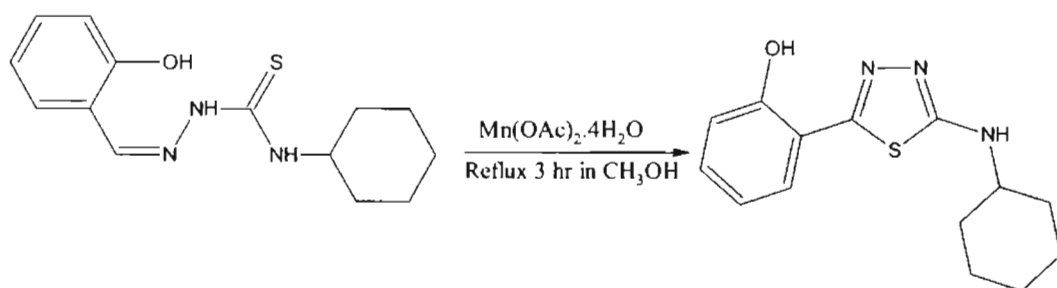


Figure 2.13. ^1H NMR spectrum of the ligand H_2L^3

2.5. Unusual isolation of the compound 2-[5-(cyclohexylamino)-1,3,4-thiadiazol-2-yl]phenol (TDZ)

The compound (TDZ) is obtained by the reaction of salicylaldehyde N(4)-cyclohexylthiosemicarbazone (1 mmol, 0.277 g) with $\text{Mn}(\text{OAc})_2 \cdot 4\text{H}_2\text{O}$ (1 mmol, 0.291 g) in methanol solution. Golden-yellow block crystals suitable for single crystal X-ray analysis were obtained from the mixture of CH_3CN and DMF solution. It is reported that thiosemicarbazones were subjected to ring closure by means of acetylating agents to obtain the corresponding 1,3,4-thiadiazolines with good yields [29]. The reaction scheme for the above compound (TDZ) is given below:



Scheme for the synthesis of 2-[5-(cyclohexylamino)-1,3,4-thiadiazol-2-yl]phenol

The structure and labeling diagram for the compound 2-[5-(cyclohexylamino)-1,3,4-thiadiazol-2-yl]phenol (TDZ) is shown in Figure 2.14. The compound (TDZ) crystallizes with monoclinic crystal system with a space group $P2_1/c$. A crystal having dimensions 0.33 x 0.26 x 0.21 mm was sealed in a glass capillary. The X-ray diffraction data were measured at 293(2) K, data acquisition and cell refinement were done using the Argus (Nonius, MACH3 software) [11]. The Maxus software package (Nonius) was used for data reduction [12]. The structure was solved by direct methods and full-matrix least-squares refinement using SHELXL-97 [13] package. The positions of all the non-hydrogen atoms were

included in the full-matrix least-squares refinement using SHELXL-97 program and all the hydrogen atoms were fixed in calculated positions. The structure of the compound TDZ were plotted using the program Diamond Version 3.0 [10] and PLATON [11].

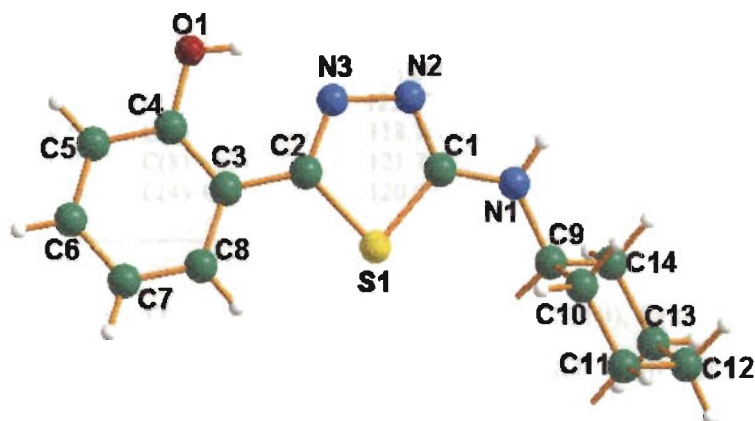


Figure 2.14. Structure and labeling diagram for TDZ

According to the crystal structure, the compound exist in the *E* configuration with respect to the C(2)–N(3) and C(1)–N(2) bonds. This is confirmed by the torsion angles of 179.76° and 178.24° respectively for C(3)–C(2)–N(3)–N(2) and N(1)–C(1)–N(2)–N(3) moieties [30]. In the thiadiazoline ring, S(1)–C(1)–N(2)–N(3)–C(2), the observed bond lengths are C(1)–S(1) [1.7431(17) Å], C(2)–S(1) [1.7369(17) Å], C(1)–N(2) [1.313(2) Å], C(2)–N(3) [1.298(2) Å] and N(2)–N(3) [1.376(2) Å]. The C(1)–S(1) and C(2)–S(1) bond lengths are closer to C–S single bond length [1.81 Å] than to C=S double bond length [1.60 Å] [16]. However, the C(1)–N(2) and C(2)–N(3) bond distances are closer to C=N double bond distance [1.28 Å]. The N(2)–N(3) bond distance is closer to N–N single bond length [N–N, 1.45 Å] [18]. This supports the ring consisting of atoms S(1)–C(1)–N(2)–N(3)–C(2)

is thiadiazoline. The selected bond lengths and bond angles are presented in Table 2.8.

Table 2.8. Selected bond lengths (Å) and bond angles (°) for TDZ.

<i>Bond lengths</i>		<i>Bond angles</i>		<i>Bond angles</i>	
C(1)–N(2)	1.313(2)	N(2)–C(1)–N(1)	122.97(16)	O(1)–C(4)–C(5)	117.94(17)
C(1)–N(1)	1.334(2)	N(2)–C(1)–S(1)	113.91(13)	O(1)–C(4)–C(3)	122.12(16)
C(1)–S(1)	1.7431(17)	N(1)–C(1)–S(1)	123.10(13)	C(1)–N(1)–C(9)	125.20(15)
C(2)–N(3)	1.298(2)	N(3)–C(2)–C(3)	123.54(15)	C(1)–N(1)–H(1N)	115.5(14)
C(2)–C(3)	1.461(2)	N(3)–C(2)–S(1)	113.09(13)	C(9)–N(1)–H(1N)	117.3(14)
C(2)–S(1)	1.7369(17)	C(3)–C(2)–S(1)	123.37(12)	C(1)–N(2)–N(3)	111.52(14)
N(2)–N(3)	1.376(2)	C(8)–C(3)–C(4)	118.16(16)	C(2)–N(3)–N(2)	114.48(14)
C(3)–C(4)	1.399(2)	C(8)–C(3)–C(2)	121.74(16)	C(4)–O(1)–H(1)	109.5
C(4)–O(1)	1.353(2)	C(4)–C(3)–C(2)	120.09(15)	C(2)–S(1)–C(1)	86.98(8)

The cyclohexyl ring Cg(3) consists of atoms C(9), C(10), C(11), C(12), C(13), C(14), itself is puckered, makes a dihedral angle of 64.04° with the neighbouring thiadiazoline ring S(1), C(1), N(2), N(3), C(2). The ring puckering analysis and least square calculations show that the cyclohexyl ring is in chair conformation ($Q_T = 0.5621$ Å) with the equatorial substitution at C(9) for N(1). One intra and one intermolecular hydrogen bonding interactions are observed in the case of this compound TDZ (Figure 2.15). Intramolecular hydrogen bonding interactions, viz. O(1)–H(1)...N(3) [O(1)...N(3) = 2.6223, O(1)---H(1) = 0.82, H(1)...N(3) = 1.89, O(1)---H(1)...N(3) = 148°] leads to the formation of six membered ring comprising of atoms O(1), C(4), C(3), C(2), N(3) and H(1)O and intermolecular hydrogen bonding interactions are between N(1)–H(1N) and N(2) [N(1)...N(2) = 2.9672, N(1)---H(1N) = 0.85, H(1N)...N(2) = 2.12, N(1)---H(1N)...N(2) = 175°]. The unit cell packing diagram for the compound (TDZ) viewed along the *a* axis is shown in Figure 2.16.

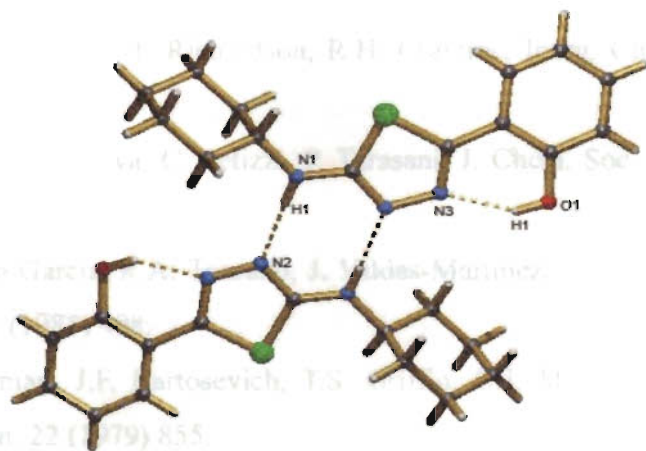


Figure 2.15. Hydrogen bonding interactions for TDZ

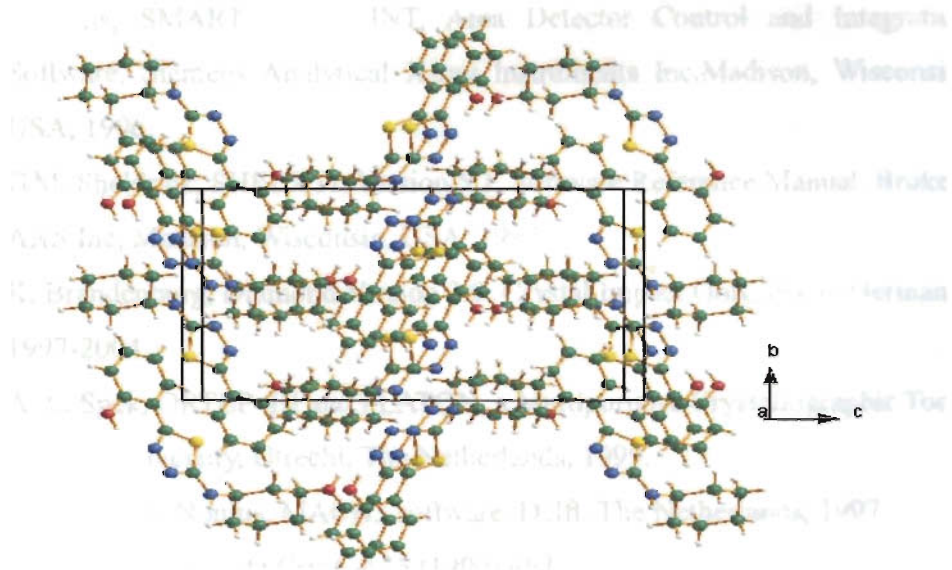


Figure 2.16. Unit cell packing diagram for H_2L^4 viewed along the a axis

References

1. D.X. West, S.B. Padhye, P.B. Sonawane, R.C. Chikate, *Asian J.Chem.Rev.* 1 (1990) 125.
2. D.E. Barber, Z. Lu, T. Richardson, R.H. Crabtree, *Inorg. Chem.* 31 (1992) 4709.
3. M.B. Ferrari, G. Fava, C. Pelizzi, P. Tarasani, *J. Chem. Soc., Dalton Trans.* (1992) 2153.
4. M. Soriano-Garcia, R.A. Toscano, J. Valdes-Martinez, J.M. Fernandez, *Acta Cryst.* C41 (1985) 498.
5. D.L. Klayman, J.F. Bartosevich, T.S. Griffin, C.J. Mason, J.P. Scovill, *J. Med. Chem.* 22 (1979) 855.
6. P. Bindu, M.R.P. Kurup, *Trans. Met. Chem.* 22 (1997) 578.
7. G. F. de Sousa, R. H. P. Francisco, M. T. P. Gambardella, R. H. de A. Santos, A. Abras, *J. Braz. Chem. Soc.* 12 (2001) 722.
8. Siemens, SMART and SAINT, Area Detector Control and Integration Software, Siemens Analytical X-ray Instruments Inc. Madison, Wisconsin, USA, 1996.
9. G.M. Sheldrick, SHELXTL Version 5.1, Software Reference Manual, Bruker AXS Inc, Madison, Wisconsin, USA, 1997.
10. K. Brandenburg, Diamond Version 3.0, Crystal Impact GbR, Bonn, Germany, 1997-2004.
11. A. L. Spek, ORTEP-III and PLATON, a Multipurpose Crystallographic Tool, Utrecht University, Utrecht, The Netherlands, 1999.
12. B.V. Nonius, Nonius, MACH3 software, Delft, The Netherlands, 1997.
13. G.M. Sheldrick, *Acta Cryst.* A46 (1990) 467.

14. G.M. Sheldrick, SHELXL97 and SHELXS97, University of Gottingen, Germany, 1997.
15. D. Chattopadhyay, T. Banerjee, S. K. Mazumdar, S. Ghosh, R. Kuroda, *Acta Cryst. C* 43 (1987) 974.
16. V. Suni, M.R.P. Kurup, M. Nethaji, *Spectrochim. Acta* 63A (2006) 174.
17. M. Joseph, V. Suni, C.R. Nayar, M.R.P. Kurup, H.-K. Fun, *J. Mol. Struct.* 705 (2004) 63.
18. G.J. Palenik, D.F. Rendle, W.S. Carter, *Acta Cryst. B* 30 (1974) 2390.
19. E.B. Seena, B.N. Bessy Raj, M.R.P. Kurup, E. Suresh, *J. Chem. Cryst.* (2006), in press.
20. A. Usman, I.A. Razak, S. Chantrapromma, H.-K. Fun, V. Philip, A. Sreekanth, M.R.P. Kurup, *Acta Cryst. C* 68 (2002) o652.
21. L. Latheef, E. Manoj, M.R.P. Kurup, *Acta Cryst. C* 62 (2006) o16.
22. E. Bermejo, A. Castineiras, R. Dominguez, R. Carballo, C. Maichle-Mossmer, J. Strahle, D.X. West, *Z. Anorg. Allg. Chem.* 625 (1999) 961.
23. F. Jian, Y. Li, H. Xiao, *Acta Cryst. E* 61 (2005) o2219.
24. S.K. Jain, B.S. Garg, Y.K. Bhoon, D.L. Klayman, J.P. Scovill, *Spectrochim. Acta* 41A (1985) 407.
25. R.M. Silverstein, G.C. Bassler, T.C. Morrill, *Spectrometric Identification of Organic Compounds*, 4th edn, Wiley, New York, 1981.
26. R.P. John, A. Sreekanth, M.R.P. Kurup, A. Usman, A.R. Ibrahim, H.-K. Fun, *Spectrochim. Acta* 59A (2003) 1349.
27. D.X. West, I.S. Billeh, J.P. Jasinski, J.M. Jasinski, R.J. Butcher, *Trans. Met. Chem.* 23 (1998) 209.
28. P. Bindu, M.R.P. Kurup, *Indian J. Chem.* 36A (1997) 1094.

29. M.A. Martins Alho, A.G. Moglioni, B. Brousse, G.Y. Moltrasio, N.B. D'Accorso, *ARKIVOC*, 1 (2000) 627.
30. Y. Nagao, T. Hirata, S. Goto, S. Sano, A. Kakehi, K. Iizuka, M. Shiro, *J. Am. Chem. Soc.* 120 (1998) 3104.

CHAPTER 3

**SYNTHESIS, SPECTRAL AND STRUCTURAL STUDIES OF Cu(II)
COMPLEXES OF N(4)-SUBSTITUTED THIOSEMICARBAZONES
OF SALICYLALDEHYDE AND 2-HYDROXYACETOPHENONE**

3.1. Introduction

The growing interest in copper complexes of thiosemicarbazone ligands containing phenolic group is due to the presence of such moieties in a number of mono- and binuclear copper proteins. In recent years, a number of binuclear and to a lesser extent mononuclear copper complexes containing the phenolate ion have been investigated as models of copper proteins.

Copper forms a variety of octahedral, square planar, square pyramidal and trigonal bipyramidal complexes with thiosemicarbazones [1]. Copper generally shows the +1 and +2 oxidation states. The +2 oxidation state is the most common one. Copper forms mononuclear as well as binuclear complexes with thiosemicarbazones. Binuclear copper(II) complexes display interesting and varied magnetic behaviour. Copper(II) shows the $3d^9$ configuration. Because of the presence of one unpaired electron in the d orbital, all the copper(II) complexes are paramagnetic.

This chapter describes the synthesis and characterization of mononuclear and binuclear Cu(II) complexes with different N(4)-substituted ONS donor ligands. It also reports single crystal X-ray diffraction studies of two of the synthesized complexes.

3.2. Experimental

3.2.1. Materials

The reagents used for the synthesis of the thiosemicarbazone ligands were discussed in Chapter 2 and were purified by standard methods and solvents were

purified by distillation. 2,2'-Bipyridine (bipy) (Central drug house chemicals), 1,10-phenanthroline (phen) (Ranboxy fine chemicals) and 4,4'-dimethyl 2,2'-bipyridine (dmbipy) (Sigma Aldrich), Cu(OAc)₂·H₂O (Fluka), CuCl₂·2H₂O (E-Merck), CuBr₂ (Sigma Aldrich) and Cu(NO₃)₂·3H₂O (S.D.fine-chemicals Ltd) were used as received.

3.2.2. Synthesis of the complexes

[(CuL¹)₂] (1)

This complex was synthesized by refluxing an ethanolic solution of H₂L¹ (1 mmol, 0.277 g) with an aqueous solution of Cu(OAc)₂·H₂O (1 mmol, 0.199 g) for 4 h. The complex formed was filtered, washed with ethanol and finally with ether and dried over P₄O₁₀ *in vacuo*.

[CuL¹dmbipy] (2)

This complex was synthesized by refluxing an ethanolic solution of H₂L¹ (1 mmol, 0.277 g) and heterocyclic base dmbipy (1 mmol, 0.184 g) with an aqueous solution of Cu(OAc)₂·H₂O (1 mmol, 0.199 g) for 4 h. The complex formed was filtered, washed with ethanol and finally with ether and dried over P₄O₁₀ *in vacuo*.

[(CuL²)₂] (3)

This complex was synthesized by refluxing an ethanolic solution of H₂L² (1 mmol, 0.291 g) with an aqueous solution of Cu(OAc)₂·H₂O (1 mmol, 0.199 g) for 4 h. The complex formed was filtered, washed with ethanol and finally with ether and dried over P₄O₁₀ *in vacuo*.

[CuL²dmbipy] (4)

This complex was synthesized by refluxing an ethanolic solution of H₂L² (1 mmol, 0.291 g) and heterocyclic base dmbipy (1 mmol, 0.184 g) with an aqueous solution of Cu(OAc)₂·H₂O (1 mmol, 0.199 g) for 4 h. The complex formed was filtered, washed with ethanol and finally with ether and dried over P₄O₁₀ *in vacuo*.

$[\text{Cu}(\text{HL}^2)\text{Cl}] \cdot 2\text{H}_2\text{O}$ (5)

This complex was synthesized by refluxing an ethanolic solution of H_2L^2 (0.250 g) with an aqueous solution of $\text{CuCl}_2 \cdot 2\text{H}_2\text{O}$ (0.250 g) for 4 h. The complex formed was filtered, washed with ethanol and finally with ether and dried over P_4O_{10} *in vacuo*.

 $[\text{Cu}(\text{HL}^2)\text{Br}] \cdot 4\text{H}_2\text{O}$ (6)

This complex was synthesized by refluxing an ethanolic solution of H_2L^2 (0.50 g) with an aqueous solution of CuBr_2 (0.50 g) for 4 h. The complex formed was filtered, washed with ethanol and finally with ether and dried over P_4O_{10} *in vacuo*.

 $[\text{Cu}(\text{HL}^2)\text{NO}_3] \cdot \text{C}_2\text{H}_5\text{OH}(\text{H}_2\text{O})$ (7)

This complex was synthesized by refluxing an ethanolic solution of H_2L^2 (0.50 g) with an aqueous solution of $\text{Cu}(\text{NO}_3)_2 \cdot \text{H}_2\text{O}$ (0.50 g) for 4 h. The complex formed was filtered, washed with ethanol and finally with ether and dried over P_4O_{10} *in vacuo*.

 $[(\text{CuL}^3)_2] \cdot \frac{1}{2}\text{H}_2\text{O}$ (8)

This complex was synthesized by refluxing an ethanolic solution of H_2L^3 (1 mmol, 0.271 g) with an aqueous solution of $\text{Cu}(\text{OAc})_2 \cdot \text{H}_2\text{O}$ (1 mmol, 0.199 g) for 4 h. The complex formed was filtered, washed with ethanol and finally with ether and dried over P_4O_{10} *in vacuo*.

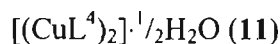
 $[\text{Cu}(\text{HL}^3)_2] \cdot \text{H}_2\text{O}$ (9)

This complex was synthesized by refluxing an ethanolic solution of H_2L^3 (2 mmol, 0.542 g) with an aqueous solution of $\text{Cu}(\text{OAc})_2 \cdot \text{H}_2\text{O}$ (1 mmol, 0.199 g) for 4 h. The complex formed was filtered, washed with ethanol and finally with ether and dried over P_4O_{10} *in vacuo*.

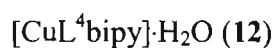
 $[\text{CuL}^3\text{dmbipy}] \cdot \text{H}_2\text{O}$ (10)

This complex was synthesized by refluxing an ethanolic solution of H_2L^3

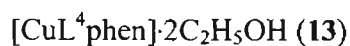
(1 mmol, 0.271 g) and heterocyclic base dmbipy (1 mmol, 0.184 g) with an aqueous solution of $\text{Cu}(\text{OAc})_2 \cdot \text{H}_2\text{O}$ (1 mmol, 0.199 g) for 4 h. The complex formed was filtered, washed with ethanol and finally with ether and dried over P_4O_{10} *in vacuo*.



This complex was synthesized by refluxing an ethanolic solution of H_2L^4 (1 mmol, 0.285 g) with an aqueous solution of $\text{Cu}(\text{OAc})_2 \cdot \text{H}_2\text{O}$ (1 mmol, 0.199 g) for 4 h. The complex formed was filtered, washed with ethanol and finally with ether and dried over P_4O_{10} *in vacuo*.



This complex was synthesized by refluxing an ethanolic solution of H_2L^4 (1 mmol, 0.285 g) and heterocyclic base bipy (1 mmol, 0.156 g) with an aqueous solution of $\text{Cu}(\text{OAc})_2 \cdot \text{H}_2\text{O}$ (1 mmol, 0.199 g) for 4 h. The complex formed was filtered, washed with ethanol and finally with ether and dried over P_4O_{10} *in vacuo*.



This complex was synthesized by refluxing an ethanolic solution of H_2L^4 (1 mmol, 0.285 g) and heterocyclic base phen (1 mmol, 0.198 g) with an aqueous solution of $\text{Cu}(\text{OAc})_2 \cdot \text{H}_2\text{O}$ (1 mmol, 0.199 g) for 4 h. The complex formed was filtered, washed with ethanol and finally with ether and dried over P_4O_{10} *in vacuo*.



This complex was synthesized by refluxing an ethanolic solution of H_2L^4 (1 mmol, 0.285 g) and heterocyclic base dmbipy (1 mmol, 0.184 g) with an aqueous solution of $\text{Cu}(\text{OAc})_2 \cdot \text{H}_2\text{O}$ (1 mmol, 0.199 g) for 4 h. The complex formed was filtered, washed with ethanol and finally with ether and dried over P_4O_{10} *in vacuo*.

3.2.3. X-Ray crystallography

A dark green crystal of the compound **2** and a brown block crystal of the compound **3** having approximate dimensions of 0.32 x 0.30 x 0.30 and 0.35 x 0.30 x 0.30 mm respectively were sealed in glass capillaries. The crystallographic data and

structure refinement parameters for the complexes **2** and **3** at 293(2) K are given in Table 3.1.

Table 3.1. Crystal Data and Structure refinement parameters for [CuL¹dmbipy] (**2**) and [(CuL²)₂] (**3**).

	(2)	(3)
Empirical formula	C ₂₆ H ₂₉ Cu N ₅ O S	C ₆₀ H ₇₆ Cu ₄ N ₁₂ O ₄ S ₄
Formula weight	523.14	1411.73
Temperature	293(2) K	293(2) K
Wavelength	0.71073 Å	0.71073 Å
Crystal system	Monoclinic	Triclinic
Space group	C2/c	P $\bar{1}$
Unit cell dimensions	a = 25.6690(19) Å b = 14.4860(8) Å c = 15.6400(10) Å $\alpha = 90^\circ$ $\beta = 95.678(6)^\circ$ $\gamma = 90^\circ$	a = 13.0420(14) Å b = 14.182(3) Å c = 18.865(2) Å $\alpha = 103.689(12)^\circ$ $\beta = 107.098(10)^\circ$ $\gamma = 96.896(13)^\circ$
Volume	5787.1(7) Å ³	3172.1(9) Å ³
Z	8	2
Density (calculated)	1.201 Mg/ m ³	1.478 Mg/ m ³
Absorption coefficient	0.851 mm ⁻¹	1.510 mm ⁻¹
F(000)	2184	1464
Crystal size	0.35 x 0.30 x 0.30 mm	0.35 x 0.30 x 0.30 mm
θ range for data collection	2.03 to 24.98°	1.51 to 24.99°
Index ranges	0 ≤ h ≤ 30, 0 ≤ k ≤ 17, -18 ≤ l ≤ 18	-15 ≤ h ≤ 15, -16 ≤ k ≤ 0, -21 ≤ l ≤ 22
Reflections collected	5160	11599
Independent reflections	5041 [R(int) = 0.0361]	11109 [R(int) = 0.0464]
Refinement method	Full-matrix least-squares on F ²	Full-matrix least-squares on F ²
Data / restraints / parameters	5041 / 0 / 313	11109 / 0 / 769
Goodness-of-fit on F ²	0.981	1.013
Final R indices [I > 2σ(I)]	R ₁ = 0.0586, wR ₂ = 0.1291	R ₁ = 0.0602, wR ₂ = 0.1301
R indices (all data)	R ₁ = 0.1830, wR ₂ = 0.1619	R ₁ = 0.1997, wR ₂ = 0.1704
Largest diff. peak and hole	0.401 and -0.320 e.Å ⁻³	0.677 and -0.514 e.Å ⁻³

The X-ray diffraction data for the two compounds were measured at 293(2) K, data acquisition and cell refinement were done using the Argus (Nonius, MACH3 software) [2]. The Maxus software package (Nonius) was used for data reduction [3].

The structure was solved by direct methods and full-matrix least-squares refinement using SHELX97 [4] package. The positions of all the non-hydrogen atoms were included in the full-matrix least-squares refinement using SHELX97 program and all the hydrogen atoms were fixed in calculated positions for compounds **2** and **3**. The structures of the compounds **2** and **3** were plotted using the program Diamond Version 3.0 [5] and PLATON [6].

3.3. Results and discussion

3.3.1. Physical measurements

The complexes **1**, **3**, **8** and **11** were readily formed by refluxing their respective ligands and $\text{Cu}(\text{OAc})_2 \cdot \text{H}_2\text{O}$ in 1:1 ratio and the complex **9** in 2:1 ratio. The complexes **2**, **4**, **10**, **12**, **13** and **14** were prepared by using their respective ligands, polypyridyl bases like bipy, phen or dmbipy and $\text{Cu}(\text{OAc})_2 \cdot \text{H}_2\text{O}$ in 1:1:1 ratio. The complexes **5**, **6** and **7** were prepared by refluxing equal grams of the ligand H_2L^2 with $\text{CuX}_2 \cdot n\text{H}_2\text{O}$ [$\text{X} = \text{Cl}$, Br and NO_3 respectively] for the compounds **5**, **6** and **7**.

After double deprotonation, thiosemicarbazones coordinate as tridentate ligands in the thiolate form (L^{2-}) in majority of the complexes, except in complexes **5**, **6**, **7** and **9**. In complexes **5**, **6**, **7** and **9**, the ligands were coordinated as monoanionic (HL^-) forms. The elemental analyses of the complexes are in agreement with the general formula $[(\text{ML})_2]$ (for complexes **1**, **3**, **8** and **11**); $[\text{MLB}]$ (for complexes **2**, **4**, **10**, **12**, **13** and **14**); $[\text{M}(\text{HL})\text{X}]$ (for complexes **5**, **6** and **7**) and $[\text{M}(\text{HL})_2]$ (for complex **9**). X-Ray quality single crystals of the compound **2** were obtained by slow evaporation of its ethanol solution over a period of 7 days and single crystals for the compound **3** were obtained by slow evaporation of its solution in $\text{CH}_3\text{CN} / \text{CH}_2\text{Cl}_2$ mixture over a period of 2 weeks. The colors, partial elemental analyses and magnetic moments of the complexes are presented in Table 3.2.

Table 3.2. Analytical data

Compound	Color	Found (Calculated) %			μ (B.M.)
		C	H	N	
$[(CuL^1)_2]$ (1)	Brown	49.43(49.61)	5.23(5.06)	12.22(12.40)	1.25
$[CuL^1dmbipy]$ (2)	Green	60.57(59.69)	6.12(5.59)	12.72(13.39)	1.82
$[(CuL^2)_2]$ (3)	Brown	51.09(51.05)	5.39(5.43)	11.80(11.91)	1.15
$[CuL^2dmbipy] \cdot \frac{1}{2}H_2O$ (4)	Green	59.23(59.37)	5.88(5.91)	12.95(12.82)	1.56
$[Cu(HL^2)Cl] \cdot 2H_2O$ (5)	Green	42.03(42.35)	6.00(5.69)	9.37 (9.88)	1.68
$[Cu(HL^2)Br] \cdot 4H_2O$ (6)	Brown	36.15(35.61)	5.43(5.58)	8.44 (8.31)	1.51
$[Cu(HL^2)NO_3] \cdot C_2H_5OH(H_2O)$ (7)	Green	42.07(42.53)	5.69(5.88)	11.69(11.67)	1.64
$[(CuL^3)_2] \cdot \frac{1}{2}H_2O$ (8)	Brown	49.80(50.36)	3.32(3.62)	13.06(12.59)	1.24
$[Cu(HL^3)_2] \cdot H_2O$ (9)	Brown	54.54(54.05)	4.20(4.21)	13.50(13.51)	1.51
$[CuL^3dmbipy] \cdot H_2O$ (10)	Brown	58.08(58.36)	4.79(4.71)	12.98(13.09)	1.72
$[(CuL^4)_2] \cdot \frac{1}{2}H_2O$ (11)	Brown	51.46(51.27)	4.00(3.87)	11.73(11.96)	1.39
$[CuL^4bipy] \cdot H_2O$ (12)	Brown	57.20(57.62)	4.28(4.45)	13.26(13.44)	1.77
$[CuL^4phen] \cdot 2C_2H_5OH$ (13)	Green	59.83(60.13)	5.07(5.37)	11.90(11.31)	1.82
$[CuL^4dmbipy] \cdot 3H_2O$ (14)	Brown	55.02(55.42)	4.62(5.34)	12.34(11.97)	1.91

Magnetic moments of the complexes were calculated from magnetic susceptibility measurements using diamagnetic corrections. Mononuclear Cu(II) complexes exhibit magnetic moments in the range 1.5-1.9 B.M., which are close to the spin-only value [7]. The magnetic moments of the binuclear Cu(II) complexes (1, 3, 8 and 11) were found to be in the range 1.15-1.40 B.M. This low magnetic moment may be attributed to the presence of a strong antiferromagnetic spin-spin interaction involving an oxygen-bridged binuclear structure similar to those proposed for the Cu(II) complexes of analogous tridentate ligands [8].

3.3.2. Crystal structure of the compound [CuL¹dmbipy] (2)

The molecular structure of the compound **2** along with atom numbering scheme is given in Figure 3.1 and selected bond lengths and bond angles are summarized in Table 3.3. Compound **2** crystallizes in the monoclinic space group *C2/c*. The copper atom in [CuL¹dmbipy] (**2**) is coordinated by phenolato oxygen, O(1), azomethine nitrogen, N(1), thiolato sulfur, S(1) of the thiosemicarbazone and the pyridine nitrogens, N(4) and N(5) of bipyridine derivative and is having an approximately trigonal bipyramidal geometry in which the equatorial positions are occupied by S(1), O(1) and N(5) and the axial positions by N(1) and N(4) [Cu(1)–N(1), 1.951(4) Å, Cu(1)–N(4), 2.016(4) Å] with the N(1)–Cu(1)–N(4) angle of 177.94(16)° being close to the ‘ideal’ value of 180° which is usual for such systems.

In a five-coordinate system, the angular structural parameter (τ) is used to propose an index of trigonality. The value of τ is defined by an equation represented by $\tau = (\beta - \alpha)/60$, where β is the greatest basal angle and α is the second greatest angle; τ is 0 for rectangular pyramidal forms and 1 for trigonal bipyramidal forms [9,10]. However, in the case of five-coordinate systems, the structure varies from near regular trigonal bipyramidal (RTB) to near square based pyramidal (SBP). The value of τ for the compound **2** is 0.35, indicates that the coordination geometry around Cu(II) is best described as trigonal bipyramidal distorted square based pyramidal (TBDSBP) [11] with copper displaced 0.2174 Å above the N(1), N(4), S(1) and O(1) coordination plane and towards the elongated apical N(5) atom, at a larger distance of 2.226(5) Å. This value is larger than the normal Cu–N bond lengths reported [12,13]. One of the reasons for the deviation from an ideal stereochemistry is the restricted bite angle imposed by both the L²⁻ and dmbipy ligands. The bite angle around the metal viz, N(4)–Cu(1)–N(5) of 77.23(18)° may be

considered normal, when compared with an average value of 77° cited in the literature [14,15]. The O(1)–Cu(1)–N(5) bond angle, $96.36(16)$, and S(1)–Cu(1)–N(5) bond angle, $106.84(12)$, indicate a slight tilting of the apical Cu(1)–N(5) bond in the direction of the O(1)–Cu(1) bond and away from S(1)–Cu(1) bond. The dihedral angle formed by the least square planes Cg(4) and Cg(5) is 6.13° for the compound **2**. Ring puckering analyses and least-square plane calculations show that the Cg(3) ring comprising of atoms Cu(1), O(1), C(1), C(6), C(7) and N(1) adopts a screw-boat conformation and Cg(7) ring comprising of atoms C(9), C(10), C(11), C(12), C(13) and C(14) adopts a chair conformation.

Table 3.3. Selected bond lengths (Å) and bond angles ($^\circ$) for [CuL¹dmbipy]

<i>Bond lengths</i>			
Cu(1)–N(1)	1.951(4)	Cu(1)–S(1)	2.272(15)
O(1)–C(1)	1.301(6)	Cu(1)–N(4)	2.016(4)
N(1)–N(2)	1.387(5)	Cu(1)–O(1)	1.965(3)
N(4)–C(15)	1.330(7)	N(3)–C(8)	1.343(7)
N(5)–C(26)	1.315(8)	S(1)–C(8)	1.732(6)
Cu(1)–N(5)	2.226(5)	N(1)–C(7)	1.291(6)
N(2)–C(8)	1.325(6)	N(3)–C(9)	1.467(7)
<i>Bond angles</i>			
N(1)–Cu(1)–O(1)	92.28(16)	O(1)–Cu(1)–N(4)	89.94(15)
O(1)–Cu(1)–N(5)	96.36(16)	N(1)–Cu(1)–S(1)	84.88(13)
N(4)–Cu(1)–S(1)	93.41(12)	C(8)–S(1)–Cu(1)	94.53(19)
C(7)–N(1)–N(2)	113.5(4)	N(2)–N(1)–Cu(1)	122.3(3)
C(8)–N(3)–C(9)	124.2(5)	C(15)–N(4)–Cu(1)	124.5(4)
C(26)–N(5)–C(21)	117.5(5)	C(21)–N(5)–Cu(1)	112.5(4)
O(1)–C(1)–C(6)	124.0(5)	N(2)–C(8)–S(1)	125.6(4)
N(3)–C(9)–C(14)	109.9(5)	N(1)–Cu(1)–N(4)	177.94(16)
N(1)–Cu(1)–N(5)	102.14(18)	N(4)–Cu(1)–N(5)	77.23(18)
O(1)–Cu(1)–S(1)	156.71(12)	N(5)–Cu(1)–S(1)	106.84(12)
C(1)–O(1)–Cu(1)	125.6(3)	C(7)–N(1)–Cu(1)	124.0(4)
C(8)–N(2)–N(1)	112.2(4)	C(15)–N(4)–C(20)	116.4(4)
C(20)–N(4)–Cu(1)	119.1(4)	C(26)–N(5)–Cu(1)	130.1(4)
O(1)–C(1)–C(2)	119.6(5)	N(1)–C(7)–C(6)	126.3(5)
N(3)–C(8)–S(1)	117.4(4)	N(3)–C(9)–C(10)	111.1(6)

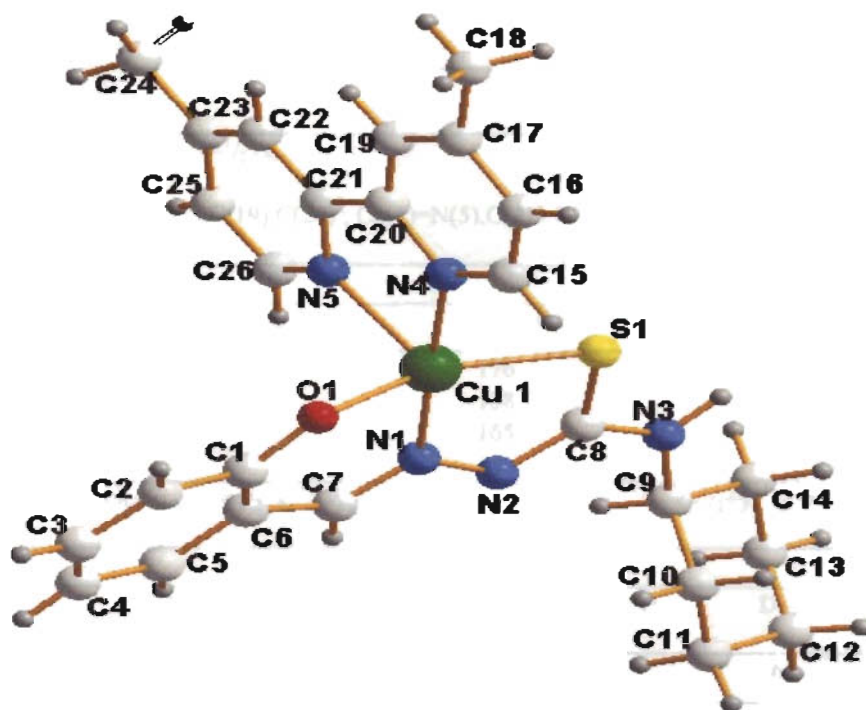


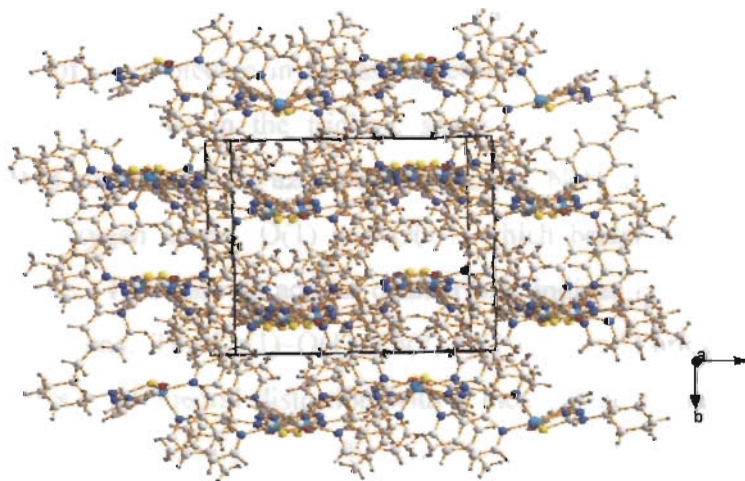
Figure 3.1. Structure and labeling scheme for $[\text{CuL}^1 \text{dmbipy}] (2)$

Figure 3.2 shows the contents of the unit cell along the a axis. The assemblage of molecules in the respective manner in the unit cell is resulted by the H-bonding, π - π and CH- π interactions as depicted in Table 3.4. The centroid Cg(4) is involved in π - π interaction with pyridyl ring of the neighbouring unit at the distance of 3.7197 Å, the CH- π interactions of the rings Cg(6) and Cg(1) with the neighbouring molecules and also intermolecular hydrogen bonding interactions between N(3)-H(3N) and S(1) contribute stability to the unit cell packing (Figure 3.3).

Table 3.4. Interaction parameters of the compound [CuL¹dmbipy]

π---π interactions				
Cg(I)-Res(1)---Cg(J)	Cg-Cg(Å)	α °	β °	
Cg(4) [1] -> Cg(5) ^a	3.7197	6.13	22.51	
Equivalent position codes : $a = 1/2-x, 1/2-y, -z$				
Cg(4)=N(4),C(15),C(16),C(17),C(19),C(20) ; Cg(5)=N(5),C(21),C(22),C(23),C(25),C(26)				
CH---π interactions				
XH(I)---Cg(J)	H..Cg(Å)	X-H..Cg (°)	X..Cg(Å)	
C(18)-H(18)[1] -> Cg(6) ^b	2.90	176	3.8605	
C(18)-H(18) [1] ->Cg(1) ^c	2.96	138	3.7250	
C(25)-H(25) [1] ->Cg(6) ^d	2.97	165	3.8788	
Equivalent position codes : $b = 1/2-x, 1/2-y, -z$; $c = x, 1-y, -1/2+z$; $d = 1/2-x, -1/2+y, 1/2-z$				
H bonding				
D--H---A	D-H (Å)	H--A (Å)	D—A (Å)	D-H--A (°)
N(3)-H(3N)--S(1)	0.94	2.62	3.5310	165

(D=Donor, A=acceptor, Cg=Centroid, α =dihedral angles between planes I & J, β = angle Cg(1)-Cg(J))

**Figure 3.2.** Unit cell packing diagram of the compound 2 viewed along the *a* axis

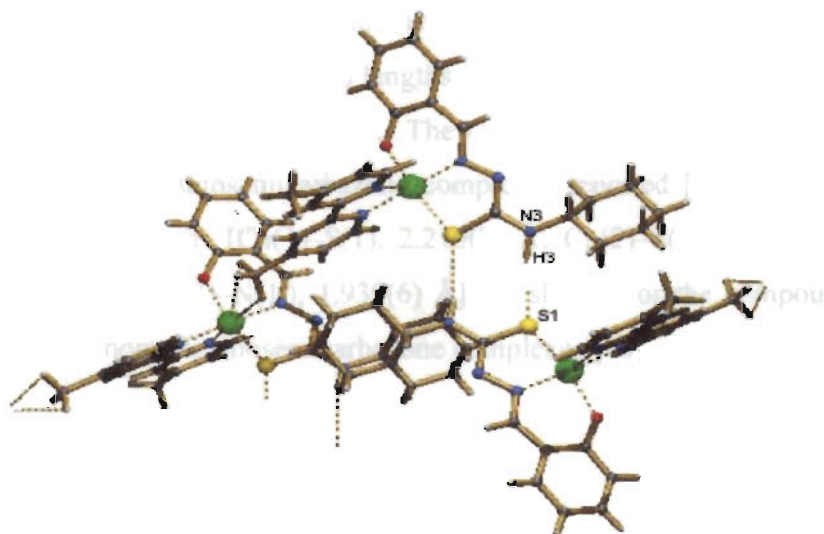


Figure 3.3. Hydrogen bonding interactions for the compound 2

3.3.3. Crystal structure of the compound $[(CuL^2)_2]$ (3)

The molecular structure of the compound 3 along with atom numbering scheme is given in Figure 3.4. In the asymmetric unit two molecules are present and bond lengths and bond angles of these two are approximately the same. So the discussion is limited to one of the molecule. The selected bond lengths and bond angles of one of the molecule in the asymmetric unit is summarized in Table 3.5. Compound 3 crystallizes in the triclinic space group $P\bar{1}$. The copper atom in $[(CuL^2)_2]$ (3) is coordinated by azomethine nitrogen, N(1), thiolato sulfur, S(1), and the phenolato oxygen atoms, O(1) and O(1'), which bridge to occupy the fourth coordination site. There are no acetate counterions, indicating loss of both the $-OH$ and $-^2NH$ hydrogens. The $Cu(1)-O(1)-Cu(2)-O(1')$ (plane 1) bridging portion of the molecule shows a tetrahedral distortion with a mean plane deviation of 0.7551 \AA , with Cu(1) above the mean plane. The two $Cu-O$ bond distances of $[(CuL^2)_2]$ are different [$Cu(1)-O(1)$, $1.911(5) \text{ \AA}$; $Cu(2)-O(1')$, $1.968(5) \text{ \AA}$]. It is reported that a

series of binuclear copper(II) complexes involving methoxy and phenoxy bridging oxygens of a macrocyclic ligand have bond lengths from the two copper atoms to the phenoxy oxygen of 1.954 and 1.962 Å [16]. The Cu–O bond distances are shorter than other binuclear Cu(II) thiosemicarbazone complexes reported [17]. Also, the Cu–S and Cu–N bond lengths [Cu(1)–S(1), 2.210(2) Å; Cu(2)–S(1'), 2.213(2) Å; Cu(1)–N(1), 1.930(6) Å; Cu(2)–N(1'), 1.939(6) Å] are shorter for the compound **3** than is found in the monomeric thiosemicarbazone complexes [18].

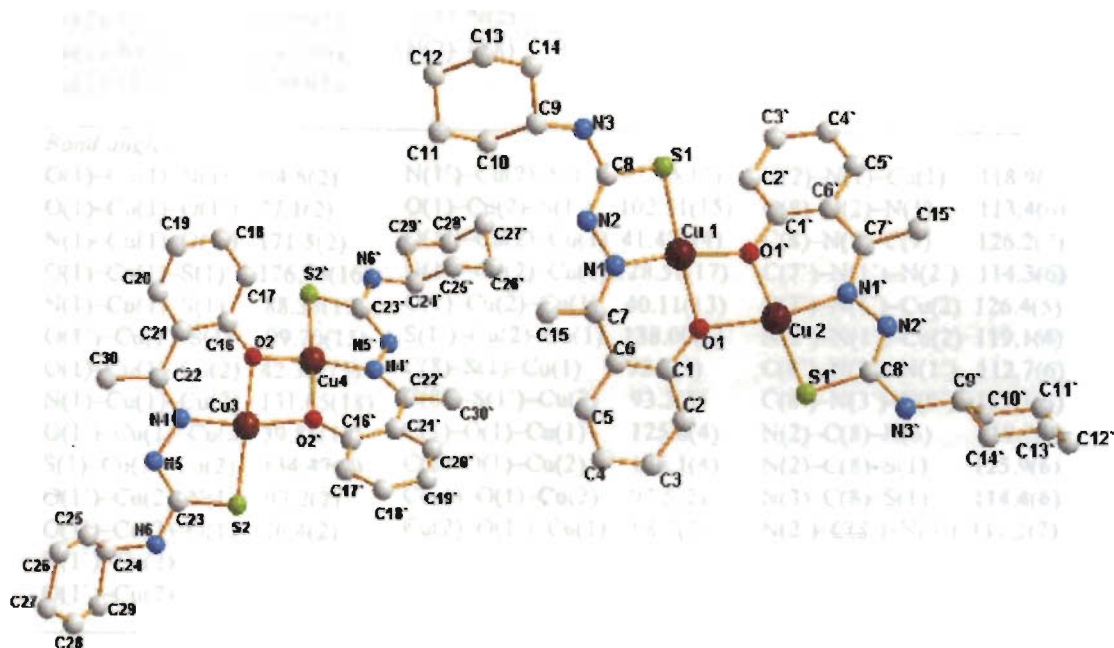


Figure 3.4. Structure and labeling scheme for $[(CuL^2)_2]$ (**3**)

The non-bonding Cu–Cu distance [Cu(1)–Cu(2), 2.9399(13) Å] in the compound **3** is approximately the same as that reported for the similar binuclear Cu(II) thiosemicarbazone complexes [19] and greater than the distance found for acetato type bridging of Cu(II) centres [20]. The geometry about each copper atom is

not planar. The mean plane deviation from the Cu(1)–O(1)–N(1)–S(1)–O(1') plane (plane 2) is 0.0184 Å, with O(1') above the mean plane. The dihedral angle formed by the least square planes / planes 1 and 2 are 31.32° and 148.68° respectively.

Table 3.5. Selected bond lengths (Å) and bond angles (°) for the compound (3).

<i>Bond lengths</i>					
Cu(1)–O(1)	1.911(5)	Cu(2)–S(1')	2.213(2)	N(3)–C(8)	1.331(9)
Cu(1)–N(1)	1.930(6)	O(1)–C(1)	1.301(6)	N(3)–C(9)	1.455(10)
Cu(1)–O(1')	1.968(5)	S(1)–C(8)	1.758(8)	N(1')–C(7')	1.315(9)
Cu(1)–S(1)	2.210(2)	S(1')–C(8')	1.739(8)	N(1')–N(2')	1.401(8)
Cu(1)–Cu(2)	2.9399(13)	N(1)–C(7)	1.303(9)	N(2')–C(8')	1.302(9)
Cu(2)–O(1')	1.906(5)	N(1)–N(2)	1.394(8)	N(3')–C(8')	1.346(9)
Cu(2)–N(1')	1.939(6)	N(2)–C(8)	1.306(9)	N(3')–C(9')	1.458(9)
Cu(2)–O(1)	1.999(5)				
<i>Bond angles</i>					
O(1)–Cu(1)–N(1)	94.8(2)	N(1')–Cu(2)–S(1')	87.90(17)	N(2)–N(1)–Cu(1)	118.9(5)
O(1)–Cu(1)–O(1')	77.1(2)	O(1)–Cu(2)–S(1')	102.51(15)	C(8)–N(2)–N(1)	113.4(6)
N(1)–Cu(1)–O(1')	171.5(2)	O(1')–Cu(2)–Cu(1)	41.42(14)	C(8)–N(3)–C(9)	126.2(7)
O(1)–Cu(1)–S(1)	176.75(16)	N(1')–Cu(2)–Cu(1)	128.51(17)	C(7')–N(1')–N(2')	114.3(6)
N(1)–Cu(1)–S(1)	88.38(19)	O(1)–Cu(2)–Cu(1)	40.11(13)	C(7')–N(1')–Cu(2)	126.4(5)
O(1')–Cu(1)–S(1)	99.70(15)	S(1')–Cu(2)–Cu(1)	138.00(6)	N(2')–N(1')–Cu(2)	119.1(4)
O(1)–Cu(1)–Cu(2)	42.38(15)	C(8)–S(1)–Cu(1)	92.8(3)	C(8')–N(2')–N(1')	112.7(6)
N(1)–Cu(1)–Cu(2)	131.65(18)	C(8')–S(1')–Cu(2)	93.3(3)	C(8')–N(3')–C(9')	125.1(6)
O(1')–Cu(1)–Cu(2)	39.86(13)	C(1)–O(1)–Cu(1)	125.6(4)	N(2)–C(8)–N(3)	119.7(7)
S(1)–Cu(1)–Cu(2)	134.47(7)	C(1)–O(1)–Cu(2)	136.1(4)	N(2)–C(8)–S(1)	125.9(6)
O(1')–Cu(2)–N(1')	93.2(2)	Cu(1)–O(1)–Cu(2)	97.5(2)	N(3)–C(8)–S(1)	114.4(6)
O(1')–Cu(2)–O(1)	76.4(2)	Cu(2)–O(1')–Cu(1)	98.7(2)	N(2')–C(8')–N(3')	117.2(7)
N(1')–Cu(2)–O(1)	168.6(2)	C(7)–N(1)–N(2)	115.4(6)	N(2')–C(8')–S(1')	126.8(6)
O(1')–Cu(2)–S(1')	178.56(17)	C(7)–N(1)–Cu(1)	125.7(5)	N(3')–C(8')–S(1')	116.0(6)

A comparison of the thiosemicarbazone moiety bond distances of [(CuL²)₂] to those of the uncoordinated thiosemicarbazone ligand (H₂L²) shows that coordination lengthens the C=N bond slightly [C(7)–N(1), 1.303(9) Å; C(7')–N(1'), 1.315(9) Å; in H₂L², 1.284(2) Å], as would be expected on coordination of the azomethine nitrogen. The delocalization of electron density of the thiosemicarbazone moiety in the complex gives rise to an increase in the N–N bond length [N(1)–N(2), 1.394(8) Å;

$N(1')-N(2')$, 1.401(8) Å; in H_2L^2 , 1.392(2) Å] as compared to the uncomplexed thiosemicarbazone ligand. The enolization and deprotonation on complexation is also confirmed by the lengthening of bonds C–S [C(8)–S(1), 1.758(8) Å; C(8')–S(1'), 1.739(8) Å] from the value of 1.688(2) Å in the uncomplexed thiosemicarbazone H_2L^2 . The decrease in the bond length of C–N [C(8)–N(2), 1.306(9) Å; C(8')–N(2'), 1.302(9) Å] from the value of 1.351(3) Å of the free ligand also supports thiolate formation [21]. Similar trend is observed in the second molecule of the asymmetric unit also.

Ring puckering analyses and least-square plane calculations show that the ring Cg(2) comprising of atoms Cu(1), N(1), N(2), C(8), and S(1) adopts an envelope on Cu(1) and Cg(8) and Cg(9) rings comprising of atoms C(9), C(10), C(11), C(12), C(13), C(14) and C(9'), C(10'), C(11'), C(12'), C(13'), C(14') adopt chair conformations.

Figure 3.5 shows the contents of the unit cell along the a axis. The assemblage of molecules in the respective manner in the unit cell is resulted by the H bonding, π - π , CH- π and ring-metal interactions as depicted in Table 3.6. The centroid Cg(3) is involved in π - π interaction with Cg(11) of the neighbouring unit (second molecule of the asymmetric unit) at a distance of 3.5383 Å, the CH- π interactions C(29)–H(29)→Cg(7) (C(29)–H(29) from the second molecule of the asymmetric unit) at a distance of 2.88 Å, the ring-metal interactions of Cg(3)→Cu(3) (Cu(3) from the second molecule of the asymmetric unit), Cg(7)→Cu(2) and Cg(11)→Cu(2) and intermolecular hydrogen bonding interactions N(3)–H(3N).....S(2') and N(6)–H(6).....S(1) also contribute stability to the unit cell packing {S(2') and N(6)–H(6) from the second molecule of the asymmetric unit}.

Table 3.6. Interaction parameters of the compound $[(CuL^2)_2]$

π---π interactions				
Cg(I)-Res(1)---Cg(J)	Cg-Cg(Å)	α °	β °	
Cg(3) [1] -> Cg(11) ^a	3.5383	10.89	16.16	
Equivalent position codes a = x, y, z Cg(3) = Cu(2),S(1'),C(8'),N(2'),N(1'); Cg(11) = Cu(3),S(2),C(23),N(5),N(4)				
CH---π interactions				
XH(I)---Cg(J)	H..Cg(Å)	X-H..Cg (°)	X..Cg(Å)	
C(29)-H(29A) [2] -> Cg(7) ^a	2.88	145	3.7188	
Equivalent position codes a = x, y, z Cg(7) = C(1'),C(2'),C(3'),C(4'),C(5'),C(6')				
Ring-Metal interactions				
Cg(I)-Res(1)---Me(J)	Cg(I)-Me(J)	Me(J)_ perp	β °	
Cg(3) [1] -> Cu(3) ^a	3.485	3.265	20.43	
Cg(7) [1] -> Cu(2) ^b	3.970	2.975	41.45	
Cg(11) [2] -> Cu(2) ^a	3.538	3.124	27.97	
Equivalent position codes a = x, y, z, b = -x, -y, -z				
H bonding				
D---H---A	D-H	H---A	D---A	D-H---A
N(3)-H(3N)-S(2') ^c	0.78	2.80	3.4627	145
N(6)-H(6)-S(1)	0.86	2.81	3.5979	154
Equivalent position codes c = x, -1+y, z				

(D=Donor, A=acceptor, Cg=Centroid, α =dihedral angles between planes I & J, β = angle Cg(1)-Cg(J)

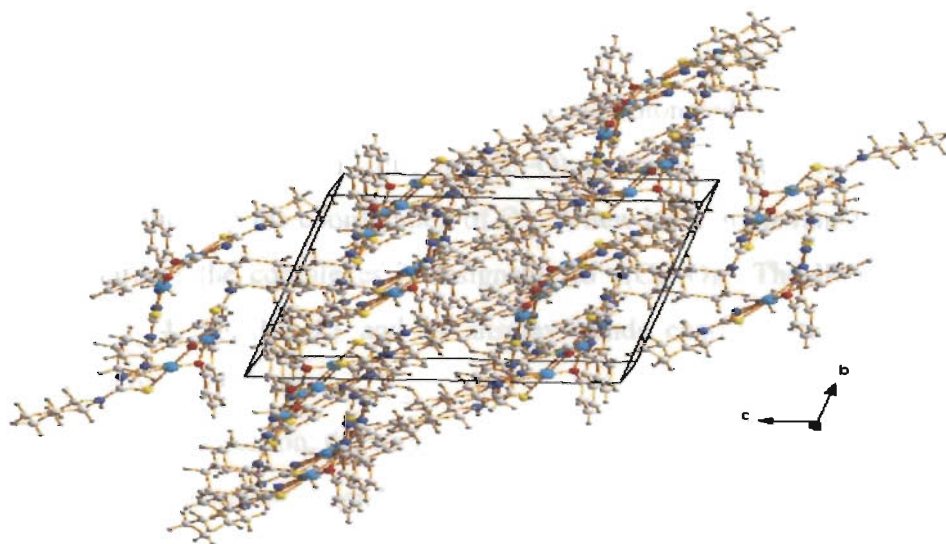


Figure 3.5. Unit cell packing diagram of the compound 3 viewed along the *a* axis

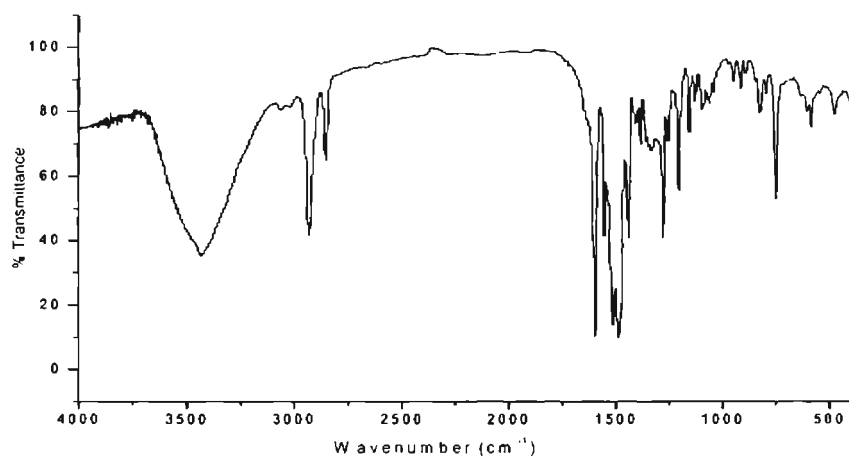
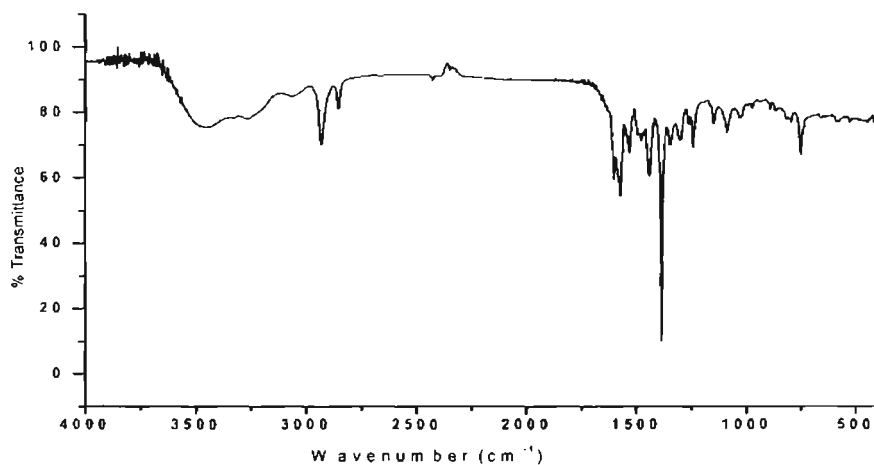
3.3.4. Infrared spectra

The infrared spectral data of the complexes 1-14 are presented in Table 3.7 with their tentative assignments. On coordination of azomethine nitrogen, $\nu(\text{C}=\text{N})$ shifts to lower wavenumbers by 10-20 cm^{-1} , as the band shifts from *ca.* 1610 cm^{-1} in the uncomplexed thiosemicarbazone spectrum to *ca.* 1588 cm^{-1} in the spectra of the complexes. Except in complexes 5, 6, 7 and 9, in all other Cu(II) complexes, another strong band is found at *ca.* 1525-1555 cm^{-1} , which may be due to the newly formed $\nu(\text{N}=\text{C})$ bond, resulting from enolization of the principal thiosemicarbazone ligands. In complexes 5, 6, 7 and 9, the principal ligand is coordinated as keto form. Coordination of azomethine nitrogen is confirmed with the presence of new bands in the range 420-470 cm^{-1} , assignable to $\nu(\text{Cu}-\text{N})$ for these fourteen complexes. The $\nu(\text{N}-\text{N})$ band of the thiosemicarbazones was found at *ca.* 1140 cm^{-1} . The increase in the frequency of this band in the spectra of the complexes, due to the increase in the bond strength, again confirms the coordination *via* the azomethine nitrogen [22].

In all the complexes, phenolic oxygen is coordinated to copper by loss of the -OH proton. The $\nu(\text{OH})$ band (3402 cm^{-1} for H_2L^1 , 3308 cm^{-1} for H_2L^2 , 3336 cm^{-1} for H_2L^3 and 3440 cm^{-1} for H_2L^4) of the free ligands disappears on complex formation and points to coordination from the deprotonated phenolic oxygen. The ligand band at *ca.* 1269 cm^{-1} due to $\nu(\text{C-O})$ is shifted to *ca.* 1229 cm^{-1} in the complexes, indicating the coordination of O^- . A new band in the range $380\text{-}395\text{ cm}^{-1}$ in the spectra of the complexes is assignable to $\nu(\text{Cu-O})$. The IR spectra of the complexes **2**, **4**, **10**, **12**, **13** and **14** display bands characteristic of coordinated heterocyclic bases [23].

Upon complexation, the stretching frequency of $\nu(\text{CS})$ band from *ca.* 852 cm^{-1} in the thiosemicarbazone ligands decreases. This indicates that coordination *via* thiolato sulfur takes place. In complexes **5-7**, anions like Cl^- , Br^- and NO_3^- were coordinated to the metal, while in complex **9**, two ligand molecules were coordinated as monoanionic (HL^-) forms. In chloro complex (**5**), the strong band observed at 297 cm^{-1} have been assigned to the terminal $\nu(\text{Cu-Cl})$ band. The $\nu(\text{Cu-Br})$ frequency is observed at 256 cm^{-1} , which is consistent with the terminal (Cu-Br) band in the bromo complex (**6**) [24]. According to Gatehouse *et al*, for nitrate complexes, the unidentate and bidentate NO_3^- groups exhibit three NO stretching bands. The separation of the two highest-frequency bands is 115 cm^{-1} for the unidentate complex, whereas it is 186 cm^{-1} for the bidentate complex. Here, in the nitrate complex (**7**), the three bands observed at 1503 , 1386 and 1079 cm^{-1} indicates the bands of the nitrate group. The fact that the nitrate group is terminally bonded is understood from the separation of 117 cm^{-1} between the two highest frequency bands just mentioned above and it is unidentate in nature [25]. Besides, from the far IR spectrum of the complex, the band observed at 258 cm^{-1} can be assigned to $\nu(\text{Cu-ONO}_2)$ in consistence with the bands at $253\text{-}280\text{ cm}^{-1}$, reported earlier for Cu-ONO_2 in metal

complexes [26]. The presence of a new band in the $320\text{-}340\text{ cm}^{-1}$ range, assignable to $\nu(\text{Cu-S})$, is another indication of the involvement of sulfur coordination. Representative IR spectra of the complexes **1**, **7**, **9** and **13** are presented in Figure 3.6.

 $[(\text{CuL}^1)_2]$ (**1**) $[\text{Cu}(\text{HL}^2)\text{NO}_3] \cdot \text{C}_2\text{H}_5\text{OH}(\text{H}_2\text{O})$ (**7**)

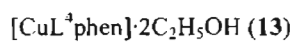
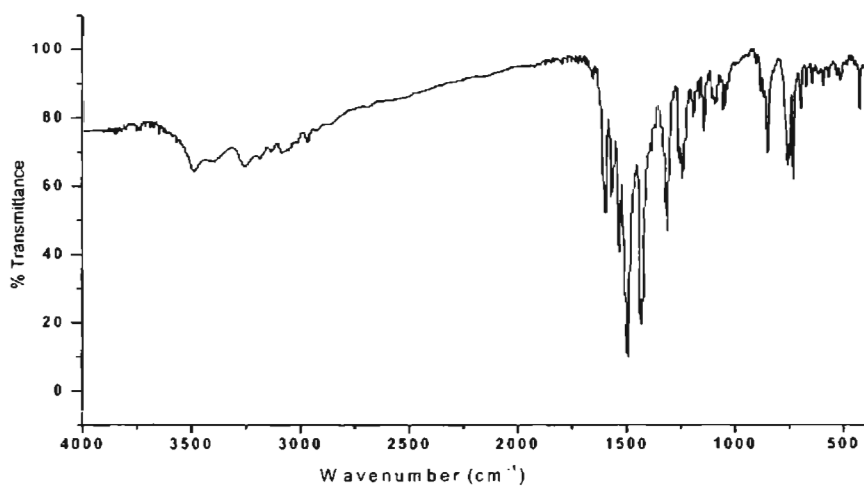
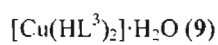
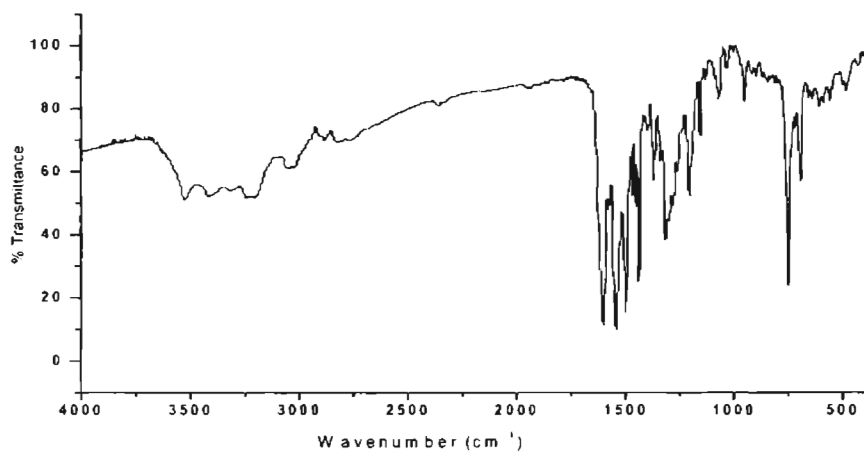


Figure 3.6. IR spectra of the compounds 1, 7, 9 and 13

Table 3.7. Selected IR bands (cm^{-1}) with tentative assignments of Cu(II) complexes

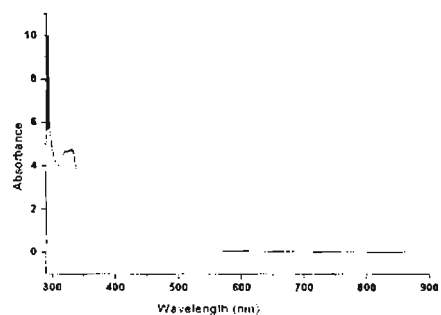
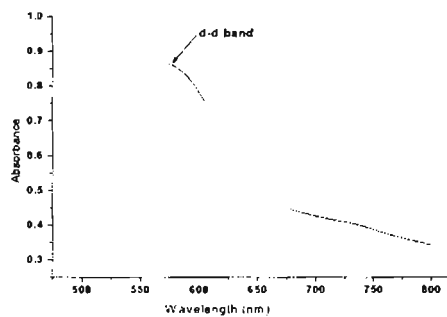
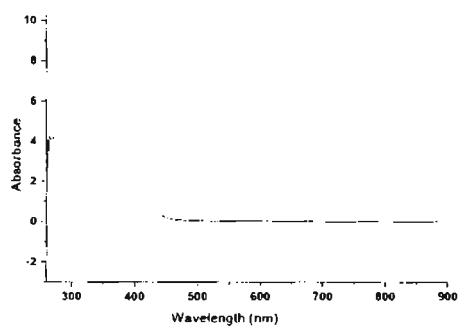
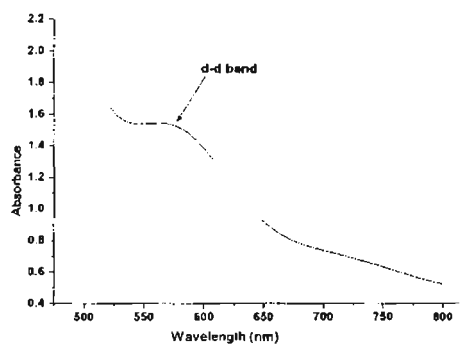
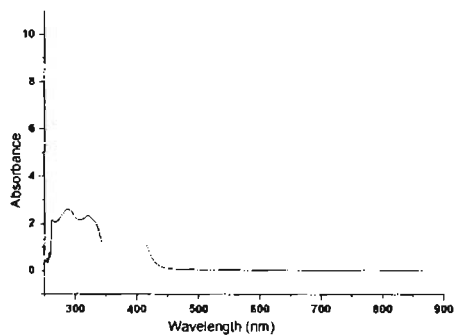
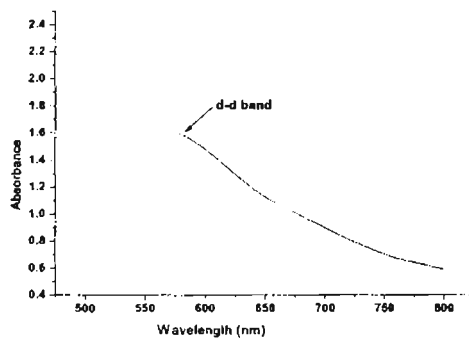
Compound	$\nu(\text{C}=\text{N})$	$\nu(\text{N}=\text{C})$	$\nu(\text{N}-\text{N})$	$\nu(\text{C}=\text{S})/\nu(\text{C}-\text{S})$	$\nu(\text{C}-\text{O})$	$\nu(\text{Cu}-\text{N})$	Bands due to heterocyclic base
H_2L^1	1614	-----	1111	1328,856	1263		
$[(\text{CuL}^1)_2]$	1594	1546	1149	1272,818	1196	421	
$[\text{CuL}^1\text{dmbipy}]$	1596	1530	1146	1313,823	1233	439	1476,627
H_2L^2	1613		1111	1358,846	1263		
$[(\text{CuL}^2)_2]$	1591	1540	1143	1305,751	1230	443	-----
$[\text{CuL}^2\text{dmbipy}] \cdot \frac{1}{2}\text{H}_2\text{O}$	1588	1527	1137	1346,824	1241	422	1473,719
$[\text{Cu}(\text{HL}^2)\text{Cl}] \cdot 2\text{H}_2\text{O}$	1572		1143	1341,740	1236	450	
$[\text{Cu}(\text{HL}^2)\text{Br}] \cdot 4\text{H}_2\text{O}$	1565		1145	1338,743	1238	470	-----
$[\text{Cu}(\text{HL}^2)\text{NO}_3] \cdot \text{C}_2\text{H}_5\text{OH}(\text{H}_2\text{O})$	1569		1144	1340,741	1236	442	
H_2L^3	1613		1149	1328,874	1255		
$[(\text{CuL}^3)_2] \cdot \frac{1}{2}\text{H}_2\text{O}$	1594	1555	1153	1314,843	1201	428	
$[\text{Cu}(\text{HL}^3)_2] \cdot \text{H}_2\text{O}$	1599		1153	1314,750	1201	431	
$[\text{CuL}^3\text{dmbipy}] \cdot \text{H}_2\text{O}$	1596	1537	1150	1313,828	1247	420	1434,697
H_2L^4	1603		1160	1362,835	1295		
$[(\text{CuL}^4)_2] \cdot \frac{1}{2}\text{H}_2\text{O}$	1596	1543	1142	1310,740	1234	425	-----
$[\text{CuL}^4\text{bipy}] \cdot \text{H}_2\text{O}$	1590	1538	1136	1311,751	1235	414	1433,687
$[\text{CuL}^4\text{phen}] \cdot 2\text{C}_2\text{H}_5\text{OH}$	1597	1532	1142	1310,752	1234	420	1427,681
$[\text{CuL}^4\text{dmbipy}] \cdot 3\text{H}_2\text{O}$	1592	1540	1136	1316,745	1246	422	1431,715

3.3.5. Electronic spectra

The electronic spectra of the complexes in DMF solution are presented in Table 3.8. Each thiosemicarbazones and its copper(II) complexes have a ring $\pi \rightarrow \pi^*$ bands in the range 32000 - 38000 cm^{-1} and $n \rightarrow \pi^*$ bands in the range 28000 - 32000 cm^{-1} . Two ligand to metal charge transfer bands are found in 21000 - 28000 cm^{-1} range. In accordance with previous studies of copper(II) thiosemicarbazone complexes [27,28], the higher energy bands in the range 25000 - 28000 cm^{-1} are assigned to $S \rightarrow \text{Cu}^{\text{II}}$ transitions. The bands in the 21000 - 25000 cm^{-1} range are assignable to phenoxy $O \rightarrow \text{Cu}^{\text{II}}$ transitions [29]. Each complex has a $d-d$ band in the range 14000 - 18000 cm^{-1} , which appears as a weak shoulder on the intraligand and charge transfer bands. Representative spectra of the complexes 2, 10 and 12 are presented in Figure 3.7.

Table 3.8. Electronic spectral assignments (cm^{-1}) for the ligands and their Cu(II) complexes

Compound	$\pi - \pi^*$	$n - \pi^*$	LMCT	d - d
H_2L^1	32150	28730		
$\{(\text{CuL}^1)_2\}$	33000	31250	26310,24630	16180
$[\text{CuL}^1\text{dmbipy}]$	34010	31050,30120	25900,25120	15430
H_2L^2	36900	30860		
$\{(\text{CuL}^2)_2\}$	35710	28980	25830,24690	17540
$[\text{CuL}^2\text{dmbipy}] \cdot \frac{1}{2}\text{H}_2\text{O}$	35210	32050,30670	26520,25180	15570
$[\text{Cu}(\text{HL}^2)\text{Cl}] \cdot 2\text{H}_2\text{O}$	35970	28980	25060	16180
$[\text{Cu}(\text{HL}^2)\text{Br}] \cdot 4\text{H}_2\text{O}$	34480	29850	26100	17660
$[\text{Cu}(\text{HL}^2)\text{NO}_3] \cdot \text{C}_2\text{H}_5\text{OH}(\text{H}_2\text{O})$	34360	28980	25770,24810	17730
H_2L^3	32250	29060		
$\{(\text{CuL}^3)_2\} \cdot \frac{1}{2}\text{H}_2\text{O}$	33110	31050	27240,26240	15520
$[\text{Cu}(\text{HL}^3)_2] \cdot \text{H}_2\text{O}$	33780	30950,30300	25970	15640
$[\text{CuL}^3\text{dmbipy}] \cdot \text{H}_2\text{O}$	37730	30950,30120	25380,24690	14160
H_2L^4	36490	31250		
$\{(\text{CuL}^4)_2\} \cdot \frac{1}{2}\text{H}_2\text{O}$	35460	30030	25830,23980	17420
$[\text{CuL}^4\text{bipy}] \cdot \text{H}_2\text{O}$	34600	30760	25770,24440	16150
$[\text{CuL}^4\text{phen}] \cdot 2\text{C}_2\text{H}_5\text{OH}$	33780	30950	26040	17530
$[\text{CuL}^4\text{dmbipy}] \cdot 3\text{H}_2\text{O}$	34240	29940	25640,24270	15920

 $[\text{CuL}^1\text{dmbipy}]$ (2) $[\text{CuL}^1\text{dmbipy}]$ (2) $[\text{CuL}^3\text{dmbipy}] \cdot \text{H}_2\text{O}$ (10) $[\text{CuL}^3\text{dmbipy}] \cdot \text{H}_2\text{O}$ (10) $[\text{CuL}^4\text{bipy}] \cdot \text{H}_2\text{O}$ (12) $[\text{CuL}^4\text{bipy}] \cdot \text{H}_2\text{O}$ (12)**Figure 3.7.** Electronic spectra of the compounds 2, 10 and 12

3.3.6. EPR spectra

The EPR parameters obtained for the compounds in the polycrystalline state at 298 K and in DMF solution at 77 K are presented in Tables 3.9 and 3.10.

The EPR spectra of compounds **1-14** in the polycrystalline state at room temperature shows different types of geometrical species. The compounds **1, 3, 8, 10, 11** and **14** gave isotropic spectra with only one broad signal at around $g = 2.080$. The spectra of the compounds **2, 5, 6, 7, 12** and **13** showed typical axial spectra with well-defined g_{\parallel} and g_{\perp} values at around 2.162 and 2.055 respectively. The spectra of the compounds **4** and **9** gave three g values indicating rhombic distortion in its geometry. The values g_1 and g_2 are very close to each other in the compounds, which means that the rhombic distortion is very small. The geometric parameter G , which is a measure of the exchange interaction between the copper centers in the polycrystalline compound, is calculated using the equation: $G = (g_{\parallel} - 2.0023)/(g_{\perp} - 2.0023)$ for axial spectra and for rhombic spectra $G = (g_3 - 2.0023)/(g_{\perp} - 2.0023)$, where $g_{\perp} = (g_1 + g_2)/2$. If $G < 4.0$ considerable exchange interaction is indicated in the solid complex [30,31]. The G value for the compounds **2, 5, 6, 7, 12** and **13** (for axial spectra) and **4, 6** and **9** (rhombic spectra) in polycrystalline state at 298 K are ≈ 2.91 , indicating considerable exchange interaction for the parent complexes. In all the copper(II) complexes $g_{\parallel} > g_{\perp} > 2.0023$ and G values within the range 2.5 - 3.5 are consistent with a $d_{x^2-y^2}$ ground state. The parameter R ($R = (g_2 - g_1)/(g_3 - g_2)$ for rhombic systems) calculated for the compounds **4** and **9** are at around 0.53, ie, $R < 1$, indicating a $d_{x^2-y^2}$ ground state of the copper(II) ion [32,33]. From the g value of a transition metal complex, we can obtain very important information about the structure of the complex.

The EPR spectra of all the compounds in frozen DMF solution at 77 K are axial. Moreover, they show well-defined four hyperfine lines in the parallel region

corresponding to the electron spin – nuclear spin interaction ($^{63,65}\text{Cu}$, $I = 3/2$). The fourth copper hyperfine line is expected to overlap with the high field component (g_{\perp}). However, the half field signal corresponding to the dimer was not observed for the compounds **1**, **3**, **8** and **11**. In all these compounds, $g_{\parallel} > g_{\perp} > 2$ corresponding to the presence of an unpaired electron in the $d_{x^2-y^2}$ orbital [34,35]. For a Cu(II) complex, g_{\parallel} is a parameter sensitive enough to indicate covalence. For a covalent complex, $g_{\parallel} < 2.3$. Here also, all the fourteen complexes are covalent in nature. In solution at 77 K, g_{\parallel} values (2.16-2.19) are almost the same for all the compounds, which indicate similar bonding nature in all of them [36]. The g_{av} and A_{av} values for the compounds in DMF solution at 77 K are calculated using the equations $g_{av} = 1/3(g_{\parallel} + 2g_{\perp})$ and $A_{av} = 1/3(A_{\parallel} + 2A_{\perp})$. In compound **1**, well resolved spectra with four copper hyperfine lines and three superhyperfine lines due to the azomethine nitrogen are observed in DMF.

The EPR parameters g_{\parallel} , g_{\perp} , g_{av} , $A_{\parallel}(\text{Cu})$ and $A_{\perp}(\text{Cu})$ and energies of $d-d$ transitions were used to evaluate the bonding parameters α^2 , β^2 and γ^2 , which may be regarded as measures of covalency of the in-plane σ bonds, in-plane π bonds and out-of-plane π bonds respectively [37].

The value of in-plane σ bonding parameter α^2 was estimated from the expression [38,39],

$$\alpha^2 = -A_{\parallel}/0.036 + (g_{\parallel} - 2.00277) + 3/7 (g_{\perp} - 2.00277) + 0.04$$

The following simplified expressions were used to calculate the bonding parameters [40,41]:

$$K^2_{\parallel} = (g_{\parallel} - 2.00277)E_{d-d}/8\lambda_0$$

$$K^2_{\perp} = (g_{\perp} - 2.00277)E_{d-d}/2\lambda_0$$

where $K_{\parallel} = \alpha^2\beta^2$ and $K_{\perp} = \alpha^2\gamma^2$, K_{\parallel} and K_{\perp} are orbital reduction factors and λ_0 represents the one electron spin orbit coupling constant which equals -828 cm^{-1}

Hathaway [42] pointed out that, for pure σ bonding, $K_{\parallel} \approx K_{\perp} \approx 0.77$, and for in-plane π bonding, $K_{\parallel} < K_{\perp}$; while for out-of-plane π bonding $K_{\perp} < K_{\parallel}$. In all the complexes it is observed that $K_{\parallel} < K_{\perp}$ which indicates the presence of significant in-plane π bonding. The values of the bonding parameters α^2 , β^2 and $\gamma^2 < 1.0$ (value of 1.0 for 100% ionic character) indicate significant in-plane σ bonding and in-plane π bonding. Representative EPR spectra of the compounds **4**, **6** and **14** in polycrystalline state at 298 K and **3**, **9** and **10** in DMF solution at 77 K are presented in Figure 3.8.

Table 3.9. EPR spectral assignments for Cu(II) complexes in polycrystalline state at 298 K and DMF solution at 77 K

Compound	Polycrystalline state (298 K)	DMF solution (77 K)					
		g_{\parallel}	g_{\perp}	g_{av}	A_{\parallel}^a	A_{\perp}^a	A_{av}^a
$[(\text{CuL}^1)_2]$	2.129 (g_{iso})	2.177	2.045	2.089	182.3	14.3	68.1
$[\text{CuL}^1\text{dmbipy}]$	2.195/2.063 (g_{\parallel}/g_{\perp})	2.167	2.056	2.093	190.5		
$[(\text{CuL}^2)_2]$	2.080 (g_{iso})	2.167	2.046	2.086	187.8	20.3	74.1
$[\text{CuL}^2\text{dmbipy}] \cdot \frac{1}{2}\text{H}_2\text{O}$	2.194/2.117/2.045 ($g_3/g_2/g_1$)	2.176	2.061	2.099	189.5	35.2	84.9
$[\text{Cu}(\text{HL}^3)\text{Cl}] \cdot 2\text{H}_2\text{O}$	2.173/2.053 (g_{\parallel}/g_{\perp})	2.181	2.059	2.100	193.4	19.2	75.1
$[\text{Cu}(\text{HL}^3)\text{Br}] \cdot 4\text{H}_2\text{O}$	2.162/2.058 (g_{\parallel}/g_{\perp})	2.193	2.040	2.091	196.2	36.5	87.3
$[\text{Cu}(\text{HL}^2)\text{NO}_3] \cdot \text{C}_2\text{H}_5\text{OH}(\text{H}_2\text{O})$	2.199/2.061 (g_{\parallel}/g_{\perp})	2.194	2.055	2.107	196.2	15.9	73.7
$[(\text{CuL}^3)_2] \cdot \frac{1}{2}\text{H}_2\text{O}$	2.059 (g_{iso})	2.195	2.053	2.100	184.5	19.1	71.9
$[\text{Cu}(\text{HL}^3)_2] \cdot \text{H}_2\text{O}$	2.120/2.040/2.030 ($g_3/g_2/g_1$)	2.191	2.053	2.099	184.1	14.4	68.6
$[\text{CuL}^3\text{dmbipy}] \cdot \text{H}_2\text{O}$	2.070 (g_{iso})	2.169	2.063	2.098	189.0		
$[(\text{CuL}^4)_2] \cdot \frac{1}{2}\text{H}_2\text{O}$	2.064 (g_{iso})	2.174	2.052	2.092	188.1	20.4	74.2
$[\text{CuL}^4\text{bipy}] \cdot \text{H}_2\text{O}$	2.186/2.060 (g_{\parallel}/g_{\perp})	2.196	2.059	2.104	203.2		
$[\text{CuL}^4\text{phen}] \cdot 2\text{C}_2\text{H}_5\text{OH}$	2.066/2.030 (g_{\parallel}/g_{\perp})	2.171	2.092	2.118	192.5	25.8	80.1
$[\text{CuL}^4\text{dmbipy}] \cdot 3\text{H}_2\text{O}$	2.079 (g_{iso})	2.168	2.050	2.089	183.8	26.3	76.9

^a Expressed in units of cm^{-1} multiplied by a factor of 10^{-4}

The Fermi contact hyperfine interaction term K may be obtained from [43]

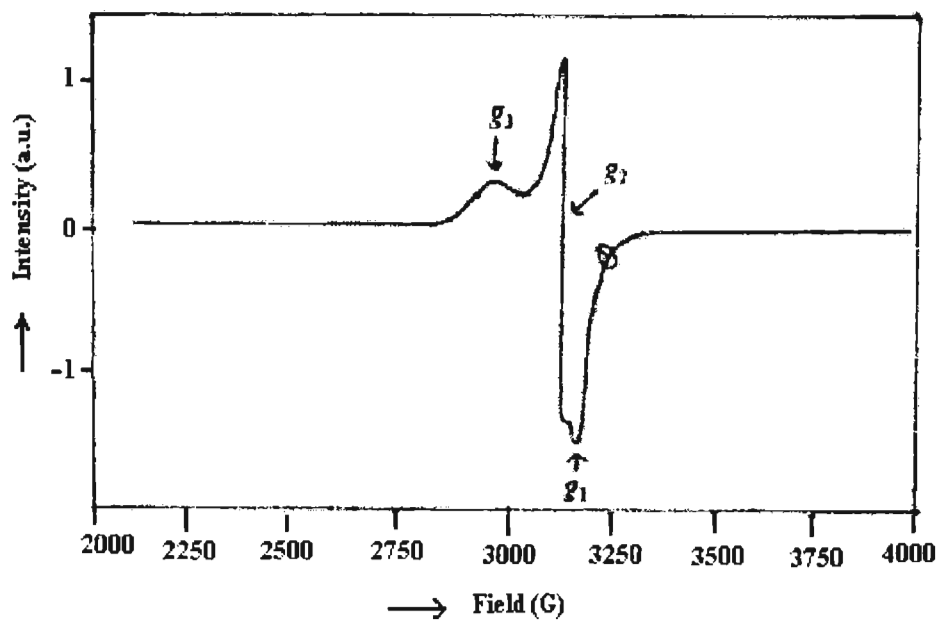
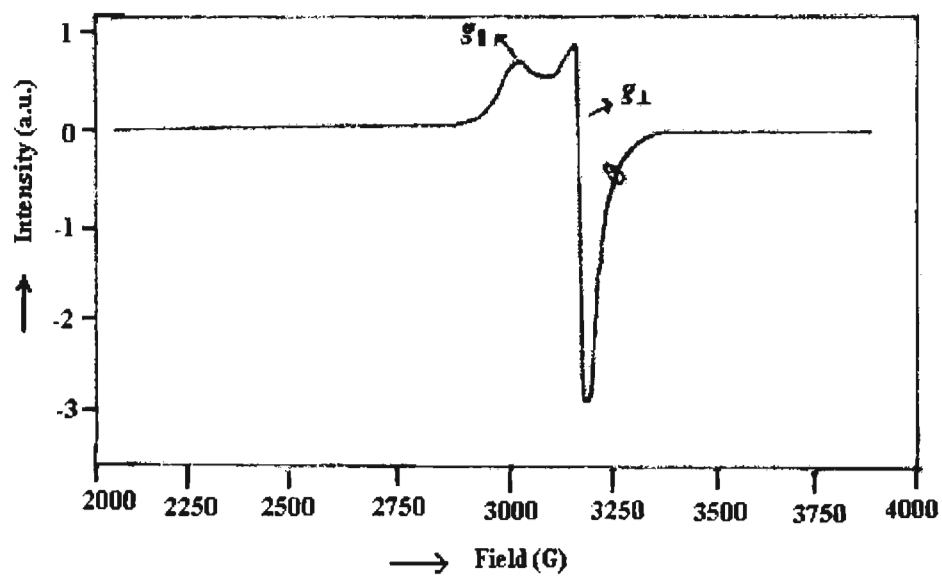
$$K = A_{iso} / P\beta^2 + (g_{av} - 2.00277) / \beta^2$$

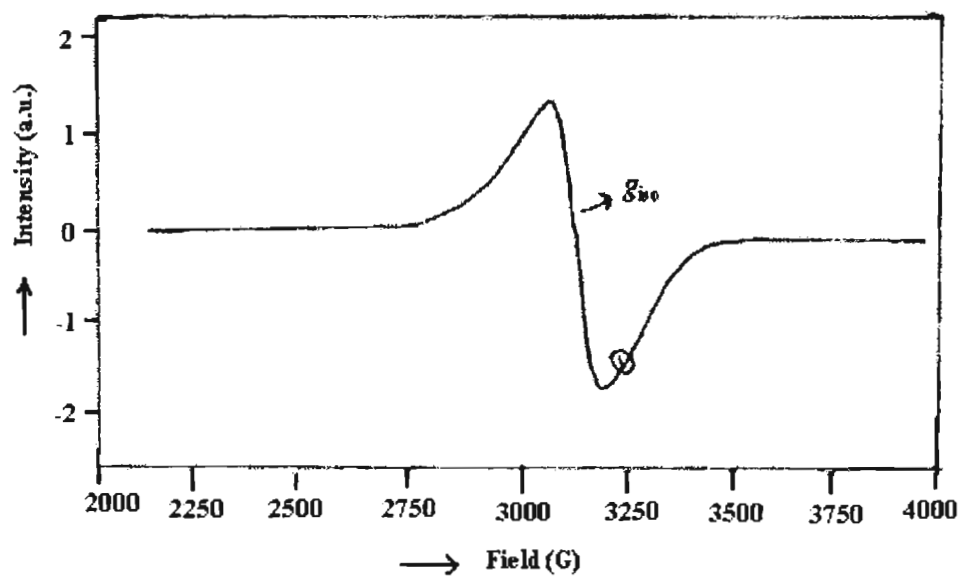
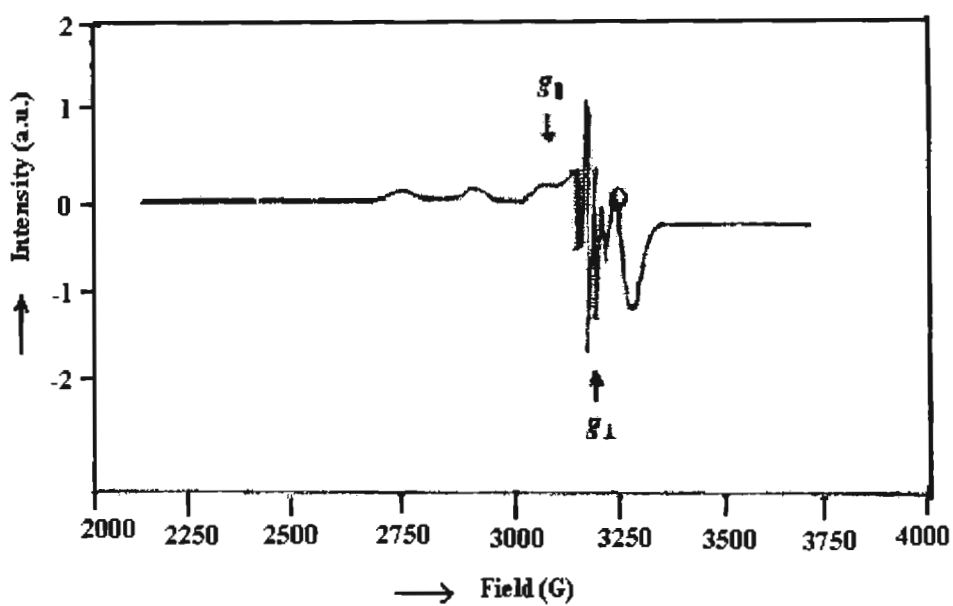
where P is the free ion dipolar term and its value is 0.036. K is a dimensionless quantity, which is a measure of the contribution of 's' electrons to the hyperfine interaction and is generally found to have a value in the range 0.30 - 0.40. The K values obtained for all the complexes are in good agreement with those estimated by Assour [44] and Abragam and Pryce [45]. The empirical factor $f = g_{\parallel} / A_{\parallel}$ (cm^{-1}) is an index of tetragonal distortion, is calculated and falls in the range 108 - 119 cm^{-1} . The value may vary from 105 - 135 cm^{-1} for small to extreme distortion. The value here indicates medium distortion from the geometry [46].

Table 3.10. EPR bonding parameters for compounds 1-14

Compound	G	R	DMF solution (77 K)							
	(298 K)		α^2	β^2	γ^2	K	K_{\parallel}	K_{\perp}	f^a	P
[(CuL ¹) ₂]			0.73	0.87	0.86	0.31	0.65	0.64	119.4	0.0236
[CuL ¹ dmbipy]	3.09		0.75	0.81	0.93		0.61	0.70	114	
[(CuL ²) ₂]			0.74	0.83	0.86	0.34	0.62	0.64	115.3	0.0237
[CuL ² dmbipy]·½H ₂ O	2.39	0.935	0.76	0.84	0.94	0.39	0.63	0.73	114.7	0.0219
[Cu(HL ³)Cl]·2H ₂ O	3.26		0.77	0.84	0.96	0.36	0.65	0.74	112.7	0.0250
[Cu(HL ²)Br]·4H ₂ O	2.84		0.79	0.89	0.79	0.37	0.71	0.63	111.8	0.0232
[Cu(HL ³)NO ₃]·C ₂ H ₅ OH(H ₂ O)	3.26		0.79	0.89	0.92	0.34	0.71	0.73	111.7	0.0264
[(CuL ³) ₂]·½H ₂ O			0.76	0.88	0.89	0.33	0.67	0.68	119.0	0.0235
[Cu(HL ³) ₂]·H ₂ O	3.42	0.125	0.76	0.86	0.90	0.33	0.66	0.69	119	0.0240
[CuL ³ dmbipy]·H ₂ O			0.75	0.78	0.94		0.59	0.71	114.8	
[(CuL ⁴) ₂]·½H ₂ O			0.75	0.89	0.95	0.33	0.67	0.72	115.5	0.0238
[CuL ⁴ bipy]·H ₂ O	3.10		0.82	0.83	0.90		0.68	0.74	108.1	
[CuL ⁴ phen]·2C ₂ H ₅ OH	2.20		0.78	0.84	1.24	0.40	0.66	0.97	112.7	0.0230
[CuL ⁴ dmbipy]·3H ₂ O			0.73	0.86	0.92	0.34	0.63	0.67	117.9	0.0220

^a Expressed in units of (cm).

(i) $[\text{CuL}^2\text{dmbipy}] \cdot \frac{1}{2}\text{H}_2\text{O}$ (4)(i) $[\text{Cu}(\text{HL}^2)\text{Br}] \cdot 4\text{H}_2\text{O}$ (6)

(i) $[\text{CuL}^+\text{dmbipy}]\cdot 3\text{H}_2\text{O}$ (14)(ii) $[(\text{CuL}^3)_2]$ (3)

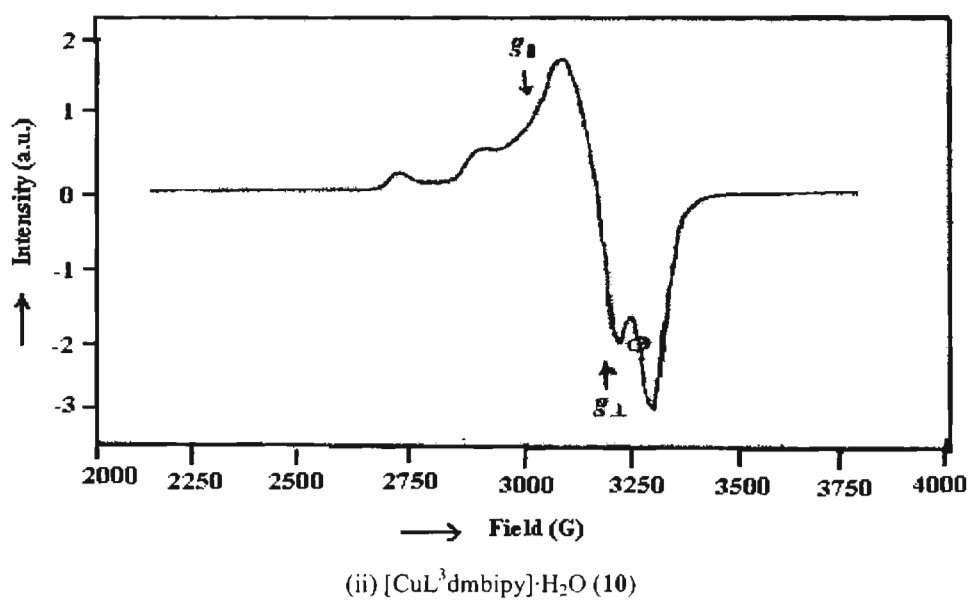
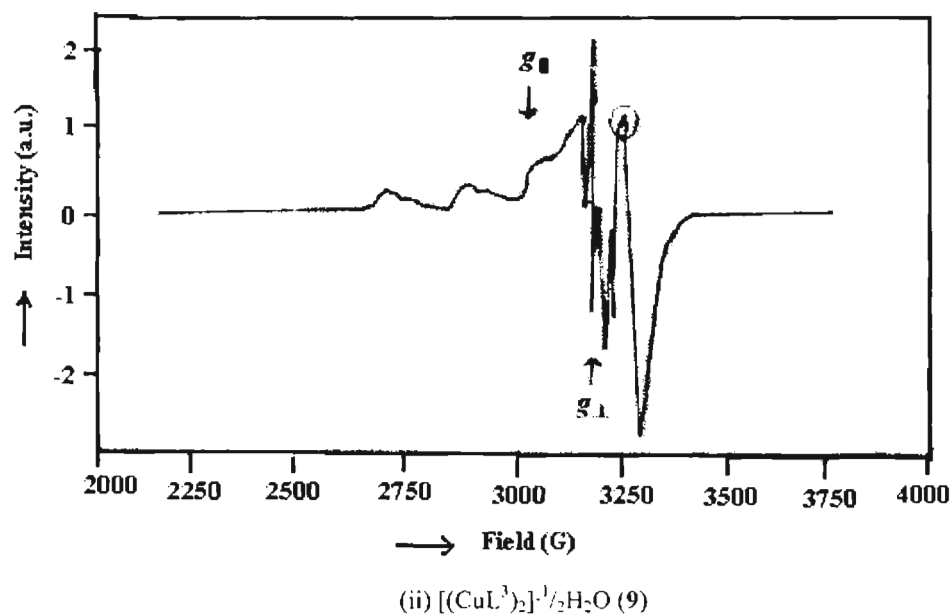


Figure 3.8. (i) EPR spectra of the compounds 4, 6 and 14 in polycrystalline state at 298 K

(ii) EPR spectra of the compounds 3, 9 and 10 in DMF at 77 K

References

1. M. A. Ali, D.A. Chowdhury, M. Nazimuddin *Polyhedron* 3 (1984) 595.
2. Nonius (1997). MACH3 software. B.V. Nonius, Delft, The Netherlands.
3. G.M. Sheldrick, *Acta Cryst.* A46 (1990) 467.
4. G.M. Sheldrick. SHELXL97, SHELXS97, University of Gottingen, Germany (1997).
5. K. Brandenburg, Diamond Version 3.0, Crystal Impact GbR, Bonn, Germany, 1997-2004.
6. A. L. Spek, ORTEP-III and PLATON, a Multipurpose Crystallographic Tool, Utrecht University, Utrecht, The Netherlands, 1999.
7. P.R. Athappan, G. Rajagopal, *Polyhedron* 15 (1996) 527.
8. G. Plesch, C. Friebel, *Polyhedron* 14 (1995) 1185.
9. A.W. Addison, T.N. Rao, J. Reedijk, J. Van Rijn, G.C. Verschoor, *J. Chem. Soc., Dalton Trans.* (1984) 1349.
10. G. Murphy, C.O. Sullivan, B. Murphy, B. Hathaway, *Inorg. Chem.* 37 (1998) 240.
11. M. Vaidyanathan, R. Balamurugan, U. Sivagnanam, M. Palaniandavar, *J. Chem. Soc., Dalton Trans.* (2001) 3498.
12. P.C. Chieh, G.J. Palenik, *Inorg. Chem.* 11 (1972) 816.
13. F. Clifford, E. Counihan, W. Fitzgerald, K. Seff, C. Simmons, S. Tyagi, B. Hathaway, *J. Chem. Soc., Chem. Commun.* (1982) 196.
14. N.J. Ray, B.J. Hathaway, *Acta Cryst.* B34 (1978) 3224.
15. G. Druhan, B.J. Hathaway, *Acta Cryst.* B35 (1979) 344.
16. S.S. Tandon, L.K. Thompson, J.N. Bridson, M. Bubenik, *Inorg. Chem.* 32 (1993) 4621.

17. R.J. Majeste, C.L. Klein, E.D. Stevens, *Acta Cryst.* C39 (1983) 52.
18. R.P. John, A. Sreekanth, M.R.P. Kurup, A. Usman, A.R. Ibrahim, H.-K. Fun, *Spectrochim. Acta* A59 (2003) 1349.
19. D.X. West, Y. Yang, T.L. Klein, K.I. Goldberg, A.E. Liberta, J.V. Martinez, R.A. Toscano, *Polyhedron* 14 (1995) 1681.
20. G. Smith, D.E. Lynch, T.C. W.Mak, W.H. Yip, C.H.L. Kennard, *Polyhedron* 12 (1993) 467.
21. Z. Lu, C. White, A.L. Rheingold, R.H. Crabtree, *Inorg. Chem.* 32 (1993) 3991.
22. B.S. Garg, M.R.P. Kurup, S.K. Jain, Y.K. Bhoon, *Trans. Met. Chem.* 13 (1988) 309.
23. P. Bindu, M.R.P. Kurup, T.R. Satyakeerty, *Polyhedron* 18 (1999) 321.
24. V. Philip, V. Suni, M.R.P. Kurup, M. Nethaji, *Polyhedron* 25 (2006) 1931
25. K. Nakamoto, *Infrared Spectra of Inorganic and Coordination Compounds*, 4th edn, Wiley-Interscience, New York, 1997, pp.256.
26. S.K. Jain, B.S. Garg, Y.K. Bhoon, *Spectrochim. Acta* 42A (1986) 701.
27. P. Bindu, M. R. P. Kurup, *Trans. Met. Chem.* 22 (1997) 578.
28. E.W. Ainscough, A.M. Brodie, N.G. Larsen, *Inorg. Chim. Acta* 60 (1982) 25.
29. M. Mikuriya, H. Okawa, S. Kida, *Bull. Chem. Soc. Japan* 53 (1980) 3717.
30. M. Joseph, M. Kuriakose, M.R.P. Kurup, E. Suresh, A. Kishore, S.G. Bhat, *Polyhedron* 25 (2006) 61.
31. I.M. Proctor, B.J. Hathaway, P. Nicholis, *J. Chem. Soc.* (1968) 1678.
32. S.S. Kandil, A. El-Dissouky, G.Y. Ali, *J. Coord. Chem.* 57 (2004) 105.
33. M.F. El-Shazly, A. El-Dissouky, T.M. Salem, M.M. Osman, *Inorg. Chim. Acta* 40 (1980) 1.

34. A. Sreekanth, M.R.P. Kurup, *Polyhedron* 22 (2003) 3321.
35. M.J. Bew, B.J. Hathaway, R.R. Faraday, *J. Chem. Soc., Dalton Trans.* (1972) 1229.
36. M. Joseph, V. Suni, M.R.P Kurup, M. Nethaji, A. Kishore, S. GBhat, *Polyhedron* 23 (2004) 3069.
37. A.H. Maki, B.R. McGarvey, *J. Chem. Phys.* 29 (1958) 31.
38. A.H. Maki, B.R. McGarvey, *J. Chem. Phys.* 29 (1958) 35.
39. D. Kivelson, R. Neiman, *J. Chem. Soc., Dalton Trans.* 35 (1961) 149.
40. B.N. Figgis, *Introduction to Ligand Fields Interscience*, New York, 1966, p 295.
41. V. Philip, V. Suni, M.R.P. Kurup, M. Nethaji, *Polyhedron* 24 (2005) 1133
42. B.J. Hathaway, *Structure and Bonding*, Springer Verlag, Heidelberg, 1973, p 60.
43. R.S. Nicholson, *Anal. Chem.* 37 (1965) 1351.
44. M. Assour, *J. Chem. Phys.* 43 (1965) 2477.
45. A. Abragam, M.H.L. Pryce, *Proc. R. Soc. London A*206 (1961) 164.
46. R.P. John, A. Sreekanth, V. Rajakannan, T.A. Ajith, M.R.P. Kurup, *Polyhedron* 23 (2004) 2549.

CHAPTER 4

**SYNTHESIS AND SPECTRAL STUDIES OF Ni(II) COMPLEXES OF
2-HYDROXYACETOPHENONE N(4)-CYCLOHEXYL
THIOSEMICARBAZONE**

4.1. Introduction

Nickel commonly shows only the +2 oxidation state in aqueous solution. The maximum coordination number shown by Ni(II) complexes is six corresponding to octahedral and distorted octahedral structures. Nickel(II) also forms five coordinate (square pyramidal and trigonal bipyramidal) and four coordinate (tetrahedral and square planar) complexes. Five coordinate geometry is quite unusual in Ni(II) complexes however, there are reports on such complexes [1]. One of the most remarkable facts about the stereochemistry of Ni(II) complexes is that equilibrium between different structural types exist in solution and these equilibria are temperature dependent also.

Nickel(II) is used as a spectroscopic probe in metal replacement studies of metalloenzyme systems. Nickel atom present in the active sites of several dehydrogenases and the chemistry of divalent and trivalent nickel complexes with nitrogen-sulfur donor ligands have received much attention [2].

This chapter describes the synthesis and characterization of three heterocyclic base adducts of Ni(II) complexes using spectral studies.

4.2. Experimental

4.2.1. Materials

The reagents used for the synthesis of 2-hydroxyacetophenone N(4)-cyclohexylthiosemicarbazone (H_2L^2) is discussed in Chapter 2. Ni(OAc)₂·4H₂O (Central drug house), 2,2'-bipyridine (bipy) (Central drug house),

1,10-phenanthroline (phen) (Ranbaxy fine chemicals) and 4,4'-dimethyl 2,2'-bipyridine (dmbipy) (E-Merck) were used. The reagents used were analar grade and used without further purification.

4.2.2. Synthesis of the complexes

[NiL²bipy]·H₂O (15)

To a hot ethanolic solution of the ligand H₂L² (1 mmol, 0.291 g), added hot methanolic solution of Ni(OAc)₂·4H₂O (1 mmol, 0.248 g) with constant stirring. This was followed by the addition of the base 2,2'-bipyridine (1 mmol, 0.156 g) in the solid form. The above brown solution was refluxed for about 3 h and allowed to cool, when brown crystalline compound was formed. The complex formed was filtered, washed with ethanol and ether and dried *in vacuo* over P₄O₁₀.

[NiL²phen]·2H₂O (16)

To a hot ethanolic solution of the ligand H₂L² (1 mmol, 0.291 g), added hot methanolic solution of Ni(OAc)₂·4H₂O (1 mmol, 0.248 g) with constant stirring. This was followed by the addition of the base 1,10-phenanthroline (1 mmol, 0.198 g) in the solid form. The above brown solution was refluxed for about 3 h and allowed to cool, when brown crystalline compound was formed. The complex formed was filtered, washed with ethanol and ether and dried *in vacuo* over P₄O₁₀.

[NiL²dmbipy]·CH₃OH (17)

To a hot ethanolic solution of the ligand H₂L² (1 mmol, 0.291 g), added hot methanolic solution of Ni(OAc)₂·4H₂O (1 mmol, 0.248 g) with constant stirring. This was followed by the addition of the base 4,4'-dimethyl 2,2'-bipyridine (1 mmol, 0.184 g) in the solid form. The above brown solution was refluxed for about 3 h and allowed to cool, when yellowish brown compound was formed. The complex formed was filtered, washed with ethanol and ether and dried *in vacuo* over P₄O₁₀.

4.3. Results and discussion

4.3.1. Physical measurements

The colors, partial elemental analyses and magnetic moments of the complexes are presented in Table 4.1. The elemental analyses data are consistent with the general empirical formula MLB , where M is the nickel metal atom, L is the doubly deprotonated thiosemicarbazone ligand and B is the bidentate heterocyclic bases *viz.* bipy, phen and dmbipy. Among the three nickel complexes, one is yellowish brown and the other two are brown in color. The complexes are insoluble in most of the common polar and non-polar solvents. They are soluble in DMF, $CHCl_3$ and DMSO.

Table 4.1. Analytical data

Compound	Color	Found (Calculated) %			μ (B.M.)
		C	H	N	
$[NiL^2bipy] \cdot H_2O$ (15)	Brown	57.49(57.06)	5.60(6.21)	13.41(12.32)	2.75
$[NiL^2phen] \cdot 2H_2O$ (16)	Brown	57.95(57.46)	6.01(5.54)	12.43(12.41)	2.56
$[NiL^2dmbipy] \cdot CH_3OH$ (17)	Yellowish brown	59.14(59.59)	6.78(6.25)	12.01(12.41)	2.01

Magnetic susceptibility measurements at 293 K suggest that the compounds **15-17** have magnetic moment values 2.75, 2.56 and 2.01 B.M. respectively. Normally five-coordinate high spin Ni(II) complexes have magnetic moment values in the range of 3.0-3.4 B.M, which are expected for a triplet spin ground state ($S=1$) of such complexes. But, in complexes **15-17**, the lower values suggest the anomalous

magnetic moment of the Ni(II) complexes. Anomalous magnetic moment for a metal ion is the one which falls outside the range of magnetic moment values predicted on the basis of the spin angular and orbital angular moment of the electrons in the metal ion [3,4]. Low magnetic moment values have already been reported for high spin pentacoordinate Ni(II) complexes with trigonal bipyramidal configuration [5], which is thought to arise from quenching of the orbital contribution to the magnetic moment due to distortion of D_{3h} symmetry [6]

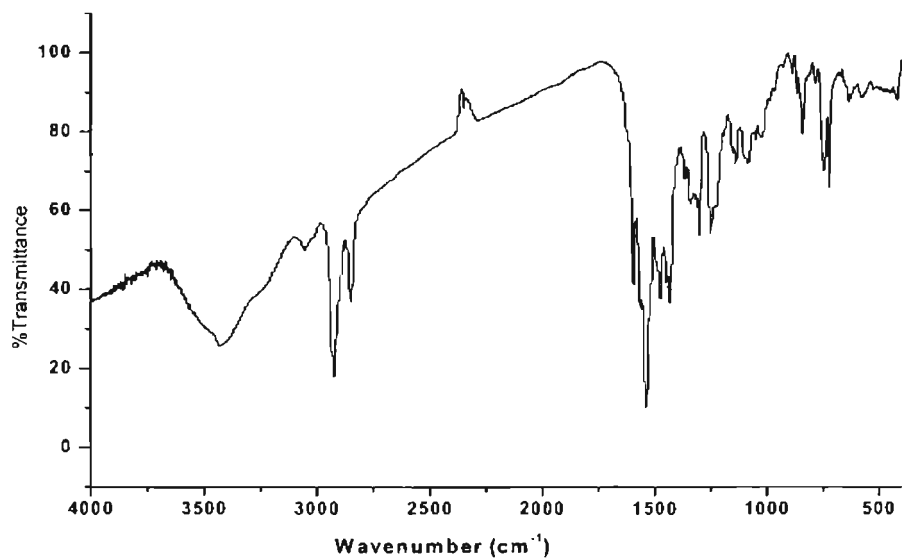
4.3.2. Infrared spectra

Table 4.2 lists the tentative assignments of main IR bands of Ni(II) complexes for the ligand H_2L^2 in 4000-50 cm^{-1} region. The spectrum of free ligand exhibits a medium band at *ca.* 3109 cm^{-1} , which is assigned to $\nu(N-H)$ vibration. The absence of $\nu(N-H)$ band in the spectra of complexes provides a strong evidence for the ligand coordination around Ni(II) ion in its deprotonated form. On coordination of azomethine nitrogen, $\nu(C=N)$ shifts to lower wavenumbers by 10-20 cm^{-1} , as the band shifts from 1613 cm^{-1} in the uncomplexed thiosemicarbazone spectrum to *ca.* 1596 cm^{-1} in the spectra of the three Ni(II) complexes. Coordination of azomethine nitrogen is confirmed with the presence of new band in the range 450-490 cm^{-1} , assignable to $\nu(Ni-N)$ for these complexes [7,8]. The $\nu(N-N)$ of the thiosemicarbazone is found at 1111 cm^{-1} . The increase in the frequency of this band in the spectra of the complexes, due to the increase in the bond strength, again confirms the coordination *via* the azomethine nitrogen.

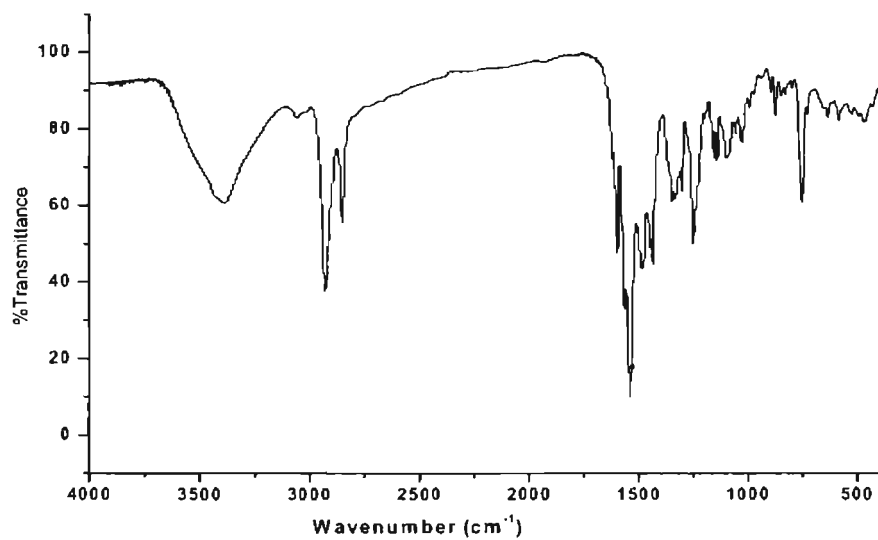
The decrease in the stretching frequency of $\nu(CS)$ band from 846 cm^{-1} in the thiosemicarbazone by 80-90 cm^{-1} upon complexation indicates coordination *via* its thiolato sulfur. Coordination of thiolato sulfur is confirmed with the presence of new band in the range 320-350 cm^{-1} , assignable to $\nu(Ni-S)$ for these complexes [9,10]. In all the three Ni(II) complexes, another strong band is found in the range 1530-1550

cm^{-1} , which may be due to the newly formed $\nu(\text{N}=\text{C})$ bond formed as a result of enolization. From this, it is clear that coordination *via* its thiolato sulfur takes place. In all the three Ni(II) complexes, phenolic oxygen is coordinated to nickel by loss of the $-\text{OH}$ proton. A new band at *ca.* 418 cm^{-1} in the spectra of the complexes is assignable to $\nu(\text{Ni}-\text{O})$ [11]. The IR spectra of the complexes **15**, **16** and **17** display bands characteristics of coordinated heterocyclic bases [12].

In the spectrum of the H_2L^2 ligand, there is a broad band at 3308 cm^{-1} , which may be due to the presence of phenolic group. But, in the complexes **15-17**, there are broad bands in the region $3200-3500$. In complexes **15** and **16**, water molecules and in complex **17**, methanol are present in non-stoichiometric proportions. In general, lattice water absorbs at $3200-3550 \text{ cm}^{-1}$ (antisymmetric and symmetric OH stretchings) and at $1600-1630 \text{ cm}^{-1}$ (HOH bending) [13]. It is clear from the spectra that the bands at 3430 cm^{-1} (in complex **15**) and at 3426 cm^{-1} (in complex **16**) are due to the presence of lattice water in these complexes. Compared to H_2L^2 ligand, the complex **17** shows a broad band at 3388 cm^{-1} . From the far IR spectrum, it is clear that phenolic oxygen is coordinated to the nickel atom in all the three complexes. Hence, in complex **17**, the broad band at 3388 cm^{-1} is due to the presence of methanolic $-\text{OH}$ group in that complex [14]. Representative spectra of the complexes **16** and **17** are presented in Figure 4.1.



[NiL²phen]·2H₂O (16)



[NiL²dmbipy]·CH₃OH (17)

Figure 4.1. IR spectra of the compounds 16 and 17

Table 4.2. Selected IR bands (cm^{-1}) with tentative assignments of Ni(II) complexes

Compound	$\nu(\text{C}=\text{N})$	$\nu(\text{N}=\text{C})$	$\nu(\text{N}-\text{N})$	$\nu(\text{C}-\text{S})$	$\nu(\text{C}-\text{O})$	$\nu(\text{Ni}-\text{O})$	$\nu(\text{Ni}-\text{N})$	$\nu(\text{Ni}-\text{N})$	$\nu(\text{Ni}-\text{S})$	Bands due to heterocyclic base
H_2L^2	1613	-----	1111	1358,846	1263	-----	-----	-----	-----	-----
$[\text{NiL}^2\text{bipy}]\cdot\text{H}_2\text{O}$	1596	1545	1155	1330,752	1247	415	490	347		1439,664
$[\text{NiL}^2\text{phen}]\cdot 2\text{H}_2\text{O}$	1595	1539	1134	1343,753	1244	407	453	329		1436,720
$[\text{NiL}^2\text{dmbipy}]\cdot\text{CH}_3\text{OH}$	1599	1533	1157	1337,757	1250	434	467	352		1430,621

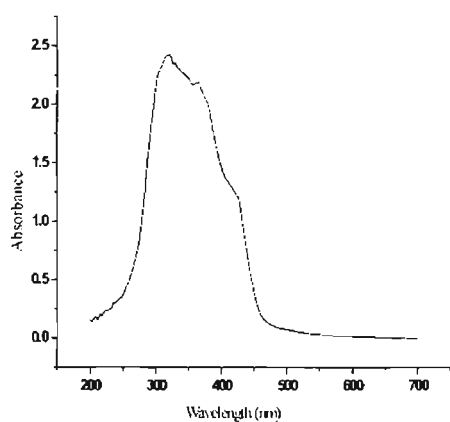
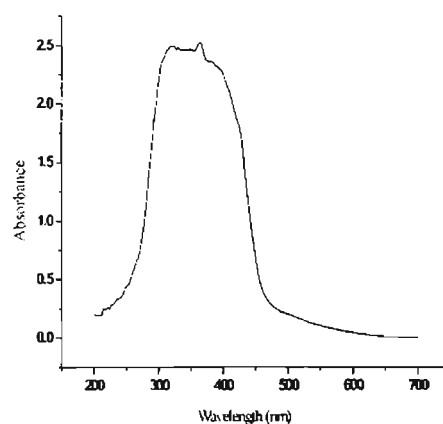
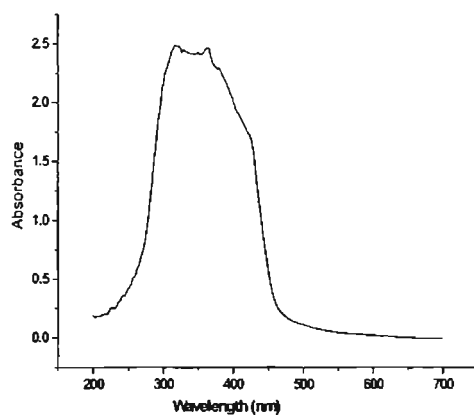
4.3.3. Electronic spectra

The electronic absorption bands of the Ni(II) complexes, recorded in DMF solution, are given in Table 4.3. The thiosemicarbazone (H_2L^2) has ring $\pi \rightarrow \pi^*$ bands at 36900 and 34120 cm^{-1} and a band at 30860 cm^{-1} due to $n \rightarrow \pi^*$ transition associated with the azomethine linkage. These bands suffer marginal shifts on complexation. The broad bands at *ca.* 31380 cm^{-1} in the spectra of the Ni(II) complexes are assigned for $n \rightarrow \pi^*$ transitions [15]. The shift of the $\pi \rightarrow \pi^*$ band to the longer wavelength region in the complexes is the result of the C=S band being weakened and conjugation system being enhanced after the formation of the complex [16].

Two ligand to metal charge transfer bands are found in the 27000 - 28000 cm^{-1} and 23000 - 24000 cm^{-1} ranges. In accordance with studies of previous Cu(II) and Ni(II) thiosemicarbazone complexes [17,18], higher energy band at *ca.* 27470 cm^{-1} is assigned to $S \rightarrow Ni^{II}$ transitions and its energy is dependent on the steric requirements of the N(4)-substituents. That is, thiosemicarbazones with bulkier N(4)-substituents have this band at somewhat higher energies. The band at *ca.* 23520 cm^{-1} is assignable to phenoxy $O \rightarrow Ni^{II}$ transitions. Each complex has a $d-d$ band in the range 14000 - 18000 cm^{-1} . Because of the presence of intense $\pi \rightarrow \pi^*$ and $n \rightarrow \pi^*$ transitions, these $d-d$ bands appear as weak shoulders on the intraligand and charge transfer bands [19]. The electronic spectra of the complexes **15-17** are very similar and show bands in the 14700 - 17240 cm^{-1} regions and at *ca.* 27470 cm^{-1} , which could be assigned to ${}^3B_1(F) \rightarrow {}^3E(F)$ and ${}^3B_1(F) \rightarrow {}^3A_2, {}^3E(P)$ transitions respectively. It has already been reported that these λ_{max} values are consistent with a distorted pentacoordinate environment around nickel(II) [20,21]. Representative spectra of the complexes **15-17** are presented in Figure 4.2.

Table 4.3. Electronic spectral assignments (cm^{-1}) for the ligand (H_2L^2) and its Ni(II) complexes

Compound	$\pi - \pi^*$	$n - \pi^*$	LMCT	d - d
H_2L^2	36900,34129	30864		
$[\text{NiL}^2\text{bipy}]\cdot\text{H}_2\text{O}$	32786	31250	27397,23474	17182
$[\text{NiL}^2\text{phen}]\cdot 2\text{H}_2\text{O}$	32894	31545	27548,23584	14749
$[\text{NiL}^2\text{dmbipy}]\cdot\text{CH}_3\text{OH}$	33003	31347	27472,23529	17211,16778

 $[\text{NiL}^2\text{bipy}]\cdot\text{H}_2\text{O}$ (15) $[\text{NiL}^2\text{phen}]\cdot 2\text{H}_2\text{O}$ (16) $[\text{NiL}^2\text{dmbipy}]\cdot\text{CH}_3\text{OH}$ (17)**Figure 4.2.** Electronic spectra of the compounds 15-17

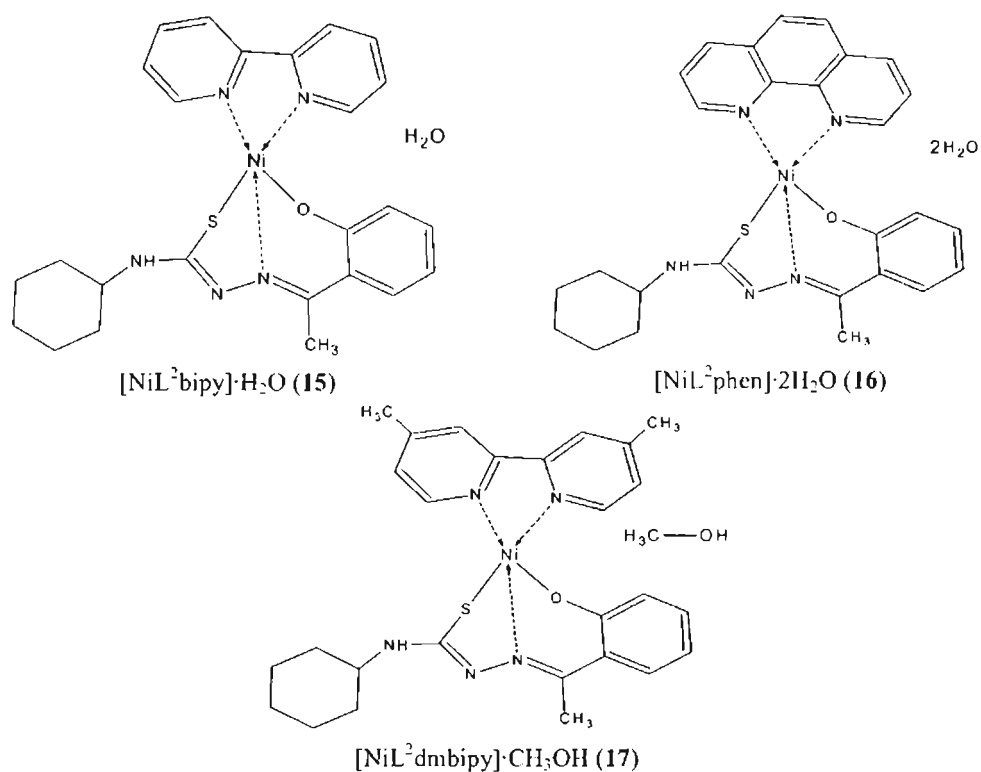


Figure 4.3. Tentative structure of the compounds 15-17

References

1. E. Bermejo, A. Castineiras, L.M. Fostiak, I. Gareia, A.L. Llamas, J.K. Swearingen, D.X. West, *J. Braz. Chem. Soc.* 56 (2001) 1297.
2. H.J. Kruger, R.H. Holm, *Inorg. Chem.* 28 (1989) 1148.
3. R.L. Dutta, A. Syamal, *Elements of Magnetochemistry*, 2nd edn, 1993, pp.157.
4. M.D. Santana, G. Garcia, A. Rufete, M.C.R. de Arellano, G. Lopez, *J. Chem. Soc., Dalton Trans.* (2000) 619.
5. S.L. Holt, R.J. Bouchard, R.L. Carlin, *J. Am. Chem. Soc.* 86 (1964) 519.
6. R.D. Bereman, G.D. Shields, *Inorg. Chem.* 18 (1979) 946.

7. P. Sousa, J.A. Garcia-Vasquez, J.R. Masaguer, *Trans. Met. Chem.* 9 (1984) 318.
8. D.X. West, A.A. Nassar, F.A. El-Saied, M.I. Ayad, *Trans. Met. Chem.* 23 (1998) 423.
9. S.K. Nag, D.S. Joarder, *Can. J. Chem.* 54 (1976) 2827.
10. R. Roy, M. Chaudhury, S.K. Mondal, K. Nag, *J. Chem. Soc., Dalton Trans.* (1984) 1681.
11. M. Mikuriya, H. Okawa, S. Kida, *Bull. Chem. Soc. Jpn.* 53 (1980) 3717.
12. P.B. Sreeja, M.R.P. Kurup, *Spectrochim. Acta* 61A (2005) 331.
13. K. Nakamoto, *Infrared Spectra of Inorganic and Coordination Compounds*, 4th edn, Wiley-Interscience, New York, 1997, pp.173.
14. M.D. Santana, G. Garcia, J. Perez, E. Molins, G. Lopez, *Inorg. Chem.* 40 (2001) 5701.
15. V. Philip, V. Suni, M.R.P. Kurup, M. Nethaji, *Polyhedron* 23 (2004) 1225.
16. Q. Li, H. Tang, Y. Li, M. Wang, L. Wang, C. Xia, *J. Inorg. Biochem.* 78 (2000) 167.
17. M.N. Alam, M. Nazimuddin, M.A. Ali, *Trans. Met. Chem.* 18 (1993) 497.
18. D.X. West, Y. Yang, T.L. Klein, K.I. Goldberg, A.E. Liberta, *Polyhedron* 14 (1995) 3051.
19. A.K. El-Sawaf, D.X. West, F.A. El-Saied, R.M. El-Bahnasawy, *Trans. Met. Chem.* 23 (1998) 417.
20. A.B.P. Lever, *Inorganic Electronic Spectroscopy*, Elsevier, Amsterdam, 1984, pp.513.
21. M.D. Santana, A.A. Lozano, G. Garcia, G. Lopez, J. Perez, *Dalton Trans.* (2005) 104.

CHAPTER 5

SYNTHESIS AND SPECTRAL STUDIES OF Mn(II) COMPLEXES OF N(4)-SUBSTITUTED THIOSEMICARBAZONES

5.1. Introduction

Manganese plays an important role in biological redox enzymes of many microorganisms, plants and animals and are exemplified by oxygen-evolving centres of photosystem II, superoxide dismutase (SOD) and catalases [1,2]. One of the most outstanding traits of manganese is its ability to adopt the widest variety of oxidation states among the 3*d* elements. The metal oxidation state is generally believed to lie in the range +2 to +4.

The (+2) oxidation state is the most common for manganese and it exists in the solid as well as in solution as complexes. In the presence of air, manganese(II) starting compounds reacted with primary hydroxamic acids producing hydroximato complexes of Mn^{III} or Mn^{IV} which invariably possess conjugated metal-ligand ring structure, but the secondary hydroxamic acids, which are incapable of forming such conjugation, produced only hydroxamato manganese(II) complexes. Manganese(III) occurs in superoxide dismutase, transferrin and catalase [3]. A sulfur function is implicated besides oxygen and nitrogen in the coordination sphere of manganese(III) in acid phosphatase [4].

Manganese(IV) is an enigmatic oxidation state. It is uncommon in coordination chemistry and is believed to be active in one of the most common reactions of nature namely photosynthetic oxygen evolution [5]. The use of mononuclear manganese(IV) complexes in the stoichiometric and catalytic oxidation of organic compounds makes the investigation of mononuclear manganese(IV) chemistry still meaningful.

This chapter describes the synthesis and characterization of two Mn(II) complexes using magnetic moment values, IR, electronic and EPR spectral studies.

5.2. Experimental

5.2.1. Materials

The reagents used for the synthesis of the ligands are discussed in Chapter 2 and were purified by standard methods and solvents were purified by distillation. Analar grade $\text{Mn}(\text{OAc})_2 \cdot 4\text{H}_2\text{O}$ (E-Merck) is used for the synthesis of complexes without further purification.

5.2.2. Synthesis of the complexes

$[\text{Mn}(\text{HL}^2)_2] \cdot \text{H}_2\text{O}$ (18)

To a hot ethanolic solution of the ligand H_2L^2 (2 mmol, 0.582 g), added hot ethanolic solution of $\text{Mn}(\text{OAc})_2 \cdot 4\text{H}_2\text{O}$ (1 mmol, 0.245 g) with constant stirring. The above brown solution was refluxed for about 3 h and allowed to cool. The yellow crystalline compound formed was filtered, washed with ethanol and ether and dried *in vacuo* over P_4O_{10} .

$[\text{Mn}(\text{HL}^3)_2]$ (19)

To a hot ethanolic solution of the ligand H_2L^3 (2 mmol, 0.542 g), added hot ethanolic solution of $\text{Mn}(\text{OAc})_2 \cdot 4\text{H}_2\text{O}$ (1 mmol, 0.245 g) with constant stirring. The above brown solution was refluxed for about 3 h and allowed to cool. The brown compound formed was filtered, washed with ethanol and ether and dried *in vacuo* over P_4O_{10} .

5.3. Results and discussion

5.3.1. Physical measurements

The colors, partial elemental analyses and magnetic moments values of the two

Mn(II) complexes are presented in Table 5.1. The two complexes synthesized using the two ligands have the same composition, $Mn(HL)_2$, ie, a structure in which two monoanionic ligands are coordinated to the Mn(II) ion. Compound **18** is yellow and the compound **19** is brown in color. All the compounds are soluble in polar organic solvents like CH_2Cl_2 , $CHCl_3$, DMF and DMSO.

The magnetic moments of the two Mn(II) complexes at 296 K were calculated from the magnetic susceptibility measurements. The diamagnetic corrections were applied using Pascals' constants. It is reported that for high spin Mn(II) compounds with d^5 configuration, the magnetic moment values are in the range 5.65 – 6.10 B.M [6]. The magnetic moments for the compounds **18** and **19** are 5.92 and 5.67 B.M respectively, indicating the presence of five unpaired electrons and hence these are high spin complexes [7].

Table 5.1. Analytical data

Compound	Color	Found (Calculated) %			μ (B.M.)
		C	H	N	
$[Mn(HL^2)_2] \cdot H_2O$ (18)	Yellow	54.96(55.11)	6.46(6.48)	12.70(12.85)	5.92
$[Mn(HL^3)_2]$ (19)	Brown	56.11(56.46)	3.71(4.06)	13.92(14.11)	5.67

5.3.2. Infrared spectra

The infrared spectral assignments (cm^{-1}) of ligands H_2L^2 and H_2L^3 and their Mn(II) complexes are given in Table 5.2. The $\nu(C=N)$ band of thiosemicarbazones are found to be shifted to lower wavenumbers by 10-20 cm^{-1} , as the band shifts from *ca.* 1613 cm^{-1} in the uncomplexed thiosemicarbazone spectrum to *ca.* 1596 cm^{-1} in the spectra of the two Mn(II) complexes suggesting the coordination of the

azomethine nitrogen to the Mn(II) ion. The involvement of this nitrogen in bonding is also supported by a shift in $\nu(\text{N-N})$ to higher frequencies. Coordination of azomethine nitrogen is confirmed with the presence of new band in the range $450\text{-}470\text{ cm}^{-1}$, assignable to $\nu(\text{Mn-N})$ for these complexes [8,9].

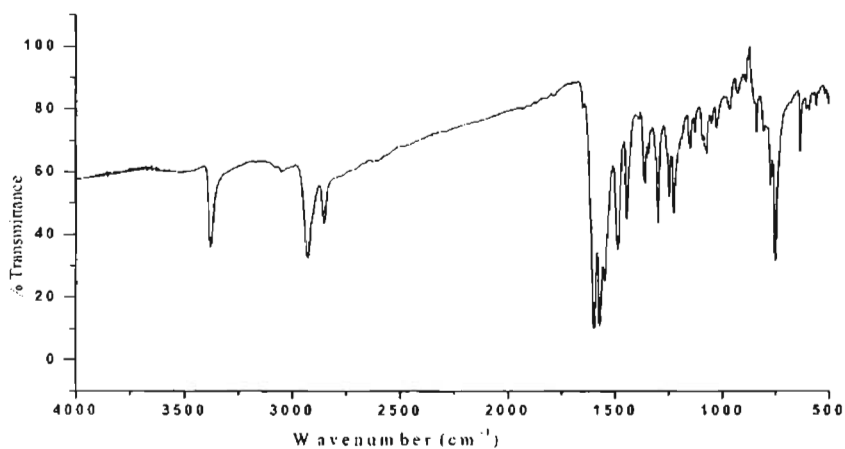
Upon complexation, the $\nu(\text{C=S})$ band shifts to lower wavenumbers and that may be due to the formation of strong metal-sulfur bonds [10]. The IR spectra of the thiosemicarbazone ligands display strong bands at *ca.* 860 cm^{-1} , which may be due to $\nu(\text{C=S})$. In complexes **18** and **19**, the $\nu(\text{C=S})$ band was found to be shifted to lower wavenumbers compared to that in the ligands. The absence of a second $\nu(\text{N=C})$ band is due to lack of enolization of the ligands. This supports that coordination takes place through the thioketo sulfur atom.

Table 5.2. Selected IR bands (cm^{-1}) with tentative assignments of ligands and Mn(II) complexes

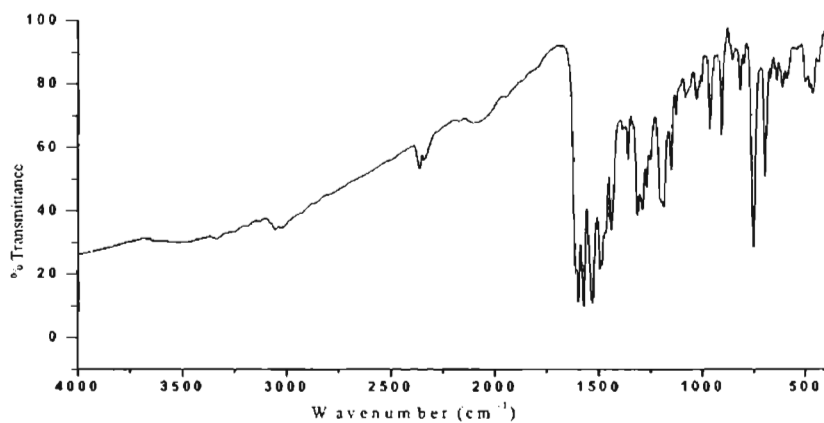
Compound	$\nu(\text{C=N})$	$\nu(\text{N-N})$	$\nu(\text{C=S})$	$\nu(\text{C-O})$	$\nu(\text{Mn-O})$	$\nu(\text{Mn-N})$
H_2L^2	1613	1111	1358,846	1263		
$[\text{Mn}(\text{HL}^2)_2] \cdot \text{H}_2\text{O}$ (18)	1599	1154	1362,748	1295	554	463
H_2L^3	1613	1149	1328,874	1255		
$[\text{Mn}(\text{HL}^3)_2]$ (19)	1594	1185	1354,744	1265	584	456

In the spectra of the ligands H_2L^2 and H_2L^3 , there are broad bands at 3308 and 3336 cm^{-1} respectively, which may be due to the presence of $\nu(\text{OH})$ of the phenolic group. The disappearance of these bands in the spectra of the complexes **18** and **19** indicates that the phenolic proton is lost upon complexation with metal ion. In thiosemicarbazone ligands, the band at *ca.* 1259 cm^{-1} is due to $\nu(\text{C-O})$, which is shifted to *ca.* 1280 cm^{-1} in the complexes, indicating the coordination of O^-

Coordination of phenoxy oxygen is confirmed with the presence of a new band in the range $550\text{-}570\text{ cm}^{-1}$, assignable to $\nu(\text{Mn-O})$ for these two Mn(II) complexes [11]. Representative spectra of the complexes **18** and **19** are shown in Figure 5.1.



[Mn(HL²)₂]·H₂O (18)



[Mn(HL³)₂] (19)

Figure 5.1. IR spectra of the compounds **18** and **19**

5.3.3. Electronic spectra

The electronic absorption bands and ligand field parameters of the Mn(II) complexes, recorded in DMF solution, are given in Table 5.3 and representative spectra are in Figure 5.2. The Mn(II) belongs to the $3d^5$ system. The ground state term for high spin d^5 configuration is 6S . In the Tanabe-Sugano diagram for d^5 octahedral Mn(II), the notation for ground state changes to ${}^6A_{1g}$, which is taken as the abscissa, with the energies of the other states being plotted relative to it. Since there is no excited state with the spin multiplicity 6, all electronic transitions in a high-spin d^5 complexes are doubly forbidden, *ie*, Laporte as well as spin forbidden [12].

The absorption bands observed at *ca.* 29960 and 34570 cm^{-1} are due to $n \rightarrow \pi^*$ and $\pi \rightarrow \pi^*$ transitions of the ligands which suffer marginal shifts on complexation. The intense band at *ca.* 23250 cm^{-1} is assignable to the $S_{(p\pi)} \rightarrow M_{(d\pi)}$ LMCT transition, while the broad high intensity peak at *ca.* 25390 cm^{-1} is assignable to the phenolato oxygen \rightarrow Mn charge transfer band, which is identical to octahedral Mn^{2+} complexes [13,14,15].

For octahedral Mn(II) complexes, the electronic spectra were expected to show bands at *ca.* 17930, 23250 and 25400 cm^{-1} represents three spin-allowed d-d transitions *ie*, ${}^6A_{1g} \rightarrow {}^4T_{1g}(G)$, ${}^6A_{1g} \rightarrow {}^4T_{2g}(G)$ and ${}^6A_{1g} \rightarrow {}^4E_g$, ${}^4A_{1g}(G)$ transitions respectively. These bands fit the Tanabe-Sugano diagram for d^5 octahedral at $Dq/B = 1.1$. At this Dq/B , the ratio of the first transition energy and B (*ie*, E/B) is found to be 24.0. The electronic repulsion parameter (Racah parameter) 'B' is a function of the ligand and the metal ion and is a built in feature of these Tanabe-Sugano diagrams [12]. The extent of covalence in the metal ligand bond may be evaluated from the electronic spectrum by estimating the nephelauxetic ratio (β) = B/B_0 . The free ion value of B_0 for Mn^{2+} is 860 cm^{-1} . The value of β is always less than one and it decreases with increasing delocalization [16].

Table 5.3. Electronic spectral assignments (cm^{-1}) and ligand field parameters of Mn(II) complexes

Compound	${}^6A_{1g} \rightarrow {}^4T_{1g}(G)$	${}^6A_{1g} \rightarrow {}^4T_{2g}(G)$	${}^6A_{1g} \rightarrow {}^4E_g,$ ${}^4A_{1g}(G)$	$n - \pi^*$	$\pi - \pi^*$	B	10Dq (Δ)	β
$[\text{Mn}(\text{HL}^2)_2] \cdot \text{H}_2\text{O}$ (18)	18348	23094	24752	28735	37878	764.5	8409.5	0.88
$[\text{Mn}(\text{HL}^3)_2]$ (19)	17513	23419	26041	28818	38022	729.7	8026.7	0.84

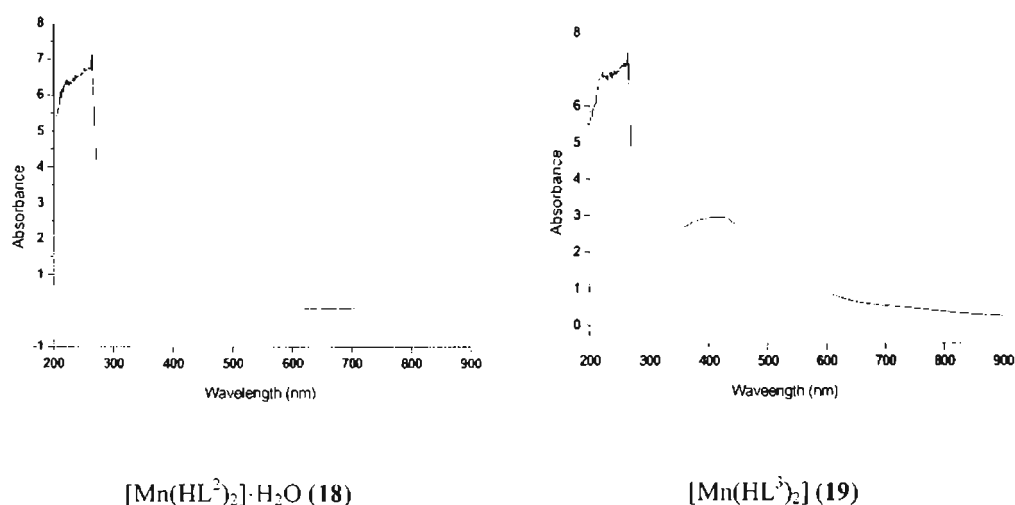


Figure 5.2. Electronic spectra of the compounds 18 and 19

5.3.4. EPR spectra

The high spin Mn(II) has ${}^6S_{5/2}$ ground state which should not interact with the electric field in the first order case. Consider a system with $S = 5/2$, $I = 5/2$, the spin Hamiltonian

$$\hat{H} = g\beta H \cdot S + D[S_z^2 - 1/3 S(S+1)] + AS \cdot I \quad \text{----- (1)}$$

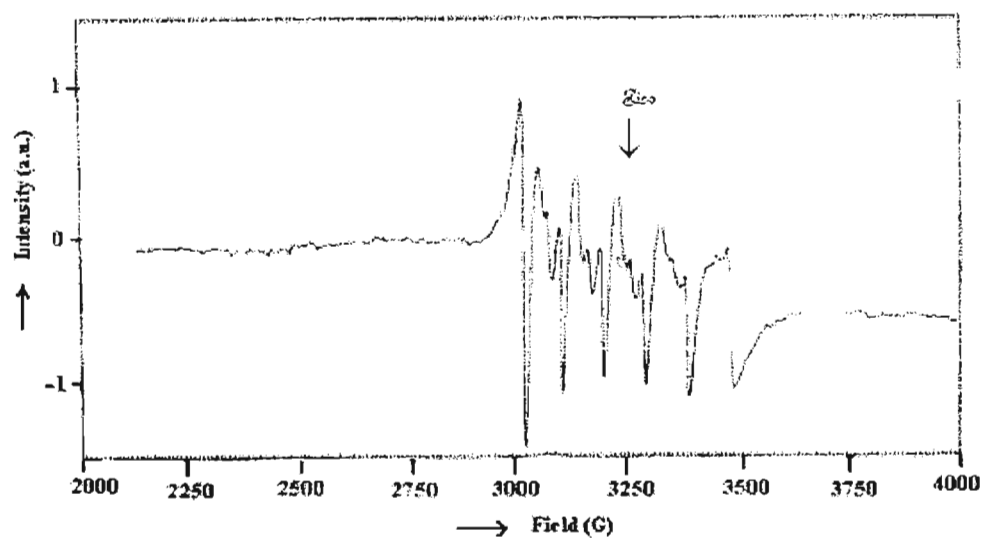
where H is the magnetic field vector, g is the spectroscopic splitting factor, β is the Bohr magneton, D is the axial zero field splitting term, S is the electron spin vector and A is the nuclear hyperfine splitting term [17]. The nuclear hyperfine splitting term (A) from the spin Hamiltonian (Eq.1) is usually applicable to high-spin manganese ion and can be determined directly from the spectra. The interpretation of the spectra in Figure 5.3 are basically the same as that proposed earlier by Allen and Nebert [18], in which both allowed and forbidden hyperfine lines occurred in the observed spectrum and were supposed to be due to a mixing of the hyperfine levels

by an axial zero-field splitting term D in the spin Hamiltonian. The same basic interpretation of the spectra is used here in the two Mn(II) complexes, but attention is centered upon the allowed transitions only. The hyperfine spectrum consists of six allowed lines corresponding to $m = +5/2, +3/2, +1/2, -5/2$ and $\Delta m_l = 0$ in the transition, in between each of which is a forbidden doublet, corresponding to $\Delta m_l = \pm 1$. Such forbidden transitions are brought about according to Bleaney and Low [19,20] by a mixing of the nuclear hyperfine levels by the zero-field splitting parameter D of (1).

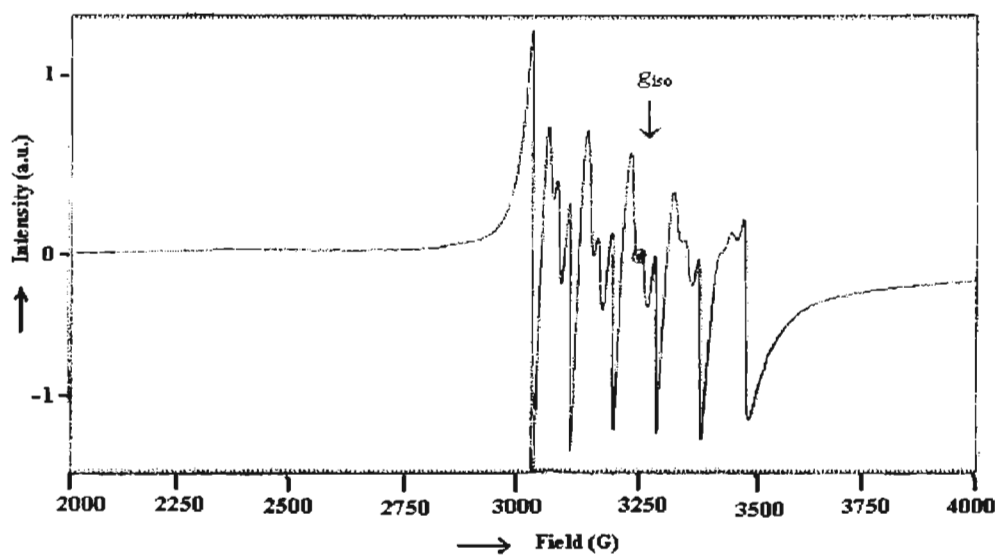
The EPR spectra of the Mn(II) compounds **18** and **19** in the polycrystalline state at 298 K gave broad signal with g values 1.993 and 2.004 respectively. In polycrystalline samples at 298 K, Mn(II) complexes give very broad signals, which are due to dipolar interactions and enhanced spin lattice relaxation [21].

The EPR spectra of the compounds **18** and **19** in frozen DMF solution at 77 K are almost similar exhibiting six-line hyperfine splitting for ^{55}Mn ($I = 5/2$) and is centered at $g = 2.001$ and 1.999 respectively. At 77 K, the electron paramagnetic resonances are at 480 and 486 G respectively for compounds **18** and **19** with an average hyperfine coupling constant (A_{iso}) of 96 G ($89.76 \times 10^{-4} \text{ cm}^{-1}$) and 97.2 G ($90.73 \times 10^{-4} \text{ cm}^{-1}$) respectively.

The observed g values are very close to the free-spin value of 2.0, indicating the absence of spin-orbit coupling in the ground state 6A_1 . The A_{iso} values are consistent with an octahedral environment. The A_{iso} values are somewhat lower than for pure ionic compounds and effect the covalent nature of the metal-ligand bonds [22].



[Mn(HL²)₂]·H₂O (18)



[Mn(HL³)₂] (19)

Figure 5.3. EPR spectra of the compounds 18 and 19 in DMF at 77 K

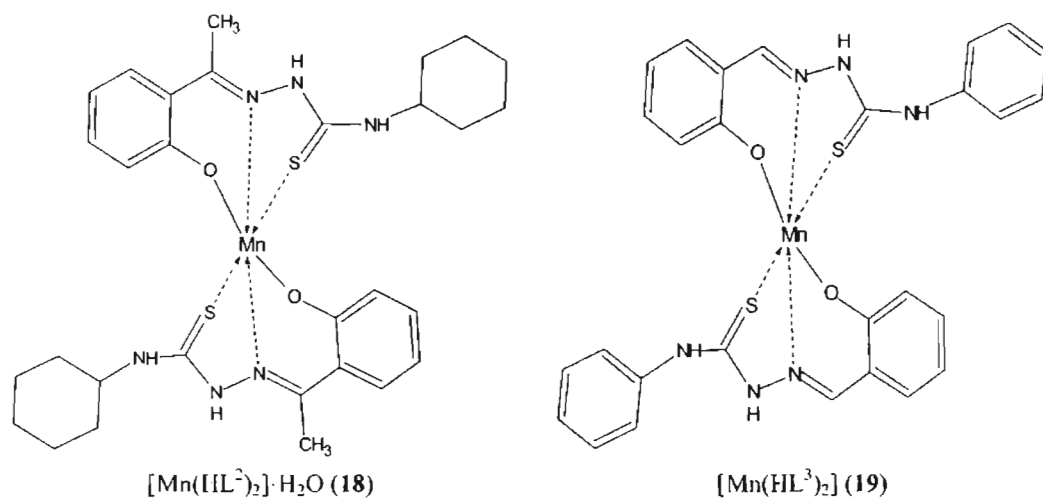


Figure 5.4. Tentative structure of the compounds 18 and 19

References

1. M. Yagi, M. Kaneko, *Chem. Rev.* 101 (2001) 21.
2. J.C. Vites, M.M. Lynam, *Coord. Chem. Rev.* 131 (1994) 95.
3. R. Mukhopadhyay, S. Bhattacharjee, S. Karmakar, R. Bhattacharyya, C.K. Pal, *J. Chem. Soc., Dalton Trans.* (1997) 2267.
4. J.S. Bashkin, J.C. Huffman, G. Christou, *J. Am. Chem. Soc.* 108 (1986) 5038.
5. J.C. DePaula, G.W. Brudvig, *J. Am. Chem. Soc.* 107 (1985) 2643.
6. J.E. Huheey, E.A. Keiter, R.L. Keiter, *Inorganic chemistry* 4th edn, Addison-Wesley, New York, 1993, pp.465.
7. B.N. Figgis, J. Lewis, *Prog. Inorg. Chem.* 6 (1964) 37.
8. V.B. Rana, J.N. Gurtu, M.P. Teotia, *J. Inorg. Nucl. Chem.* 42 (1980) 331.
9. R.P. John, A. Sreekanth, M.R.P. Kurup, H.-K. Fun, *Polyhedron* 24 (2005) 601.

10. D.K. Demertzi, U. Gangadharmath, M.A. Demertzis, Y. Sanakis, *Inorg. Chem. Commun.* 8 (2005) 619.
11. R. Mukhopadhyay, S. Bhattacharjee, R. Bhattacharyya, *J. Chem. Soc., Dalton Trans.* (1994) 2799.
12. R.L. Dutta, A. Syamal, *Elements of Magnetochemistry*, 2nd edn, 1993, pp.102.
13. S. Pal, P. Ghosh, A. Chakravorty, *Inorg. Chem.* 24 (1985) 3704.
14. S.K. Chandra, P. Basu, D. Ray, S. Pal, A. Chakravorty, *Inorg. Chem.* 29 (1990) 2423.
15. U. Auerbach, T. Weyhermuller, K. Wieghardt, B. Nuber, E. Bill, C. Butzlaff, A.X. Trautwein, *Inorg. Chem.* 32 (1993) 508.
16. R.L. Dutta, A. Syamal, *Elements of Magnetochemistry*, 2nd edn, 1993, pp.98.
17. B.T. Allen, *J. Chem. Phys.* 43 (1965) 3820.
18. B.T. Allen, D.W. Nebert, *J. Chem. Phys.* 41 (1964) 1983.
19. B. Bleaney, R.S. Rubins, *Proc. Phys. Soc. A* 77 (1961) 103.
20. E. Friedman, W. Low, *Phys. Rev.* 120 (1960) 408.
21. A. Sreekanth, M. Joseph, H.-K. Fun, M.R.P. Kurup, *Polyhedron* 25 (2006) 1408.
22. B.S. Garg, M.R.P. Kurup, S.K. Jain, Y.K. Bhoon, *Trans. Met. Chem.* 13 (1988) 92.

CHAPTER 6

**SYNTHESIS, SPECTRAL AND STRUCTURAL STUDIES OF
Zn(II) COMPLEXES OF SALICYLALDEHYDE
N(4)-PHENYLTHIOSEMICARBAZONE**

6.1. Introduction

Zinc atom has either a structural or analytical role in several proteins. It has been recognized as an important cofactor in biological molecules, either as a structural template in protein folding or as a Lewis acid catalyst that can readily adopt 4-, 5- or 6-coordination [1]. Zinc is able to play a catalytic role in the activation of thiols as nucleophiles at physiological pH. Mononuclear zinc complexes may serve as model compounds for zinc enzymes such as phospholipase C, bovine lens leucine aminopeptidase, ATPases, carbonic anhydrases and peptide deformylase. Binuclear cores are versatile at active sites of many metalloenzymes and play essential role in biological systems.

The Zn^{2+} ion having d^{10} configuration and display a variety of coordination numbers and geometries based on the interplay of electrostatic forces, covalence and the size factor. The zinc(II) ion is known to have a high affinity towards nitrogen and sulfur donor ligands. Perkin and co-workers investigated zinc(II) complexes with mixed N, O and S coordination to understand the reactivity of the pseudotetrahedral zinc center in proteins [2].

Complexes of Group 12 metals, mainly zinc, can provide an interesting range of stoichiometries depending on the preparative salt. This chapter describes the synthesis and characterization of five Zn(II) complexes of salicylaldehyde N(4)-phenylthiosemicarbazone using infrared, electronic and 1H NMR studies. It also describes the single crystal X-ray diffraction studies of one of the prepared compound, that is the first heterocyclic base adduct Zn(II) complex with five coordinated geometry.

6.2. Experimental

6.2.1. Materials

The reagents used for the synthesis of salicylaldehyde N(4)-phenylthiosemicarbazone (H_2L^3) are discussed in chapter 2. $Zn(OAc)_2 \cdot 2H_2O$ (S.D.Fine chemicals), 2,2'-bipyridine (bipy) (Central drug house), 1,10-phenanthroline (phen) (Ranboxy fine chemicals) and 4,4'-dimethyl 2,2'-bipyridine (dmbipy) (E-Merck) were used. The reagents used were of analar grade and used without further purification. The ligands were recrystallized from ethanol and dried *in vacuo* before complexation.

6.2.2. Synthesis of the complexes

$[(ZnL^3)_2] \cdot 3C_2H_5OH$ (20)

To a solution of H_2L^3 (1 mmol, 0.271 g) in hot ethanol was added an ethanolic solution of $Zn(OAc)_2 \cdot 2H_2O$ (1 mmol, 0.219 g) with constant stirring. The stirring was continued for about an hour when yellow compound which got separated were filtered, washed with ethanol and ether and dried *in vacuo* over P_4O_{10} .

$[Zn(HL^3)_2] \cdot C_2H_5OH$ (21)

A solution of $Zn(OAc)_2 \cdot 2H_2O$ (1 mmol, 0.219 g) in ethanol and a solution of H_2L^3 (2 mmol, 0.542 g) in hot ethanol were mixed and refluxed for 4 h. On cooling, yellow solid separated was filtered, washed with ethanol and ether and dried *in vacuo* over P_4O_{10} .

$[ZnL^3bipy] \cdot \frac{1}{2}H_2O$ (22)

To a solution of H_2L^3 (1 mmol, 0.271 g) in hot ethanol was added an ethanolic solution of $Zn(OAc)_2 \cdot 2H_2O$ (1 mmol, 0.219 g) with constant stirring. This was followed by the addition of the base 2,2'-bipyridine (1 mmol, 0.156 g) in the solid form. The stirring was continued for about an hour when yellow crystalline compound was formed, which were filtered, washed with ethanol and ether and dried *in vacuo* over P_4O_{10} .

$[ZnL^3phen] \cdot H_2O$ (23)

To a solution of H_2L^3 (1 mmol, 0.271 g) in hot ethanol was added an ethanolic

solution of $\text{Zn}(\text{OAc})_2 \cdot 2\text{H}_2\text{O}$ (1 mmol, 0.219 g) with constant stirring. This was followed by the addition of the base 1,10-phenanthroline (1 mmol, 0.198 g) in the solid form. The stirring was continued for about an hour when yellow compound began to separate. This was filtered, washed with ethanol and ether and dried *in vacuo* over P_4O_{10} .

$[\text{ZnL}^3\text{dmbipy}]$ (**24**)

To a solution of H_2L^3 (1 mmol, 0.271 g) in hot ethanol was added an ethanolic solution of $\text{Zn}(\text{OAc})_2 \cdot 2\text{H}_2\text{O}$ (1 mmol, 0.219 g) with constant stirring. This was followed by the addition of the base 4,4'-dimethyl 2,2'-bipyridine (1 mmol, 0.184 g) in the solid form. The stirring was continued for about an hour when yellow compound began to separate. This was filtered, washed with ethanol and ether and dried *in vacuo* over P_4O_{10} .

6.2.3. X-Ray crystallography

A yellow block crystal of the compound $[\text{ZnL}^3\text{bipy}]$ having approximate dimensions 0.40 x 0.35 x 0.20 mm was sealed in a glass capillary and intensity data were measured at 293(2) K. The data acquisition and cell refinement were done using the Argus (Nonius, MACH3 software) [3]. The Maxus (Nonius software) were used for data reduction [4]. The structure was solved by direct methods and full-matrix least-squares refinement using SHELX97 [5] package. The positions of all the non-hydrogen atoms were included in the full-matrix least-squares refinement using SHELX97 program and all the hydrogen atoms were fixed in calculated positions. The structure of the compound **22** was plotted using the program Diamond Version 3.0 [6] and PLATON [7]. The crystal data and structure refinement parameters for $[\text{ZnL}^3\text{bipy}]$ are given in Table 6.1.

Table 6.1. Crystal Data and Structure refinement parameters for [ZnL³bipy]

Empirical formula	C ₂₄ H ₁₉ N ₅ O S Zn
Formula weight	490.87
Temperature	293(2) K
Wavelength	0.71073 Å
Crystal system	Orthorhombic
Space group	<i>P</i> 2 ₁ <i>cn</i>
Unit cell dimensions	a = 9.8250(16) Å b = 10.5580(6) Å c = 20.7990(12) Å α = 90° β = 90° γ = 90°
Volume	2157.5(4) Å ³
Z	4
Density (calculated)	1.511 Mg/ m ³
Absorption coefficient	1.263 mm ⁻¹
F(000)	1008
Crystal size	0.40 x 0.35 x 0.20 mm
θ range for data collection	1.96 - 24.96°
Index ranges	-11 ≤ h ≤ 0, -12 ≤ k ≤ 0, -24 ≤ l ≤ 0
Reflections collected	2012
Independent reflections	2012 [R(int) = 0.0000]
Refinement method	Full-matrix least-squares on F ²
Data / restraints / parameters	2012 / 1 / 293
Goodness-of-fit on F ²	1.017
Final R indices [I > 2σ(I)]	R ₁ = 0.0383, wR ₂ = 0.0681
R indices (all data)	R ₁ = 0.0923, wR ₂ = 0.0795
Largest diff. peak and hole	0.324 and -0.380 e.Å ⁻³

6.3. Results and discussion

6.3.1. Physical measurements

The colors and partial elemental analyses of the complexes are presented in Table 6.2. The elemental analyses data are consistent with the general composition (ML)₂, M(HL)₂ and MLB, where M is the zinc atom, L is the doubly deprotonated thiosemicarbazone ligand and B is the bidentate heterocyclic bases *viz.* bipy, phen and dmbipy. All the zinc complexes are yellow in color. Elemental analyses data shows both compounds **20** and **21** having ethanol molecules and compounds **22** and **23** having water molecules present as solvents of crystallization. In compound **24**, there is neither ethanol nor water of crystallization present in it. Compound **20** is binuclear and the others are

mononuclear in nature. The complexes are insoluble in most of the common polar and non-polar solvents. They are soluble in DMF, CHCl_3 and DMSO.

Table 6.2. Analytical data

Compound	Color	Found (Calculated) %		
		C	H	N
$[(\text{ZnL}^3)_2] \cdot 3\text{C}_2\text{H}_5\text{OH}$ (20)	Yellow	50.14(50.56)	5.08(4.99)	10.55(10.41)
$[\text{Zn}(\text{HL}^3)_2] \cdot \text{C}_2\text{H}_5\text{OH}$ (21)	Yellow	54.77(55.25)	4.49(4.64)	13.35(12.89)
$[\text{ZnL}^3\text{bipy}] \cdot \frac{1}{2}\text{H}_2\text{O}$ (22)	Yellow	57.92(57.66)	3.88(4.03)	14.02(14.01)
$[\text{ZnL}^3\text{phen}] \cdot \text{H}_2\text{O}$ (23)	Yellow	58.63(58.60)	3.96(3.97)	13.13(13.14)
$[\text{ZnL}^3\text{dmbipy}]$ (24)	Yellow	59.90(60.18)	4.58(4.47)	13.38(13.50)

6.3.2. Crystal structure of the compound $[\text{ZnL}^3\text{bipy}]$

The molecular structure of the compound **22** along with the atom numbering scheme is represented in Figure 6.1 and selected bond lengths and bond angles are summarized in Table 6.3. Suitable pale yellow crystals were obtained by recrystallization from a mixture of CH_3OH and CH_3CN solutions. The compound **22** is orthorhombic with a space group $P2_1cn$. The zinc atom in **22** is mononuclear and five coordinated. In the complex $[\text{ZnL}^3\text{bipy}]$, Zn(II) is located in an approximately trigonal bipyramidal geometry in which the equatorial positions are occupied by the S(1), O(1), N(2) and the axial positions by N(1) and N(3) [$\text{Zn}(1)\text{--N}(1)$, 2.164(5), $\text{Zn}(1)\text{--N}(3)$, 2.098(5) Å] with the N(3)–Zn(1)–N(1) angle of $177.5(2)^\circ$ being close to the ‘ideal’ value of 180° which is usual for such systems [8]. In a five-coordinate system, the angular

structural parameter (τ) is used to propose an index of trigonality. The trigonality index τ of 0.53 [According to Addison *et al.*, $\tau = (\beta - \alpha)/60$, where $\beta = \text{N}(3)\text{--Zn}(1)\text{--N}(1) = 177.5(2)^\circ$ and $\alpha = \text{O}(1)\text{--Zn}(1)\text{--S}(1) = 145.18(16)^\circ$; for perfect square pyramidal and trigonal bipyramidal geometries the values of τ are zero and unity respectively] indicates that the coordination geometry around zinc is intermediate between trigonal bipyramidal and square pyramidal geometries and is better described as trigonal bipyramidal distorted square based pyramid (TBDSBP) with zinc displaced 0.3225 Å above the N(1), N(3), O(1) and S(1) coordination plane and towards the elongated apical N(2) atom [9].

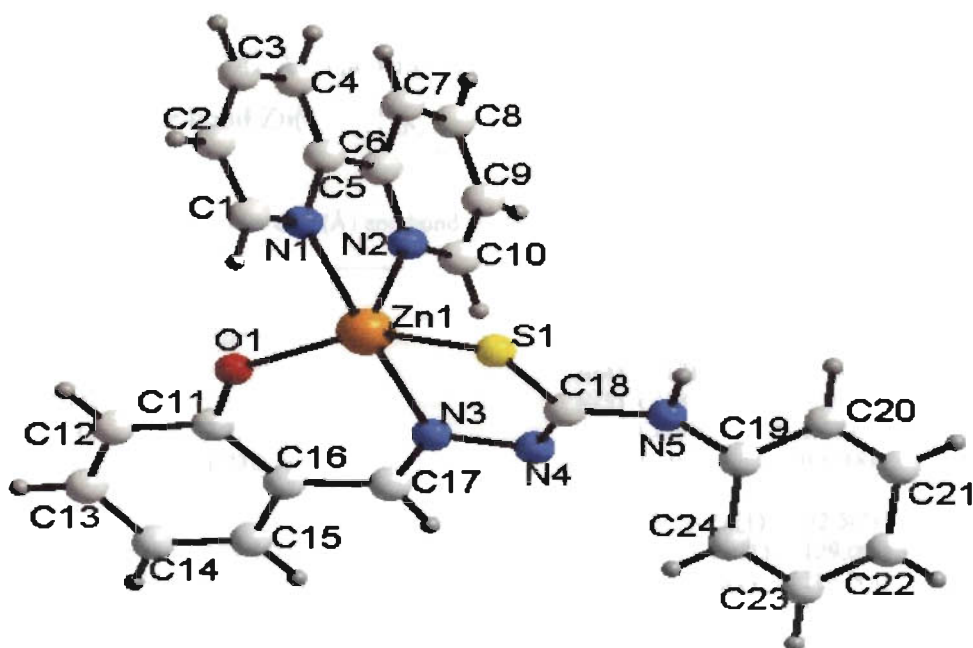


Figure 6.1. Structure and labeling diagram of the compound 22

One of the reasons for the deviation from an ideal stereochemistry is the restricted bite angle imposed by both the L^{3-} and bipy ligands. The bite angle around the metal viz. $\text{N}(2)\text{--Zn}(1)\text{--N}(1)$ of $77.1(2)^\circ$ may be considered normal, when compared with an average

value of 77° cited in the literature [10,11]. The variation in Zn–N bond distances, Zn(1)–N(2), 2.097(5), Zn(1)–N(3), 2.098(5) and Zn(1)–N(1), 2.164(5) indicate differences in the strengths of the bonds formed by each of the coordinating nitrogen atoms. The Zn–N bond lengths are shorter than those reported for mononuclear zinc(II) complexes, while there is no significant variation in the Zn–S bond lengths reported [12]. The dihedral angle formed by the least square plane Cg(5) and Cg(7) is 4.78° for the compound **22**.

Ring puckering analyses shows that the ring Cg(3) comprising of atoms Zn(1), O(1), C(11), C(16), C(17) and N(3) with puckering amplitude (Q_T) = 0.1714 Å and the ring Cg(1) comprising of atoms Zn(1), S(1), C(18), N(4) and N(3) with puckering amplitude (Q_T) = 0.3742 Å. The ring Cg(1) adopts an envelope on Zn(1) [$P = 159.1^\circ$, $\tau = 28.1^\circ$ for reference bond Zn(1)–S(1)].

Table 6.3. Selected bond lengths (Å) and bond angles ($^\circ$) for [ZnL³bipy]

<i>Bond lengths</i>		O(1)–C(11)	1.315(7)
Zn(1)–O(1)	1.958(5)	N(3)–C(17)	1.276(7)
Zn(1)–N(2)	2.097(5)	N(3)–N(4)	1.396(7)
Zn(1)–N(3)	2.098(5)	N(4)–C(18)	1.308(7)
Zn(1)–N(1)	2.164(5)	N(5)–C(18)	1.393(9)
Zn(1)–S(1)	2.3435(19)	N(5)–C(19)	1.414(9)
S(1)–C(18)	1.738(7)	N(5)–H(105)	0.81(8)
<i>Bond angles</i>		C(18)–S(1)–Zn(1)	92.5(2)
O(1)–Zn(1)–N(2)	104.3(2)	C(11)–O(1)–Zn(1)	129.0(4)
O(1)–Zn(1)–N(3)	89.19(19)	C(5)–N(1)–Zn(1)	114.0(4)
N(2)–Zn(1)–N(3)	100.8(2)	C(1)–N(1)–Zn(1)	126.9(4)
O(1)–Zn(1)–N(1)	92.68(19)	C(6)–N(2)–Zn(1)	117.1(4)
N(2)–Zn(1)–N(1)	77.1(2)	C(10)–N(2)–Zn(1)	125.0(5)
N(3)–Zn(1)–N(1)	177.5(2)	C(17)–N(3)–N(4)	115.5(5)
O(1)–Zn(1)–S(1)	145.18(16)	C(17)–N(3)–Zn(1)	126.2(5)
N(2)–Zn(1)–S(1)	110.34(15)	N(4)–N(3)–Zn(1)	118.0(4)
N(3)–Zn(1)–S(1)	81.30(15)	C(18)–N(4)–N(3)	110.9(5)
N(1)–Zn(1)–S(1)	98.10(14)	C(18)–N(5)–C(19)	126.5(7)

Figure 6.2 shows the contents of the unit cell along the a axis. The assemblage of molecules in the respective manner in the unit cell is resulted by the π - π and CH- π interactions as depicted in Table 6.4. One intermolecular hydrogen bonding is observed, *ie*, [C(9)-H(9) and O(1)] (Figure 6.3), but no classic hydrogen bonds were found. The centroid Cg(4) is involved in π - π interactions with pyridyl ring of the neighbouring unit at a distance of 3.8418 Å and the centroid Cg(5) with phenyl ring at a distance of 3.7274 Å, the CH- π interactions of the ring Cg(6) with the neighbouring molecules also contribute stability to the unit cell packing.

Table 6.4. Interaction parameters of the compound [ZnL³bipy]

π --- π interactions				
Cg(I)-Rcs(1)---Cg(J)	Cg-Cg(Å)	α °	β °	
Cg(4) [1] -> Cg(5) ^a	3.8418	23.58	5.95	
Cg(5) [1] -> Cg(4) ^b	3.8418	23.58	29.44	
Cg(5) [1] -> Cg(7) ^c	3.7274	4.78	18.80	
Cg(7) [1] -> Cg(5) ^d	3.7274	4.78	19.81	
Equivalent position codes	a = -1/2+x,-y,-z b = 1/2+x,-y,- c = -1/2+x,-1/2+y,1/2-z d = 1/2+x,1/2+y,1/2-z	Cg(4) = N(1),C(1),C(2),C(3),C(4),C(5) Cg(5) = N(2),C(6),C(7),C(8),C(9),C(10) Cg(7) = C(19),C(20),C(21),C(22),C(23),C(24)		
CH--- π interactions				
XH(1)---Cg(J)	H..Cg(Å)	X-H..Cg (°)	X..Cg(Å)	
C(4)-H(4) [1] -> Cg(6) ^a	2.75	153	3.6078	
Equivalent position codes	a = -1/2+x,-y,-z			
H bonding				
D---H---A	D-H (Å)	H---A (Å)	D ---A (Å)	D-H---A (°)
C(9)---H(9)---O(1)	0.93	2.41	3.2456	149

(D=Donor, A=acceptor, Cg=Centroid, α =dihedral angles between planes I & J, β = angle Cg(1)-Cg(J)

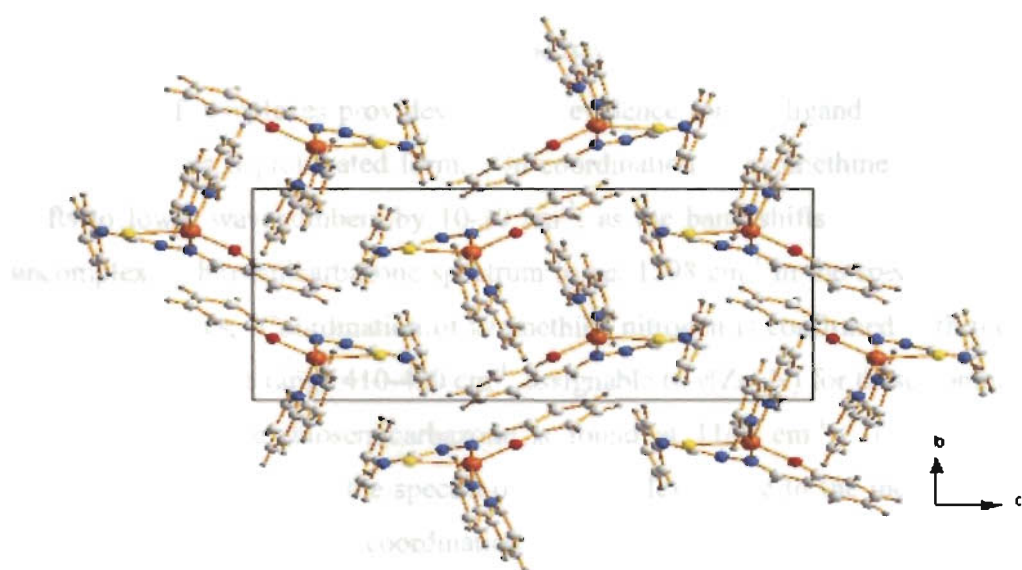


Figure 6.2. Unit cell packing diagram of the compound 22 viewed along the *a* axis

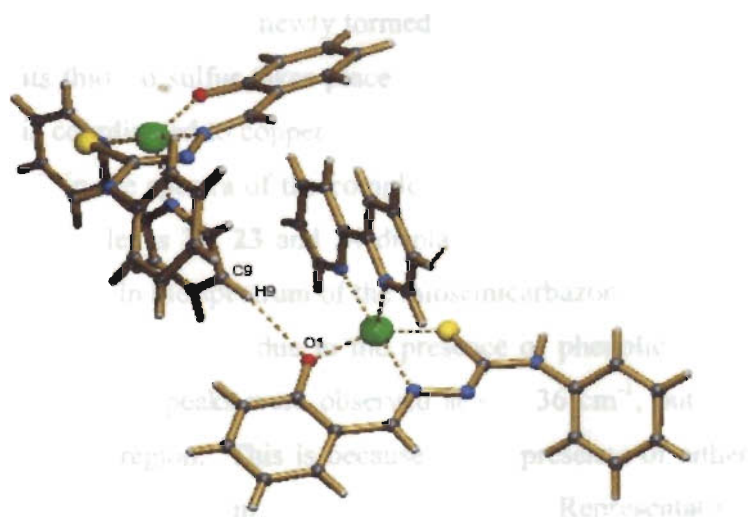


Figure 6.3. Hydrogen bonding interactions for the compound 22

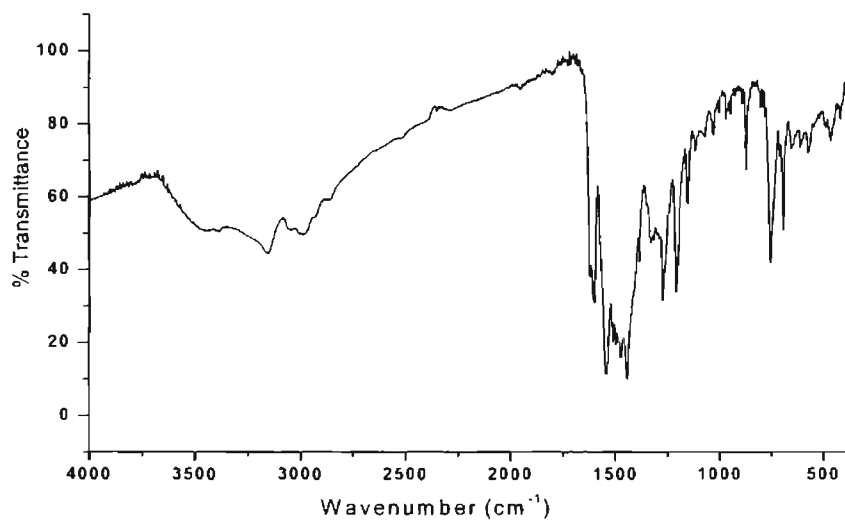
6.3.3. Infrared spectra

Table 6.5 lists the tentative assignments of main IR bands of Zn(II) complexes for the ligand H_2L^3 in 4000-50 cm^{-1} region. The spectra of free ligand exhibit a medium band at 3146 cm^{-1} , which is assigned to $\nu(N-H)$ vibration. The absence of $\nu(N-H)$ band in the spectra of complexes provides a strong evidence for the ligand coordination around Zn(II) ion in its deprotonated form. On coordination of azomethine nitrogen, $\nu(C=N)$ shifts to lower wavenumbers by 10-20 cm^{-1} as the band shifts from 1613 cm^{-1} in the uncomplexed thiosemicarbazone spectrum to *ca.* 1598 cm^{-1} in the spectra of all the five Zn(II) complexes. Coordination of azomethine nitrogen is confirmed with the presence of new bands in the range 410-420 cm^{-1} , assignable to $\nu(Zn-N)$ for these complexes [13]. The $\nu(N-N)$ of the thiosemicarbazone is found at 1149 cm^{-1} . The increase in the frequency of this band in the spectra of the complexes, due to the increase in the bond strength, again confirms the coordination *via* the azomethine nitrogen.

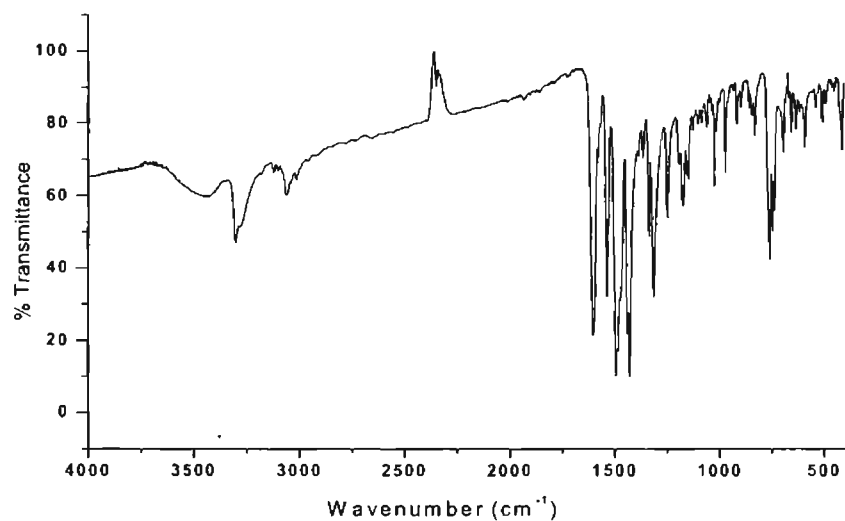
The decrease in the stretching frequency of $\nu(CS)$ bond from 874 cm^{-1} in the thiosemicarbazone by 10-50 cm^{-1} upon complexation indicates coordination *via* its thiolato sulfur. In all the five Zn(II) complexes, another strong band is found at *ca.* 1530-1550 cm^{-1} , which may be due to the newly formed $\nu(N=C)$ band. From this, it is clear that coordination *via* its thiolato sulfur takes place. In all the five complexes, except in **21**, phenolic oxygen is coordinated to copper by loss of the $-OH$ proton. A new band in the range 570-590 cm^{-1} in the spectra of the complexes is assignable to $\nu(Zn-O)$ [14]. The IR spectra of the complexes **22**, **23** and **24** display bands characteristic of coordinated heterocyclic bases [15]. In the spectrum of the thiosemicarbazone ligand, there is a sharp peak at 3336 cm^{-1} , which may be due to the presence of phenolic group. But, in the complexes **20-23**, no sharp peaks were observed at ~ 3336 cm^{-1} , but there were broad bands in the 3200-3500 region. This is because of the presence of either the alcoholic group or the lattice water present in these complexes [16]. Representative spectra of the complexes **21** and **22** are presented in Figure 6.4.

Table 6.5. Selected IR bands (cm^{-1}) with tentative assignments of Zn(II) complexes

Compound	$\nu(\text{C}=\text{N})$	$\nu(\text{N}=\text{C})$	$\nu(\text{N}-\text{N})$	$\nu(\text{C}-\text{S})$	$\nu(\text{C}-\text{O})$	$\nu(\text{Zn}-\text{O})$	$\nu(\text{Zn}-\text{N})$	Bands due to heterocyclic base
H_2L^3	1613	-----	1149	1328,874	1255	-----	-----	
$[\text{ZnL}^3]_2 \cdot 2\text{C}_2\text{H}_5\text{OH}$	1597	1548	1154	1316,824	1204	573	417	-----
$[\text{Zn}(\text{HL}^3)_2] \cdot \text{C}_2\text{H}_5\text{OH}$	1596	1542	1154	1327,864	1204		421	
$[\text{ZnL}^3 \text{bipy}] \cdot \frac{1}{2}\text{H}_2\text{O}$	1597	1534	1175	1316,824	1245	587	411	1429,758,690
$[\text{ZnL}^3 \text{phen}] \cdot \text{H}_2\text{O}$	1604	1534	1169	1309,852	1239	588	420	1426,751,693
$[\text{ZnL}^3 \text{dmbipy}]$	1597	1541	1169	1309,837	1239	583	416	1432,752,694



[Zn(HL³)₂] \cdot C₂H₅OH (21)



[ZnL³bipy] \cdot 1/2H₂O (22)

Figure 6.4. IR spectra of the compounds 21 and 22

6.3.4. Electronic spectra

The electronic absorption bands of the Zn(II) complexes, recorded in DMF solution, are given in Table 6.6 and representative spectra are in Figure 6.5. The thiosemicarbazone (H_2L^3) has a ring $\pi \rightarrow \pi^*$ band at 32250 cm^{-1} and a band at 29060 cm^{-1} due to $n \rightarrow \pi^*$ transition associated with the azomethine linkage. This band in the complexes have shown a bathochromic shift due to the donation of a lone pair of electrons to the metal and hence the coordination of azomethine nitrogen [17]. The absorption band centered around 29060 cm^{-1} in the ligand was assigned to $n \rightarrow \pi^*$ of the thioamide chromophore which suffers a blue shift in the complexes due to thioenolization.

The moderately intense broad bands for the complexes in the region $28500\text{-}23500\text{ cm}^{-1}$ are assigned to Zn(II) \rightarrow S metal to ligand charge transfer transition (MLCT). The MLCT maxima for the phenolato complexes show line broadening, with a tail running into the visible part of the spectrum. This may result from Zn(II) to phenolate MLCT band being superimposed on the low energy side of Zn(II) \rightarrow S MLCT [18]. Except this, the complexes show no appreciable absorptions in the region below 22000 cm^{-1} in DMF solution, in accordance with the d^{10} electronic configuration of the Zn(II) ion.

Table 6.6. Electronic spectral assignments (cm^{-1}) of the ligand H_2L^3 and their Zn(II) complexes

Compound	$\pi - \pi^*$	$n - \pi^*$	LMCT
H_2L^3	32250	29060	
$[(ZnL^3)_2] \cdot 3C_2H_5OH$	33670	31440,30300	27240,26240
$[Zn(HL^3)_2] \cdot C_2H_5OH$	33330	31540,30300	27470,26240
$[ZnL^3bipy] \cdot \frac{1}{2}H_2O$	33110	31540,30300	27390,26240
$[ZnL^3phen] \cdot H_2O$	33440	31940	26170,25640
$[ZnL^3dmbipy]$	33440	31740,30300	27390,26240

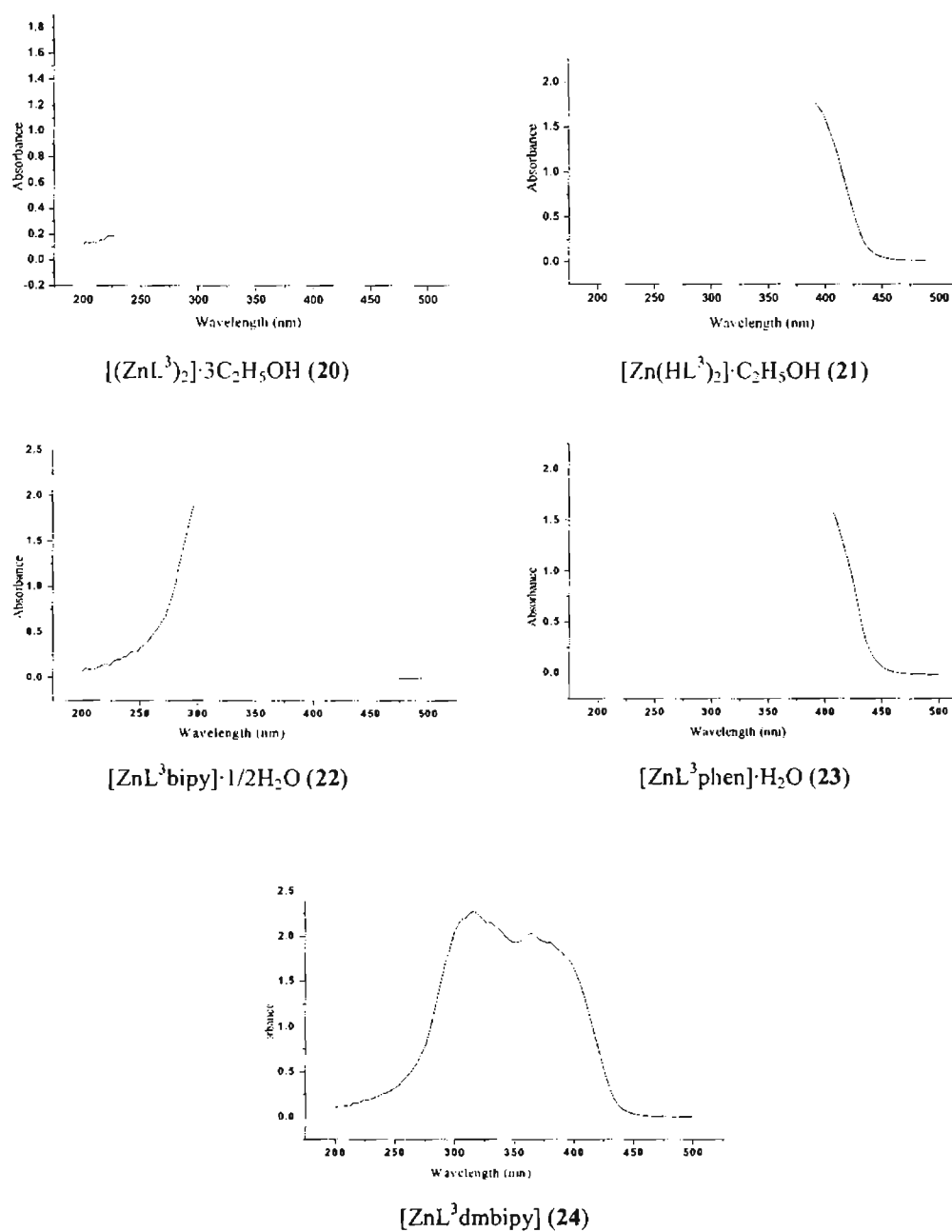


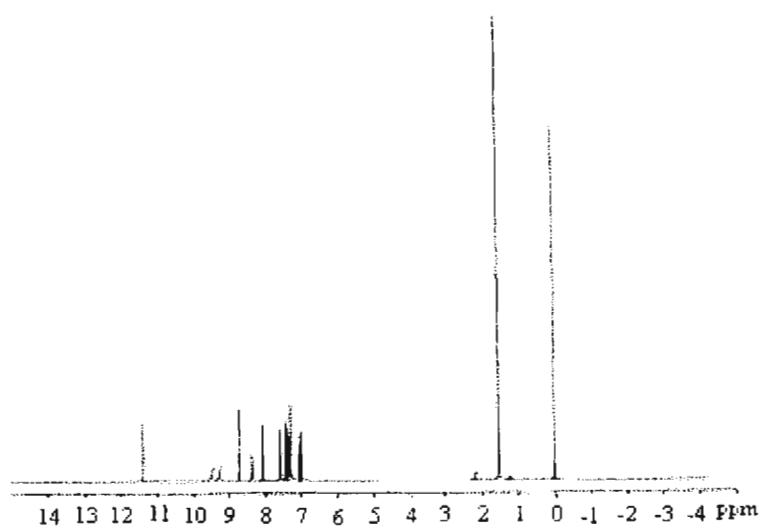
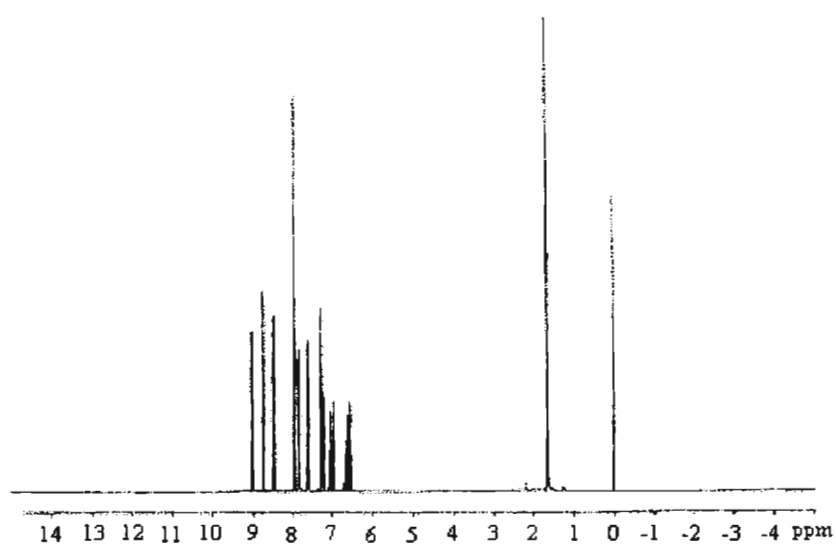
Figure 6.5. Electronic spectra of the compounds 20-24

6.3.5. ^1H NMR spectra

The ^1H NMR signals of the ligand H_2L^3 and their $\text{Zn}(\text{II})$ complexes recorded in CDCl_3 are listed in Table 6.7. The ligand has signals at $\delta = 11.36$, $\delta = 9.54$ and $\delta = 8.37$ ppm, which are due to $-\text{OH}$, $-\text{NH}$ and $-\text{CH}=\text{N}^1$ respectively (described in Chapter 2, section 2.4.5). In the $\text{Zn}(\text{II})$ complexes, signal due to $-\text{NH}$ is absent supporting thioenolization [19]. The low field position of $-\text{NH}$ ($\delta = 7.26$ ppm) could be attributable to the deshielding caused by the phenyl group and the adjacent $-\text{N}=\text{C}<$ of the system $-\text{N}=\text{C}(\text{SH})-\text{NH}-\text{C}_6\text{H}_5$. In all the complexes, except in the spectrum of the complex $[\text{Zn}(\text{HL}^3)_2]\cdot\text{C}_2\text{H}_5\text{OH}$ (**21**), the $-\text{OH}$ proton signals are absent. But in complex **21**, the $-\text{OH}$ signal appears at $\delta = 11.38$ ppm which supports for the existence of the phenoxy ($-\text{OH}$) group in the neutral form in this complex. Considerable shift of characteristic signals occurs on complexation [20,21]. Representative spectra of the complexes **21**, **23** and **24** are presented in Figure 6.6.

Table 6.7 ^1H NMR signals of H_2L^3 and their $\text{Zn}(\text{II})$ complexes (δ , ppm)

Compound	$-\text{CH}=\text{N}^1$	$-\text{NH}$	Aromatic
H_2L^3	8.37	7.26	6.84 – 7.60
$[(\text{ZnL}^3)_2]\cdot 3\text{C}_2\text{H}_5\text{OH}$		7.26	
$[\text{Zn}(\text{HL}^3)_2]\cdot\text{C}_2\text{H}_5\text{OH}$	8.72	7.26	6.85 – 7.9
$[\text{ZnL}^3\text{bipy}]\cdot\frac{1}{2}\text{H}_2\text{O}$	8.7	7.26	6.5 – 7.6
$[\text{ZnL}^3\text{phen}]\cdot\text{H}_2\text{O}$	8.74	7.26	6.5 – 7.9
$[\text{ZnL}^3\text{dmbipy}]$	8.67	7.26	6.5 – 7.9

 $[\text{Zn}(\text{HL}^3)_2] \cdot \text{C}_2\text{H}_5\text{OH}$ (21) $[\text{ZnL}^3\text{phen}] \cdot \text{H}_2\text{O}$ (23)

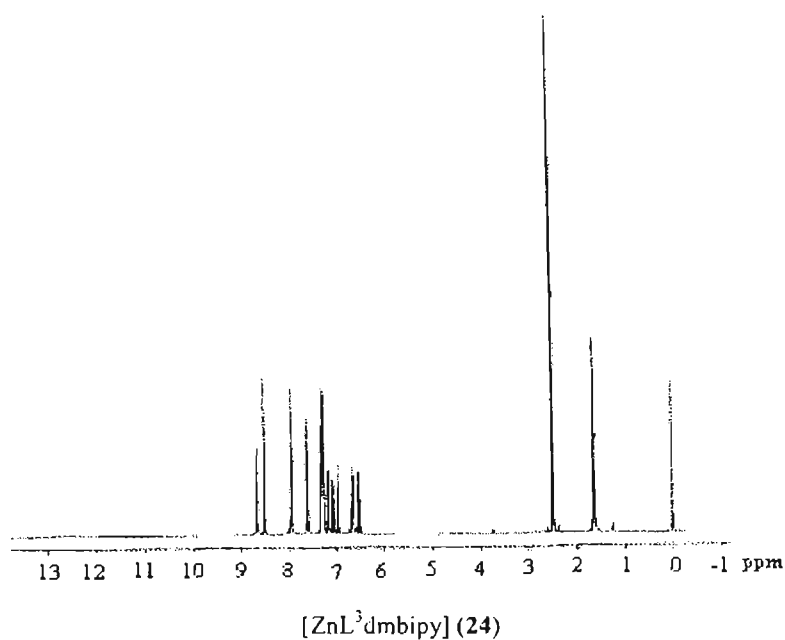


Figure 6.6. ¹H NMR spectra of the compounds 21, 23 and 24

References

1. K. Peariso, C.W. Goulding, S. Huang, R.G. Matthews, J.E. Penner-Hahn, *J. Am. Chem. Soc.* 120 (1998) 8410.
2. C. Dowling, G. Perkin, *Polyhedron* 15 (1996) 2463.
3. B.V. Nonius, Nonius, MACH3 software, Delft, The Netherlands, 1997.
4. G.M. Sheldrick, *Acta Cryst. A*46 (1990) 467.
5. G.M. Sheldrick, SHELXL97, SHELXS97, University of Gottingen, Germany, 1997.
6. K. Brandenburg, Diamond Version 3.0, Crystal Impact GbR, Bonn, Germany, 1997-2004.

-
7. A. L. Spek, ORTEP-III and PLATON, a Multipurpose Crystallographic Tool, Utrecht University, Utrecht, The Netherlands, 1999.
 8. G. Murphy, C.O. Sullivan, B. Murphy, B. Hathaway, *Inorg. Chem.* 37 (1998) 240.
 9. D. Chakraborty, H. Nagase, M. Kamijo, T. Endo, H. Ueda, *Analytical Sciences*, 21 (2005) x167.
 10. C.B. Castellani, G. Gatti, R. Millini, *Inorg. Chem.* 23 (1983) 4004.
 11. N.J. Ray, B.J. Hathaway, *Acta Cryst.* B34 (1978) 3224.
 12. C. Zhang, C. Janiak, *J. Chem. Cryst.* 31 (2001) 29.
 13. E. Bermejo, A. Castineiras, L.M. Fostiak, I.G. Santos, J.K. Swearingen, D.X. West, *Polyhedron* 23 (2004) 2303.
 14. R.P. John, Ph.D Thesis, Cochin University of Science and Technology, 2001.
 15. P. Bindu, M.R.P. Kurup, *Indian J. Chem.* 36A (1997) 1094.
 16. K. Nakamoto, *Infrared Spectra of Inorganic and Coordination Compounds*, 4th edn, Wiley-Interscience, New York, 1997, pp.228.
 17. A.D. Naik, V.K. Revankar, *Proc. Indian Acad. Sci. (Chem. Sci.)* 113 (2001) 285.
 18. A. Castineiras, E. Bermejo, D.X. West, L.J. Ackerman, J. Valdes-Martinez, S. Hernandez-Ortega, *Polyhedron* 18 (1999) 1463.
 19. A. Castineiras, R. Carballo, T. Perez, *Polyhedron* 20 (2001) 441.
 20. A. Erxleben, *Inorg. Chem.* 40 (2001) 208.
 21. Z. Popovic, V. Roje, G. Pavlovic, D.M. Calogovic, M. Rajic, I. Leban, *Polyhedron* 23 (2004) 1293.

CHAPTER 7

SYNTHESIS AND SPECTRAL STUDIES OF OXOVANADIUM(IV) COMPLEXES OF *N*(4)-SUBSTITUTED THIOSEMICARBAZONES

7.1. Introduction

Vanadium is an essential trace element and has generated increasing interest in the structure and function of its metal complexes found in the living organisms [1,2]. Many vanadium(IV) compounds contain the VO^{2+} group. The oxovanadium(IV) ion, VO^{2+} is considered to be the most stable oxocation of the first row transition metal ion [3]. It forms stable anionic, cationic and neutral complexes with various types of ligands. The common geometries of vanadium in VO^{IV} complexes are the square pyramid, distorted octahedron and trigonal bipyramid. Among the five coordinated VO^{IV} complexes, those with square-pyramidal geometry are the most common [4].

Vanadium(IV) species containing the $\text{V}=\text{O}$ grouping have spectra which are quite distinct from other vanadium(IV) derivatives and present several controversial features. Evidently the strong axial perturbation by the axial $\text{V}=\text{O}$ group plays an important role in determining the spectrum. All oxovanadium(IV) complexes are paramagnetic due to the presence of one unpaired d electron.

Design and synthesis of heterochelate complexes are generally intended to study the effect of unsymmetrical ligand fields on transition metal acceptor centres. This chapter describes the synthesis of six oxovanadium(IV) complexes of two tridentate (ONS) ligands, viz, salicylaldehyde *N*(4)-substituted thiosemicarbazones (H_2L^1 and H_2L^3) and intrinsic interest because of the formation of a basic $\text{VO}(\text{L})$ core having one or more vacant coordination sites to potentially bind an ancillary ligands. These are characterized by magnetic moment values, infrared, electronic and EPR spectral studies.

7.2. Experimental

7.2.1. Materials

The reagents used for the synthesis of the ligands (H_2L^1 and H_2L^3) are discussed in Chapter 2. $VOSO_4 \cdot H_2O$ (Sigma aldrich), 2,2'-bipyridine (bipy) (Central drug house chemicals), 1,10-phenanthroline (phen) (Ranbaxy fine chemicals) and 4,4'-dimethyl 2,2'-bipyridine (dmbipy) (E-Merck) were of analar grade and used without further purification. The ligands were recrystallized from ethanol and dried *in vacuo* before complexation.

7.2.2. Synthesis of the complexes

[VOL¹bipy] (25)

To a hot ethanolic solution of the ligand H_2L^1 (1 mmol, 0.277 g) was added aqueous solution of $VOSO_4 \cdot H_2O$ (1 mmol, 0.163 g) with constant stirring. This was followed by the addition of the base 2,2'-bipyridine (1 mmol, 0.156 g) in the solid form. The above brown solution was refluxed for about 3 h and allowed to cool. The reddish orange compound formed was filtered, washed with ethanol and ether and dried *in vacuo* over P_4O_{10} .

[VOL¹phen]· $\frac{1}{2}H_2O$ (26)

To a hot ethanolic solution of the ligand H_2L^1 (1 mmol, 0.277 g) was added aqueous solution of $VOSO_4 \cdot H_2O$ (1 mmol, 0.163 g) with constant stirring. This was followed by the addition of the base 1,10-phenanthroline (1 mmol, 0.198 g) in the solid form. The above brown solution was refluxed for about 3 h and allowed to cool. The reddish orange crystalline compound formed was filtered, washed with ethanol and ether and dried *in vacuo* over P_4O_{10} .

[VOL¹dmbipy] (27)

To a hot ethanolic solution of the ligand H_2L^1 (1 mmol, 0.277 g) was added aqueous solution of $VOSO_4 \cdot H_2O$ (1 mmol, 0.163 g) with constant stirring. This was

followed by the addition of the base 4,4'-dimethyl 2,2'-bipyridine (1 mmol, 0.184 g) in the solid form. The above brown solution was refluxed for about 3 h and allowed to cool. The reddish orange compound formed was filtered, washed with ethanol and ether and dried *in vacuo* over P_4O_{10} .

[VOL³bipy] (28)

To a hot ethanolic solution of the ligand H_2L^3 (1 mmol, 0.271 g) was added aqueous solution of $VOSO_4 \cdot H_2O$ (1 mmol, 0.163 g) with constant stirring. This was followed by the addition of the base 2,2'-bipyridine (1 mmol, 0.156 g) in the solid form. The above brown solution was refluxed for about 3 h and allowed to cool. The reddish orange compound formed was filtered, washed with ethanol and ether and dried *in vacuo* over P_4O_{10} .

[VOL³phen] (29)

To a hot ethanolic solution of the ligand H_2L^3 (1 mmol, 0.271 g) was added aqueous solution of $VOSO_4 \cdot H_2O$ (1 mmol, 0.163 g) with constant stirring. This was followed by the addition of the base 1,10-phenanthroline (1 mmol, 0.198 g) in the solid form. The above brown solution was refluxed for about 3 h and allowed to cool. The reddish orange compound formed was filtered, washed with ethanol and ether and dried *in vacuo* over P_4O_{10} .

[VOL³dmbipy]· $\frac{1}{2}H_2O$ (30)

To a hot ethanolic solution of the ligand H_2L^3 (1 mmol, 0.271 g) was added aqueous solution of $VOSO_4 \cdot H_2O$ (1 mmol, 0.163 g) with constant stirring. This was followed by the addition of the base 4,4'-dimethyl 2,2'-bipyridine (1 mmol, 0.184 g) in the solid form. The above brown solution was refluxed for about 3 h and allowed to cool. The yellowish orange compound formed was filtered, washed with ethanol and ether and dried *in vacuo* over P_4O_{10} .

7.3. Results and discussion

7.3.1. Physical measurements

The colors, partial elemental analyses and magnetic moments of the complexes (25-30) are presented in Table 7.1. Reactions of tridentate ONS donor ligands H_2L (H_2L^1 and H_2L^3) and heterocyclic bases (B) {B = bipy, phen and dmbipy} with $VOSO_4 \cdot H_2O$ in ethanol / water mixture afforded oxovanadium(IV) complexes of the type $VOL(B)$. The mononuclear complexes 25-30 are soluble in CH_2Cl_2 , DMF and DMSO. All the six complexes are orange colored. In complexes 26 and 30, small fraction of water molecules present in nonstoichiometric proportions.

Table 7.1. Analytical data

Compound	Color	Found (Calculated) %			μ (B.M.)
		C	H	N	
$[VOL^1bipy]$ (25)	Reddish orange	57.63(57.83)	5.10(5.05)	13.87(14.05)	1.70
$[VOL^1phen] \cdot \frac{1}{2}H_2O$ (26)	Reddish orange	58.74(58.75)	4.70(4.93)	13.11(13.18)	1.58
$[VOL^1dmbipy]$ (27)	Reddish orange	58.73(59.31)	5.69(5.55)	13.15(13.30)	1.83
$[VOL^3bipy]$ (28)	Reddish orange	58.35(58.54)	3.93(3.89)	13.96(14.22)	1.80
$[VOL^3phen]$ (29)	Reddish orange	60.16(60.46)	3.28(3.71)	13.39(13.56)	1.69
$[VOL^3dmbipy] \cdot \frac{1}{2}H_2O$ (30)	Yellowish orange	59.20(58.98)	4.57(4.57)	13.25(13.23)	1.73

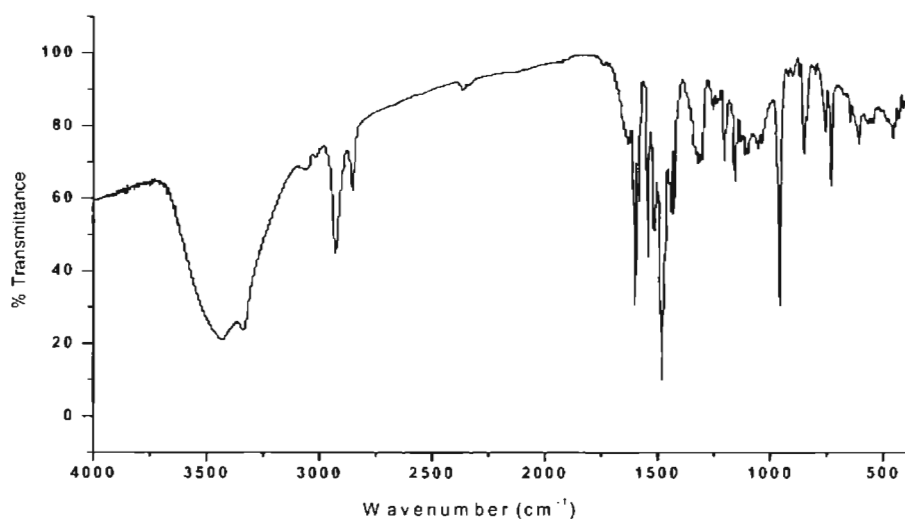
The magnetic moment obtained at 297 K for the complexes **25-30** are in the range of 1.58–1.83 B.M. The values correspond to the spin only value of systems having one electron. These are magnetically diluted complexes in which metal ion is not involved in magnetic exchange with the neighbouring metal ion [5]. The oxovanadium(IV) complexes are paramagnetic and the expected magnetic moment values for a d^1 system are ~ 1.73 B.M. [6].

7.3.2. Infrared spectra

Table 7.2 lists the tentative assignments of main IR bands of oxovanadium(IV) complexes for the ligands H_2L^1 and H_2L^3 in the 4000-50 cm^{-1} region. The free ligands H_2L^1 and H_2L^3 show bands at *ca.* 3369 and 3141 cm^{-1} , which are due to $-OH$ stretching mode and $-NH$ groups respectively. These bands are absent in complexes, which suggests deprotonation of the phenolic group indicating the coordination through phenolic oxygen and enolization of the thione sulfur followed by deprotonation. On coordination of azomethine nitrogen, $\nu(C=N)$ shifts to lower wavenumbers by 10-20 cm^{-1} as the band shifts from *ca.* 1613 to 1600 cm^{-1} in the spectra of the six oxovanadium(IV) complexes. Coordination of azomethine nitrogen is confirmed with the presence of new band in the range 430-460 cm^{-1} assignable to $\nu(V-N)$ for these complexes [7]. The $\nu(N-N)$ of the thiosemicarbazone is found at *ca.* 1154 cm^{-1} . The increase in the frequency of this band in the spectra of the complexes, due to the increase in the bond strength, again confirms the coordination *via* the azomethine nitrogen.

The decrease in the stretching frequency of C-S band from *ca.* 865 cm^{-1} in the thiosemicarbazones by 80-90 cm^{-1} upon complexation indicates coordination *via* thiolato sulfur. In the far IR spectrum of the compound **28**, a band is found at 335 cm^{-1} , which is due to $\nu(V-S)$ and the coordination of thiolato sulfur is confirmed [8]. IR spectra of the complexes **25-30** show sharp bands at *ca.* 1538 cm^{-1} due to

newly formed $\nu(\text{N}=\text{C})$ band indicating the coordination of sulfur in the enol form rather than as keto form [9]. In all the complexes, phenolic oxygen coordinated to vanadium by loss of the $-\text{OH}$ proton. A new band in the range $510\text{--}545\text{ cm}^{-1}$ in the spectra of the complexes was assignable to $\nu(\text{V}-\text{O})$, resulting from the coordination of phenolic oxygen [10]. All these indicate ONS mode of chelation by the thioenol form of the ligands in the present series of complexes. The complexes display a strong $\text{V}=\text{O}$ terminal stretch appearing at *ca.* 960 cm^{-1} , similar to that observed with the octahedral vanadium(IV) complexes [11]. Representative spectra of the complexes **26**, **29** and **30** are presented in Figure 7.1.



$[\text{VOL}^{\text{I}}\text{phen}]^{1/2}\text{H}_2\text{O}$ (**26**)

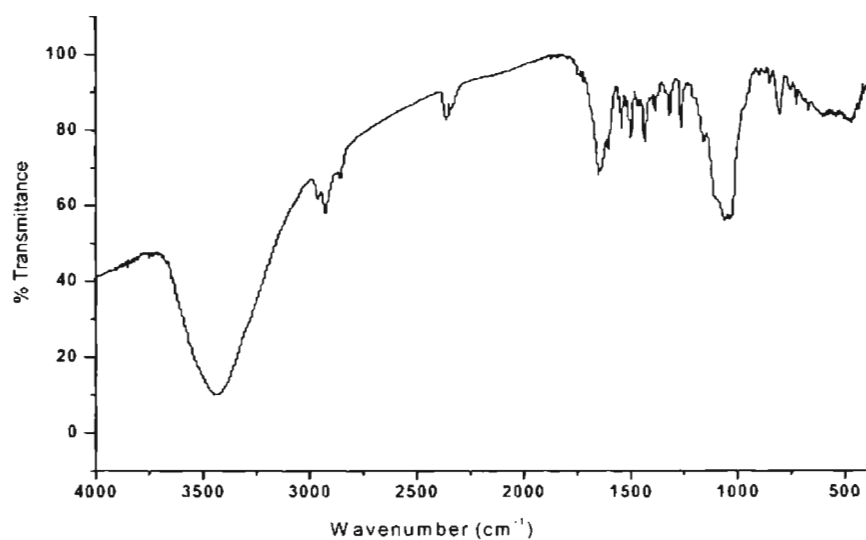
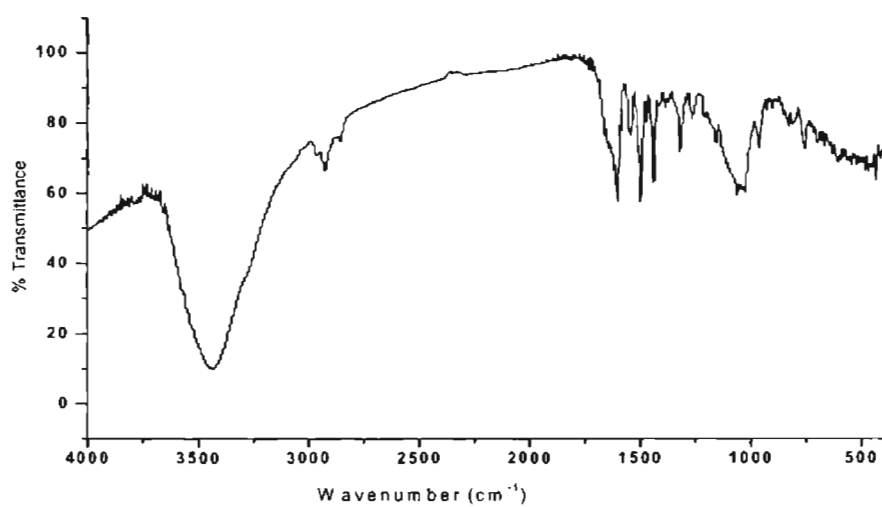
[VOL³phen] (29)[VOL³dmbipy]^{1/2}H₂O (30)

Figure 7.1. IR spectra of the compounds 26, 29 and 30

Table 7.2. Selected IR bands (cm^{-1}) with tentative assignments of oxovanadium(IV) complexes

Compound	$\nu(\text{C}=\text{N})$	$\nu(\text{N}=\text{C})$	$\nu(\text{N}-\text{N})$	$\nu(\text{C}-\text{S})$	$\nu(\text{V}=\text{O})$	$\nu(\text{C}-\text{O})$	$\nu(\text{V}-\text{O})$	$\nu(\text{V}-\text{N})$	Bands due to heterocyclic base
H_2L^1	1614		1111	1328/856		1263			
$[\text{VOL}^1\text{bipy}]$	1599	1539	1157	1320/763	954	1260	544	451	1440,604
$[\text{VOL}^1\text{phen}] \cdot \frac{1}{2}\text{H}_2\text{O}$	1595	1540	1152	1315/725	955	1250	550	447	1473,600
$[\text{VOL}^1\text{dmbipy}]$	1610	1538	1150	1321/757	960	1256	517	452	1474,607
H_2L^3	1613		1149	1328/874		1255			
$[\text{VOL}^3\text{bipy}]$	1600	1539	1158	1315/757	966	1245	548	446	1440,600
$[\text{VOL}^3\text{phen}]$	1599	1537	1157	1314/801	971	1246	540	458	1430,664
$[\text{VOL}^3\text{dmbipy}] \cdot \frac{1}{2}\text{H}_2\text{O}$	1598	1535	1155	1316/823	954	1240	542	430	1436,600

7.3.3. Electronic spectra

The electronic absorption bands of the oxovanadium(IV) complexes recorded in DMF solution, are given in Table 7.3 and their representative spectra in Figure 7.2. The thiosemicarbazones (H_2L^1 and H_2L^3) have ring $\pi - \pi^*$ band at *ca.* 36640 cm^{-1} and a band at *ca.* 32520 cm^{-1} due to $n - \pi^*$ transitions associated with the azomethine linkage. These bands suffer marginal shifts on complexation. Visible spectra of oxovanadium(IV) complexes are known to exhibit mainly three bands lying in the range 11000-15000 cm^{-1} (band I), 15000-20000 cm^{-1} (band II) and 21000-30000 (band III), corresponding to $d-d$ transitions ${}^2B_2 \rightarrow {}^2E$, ${}^2B_2 \rightarrow {}^2B_1$ and ${}^2B_2 \rightarrow {}^2A_1$ respectively. These are followed by one or many high intensity bands in the ultraviolet region [12]. In the electronic spectra of the present complexes the first absorption band at *ca.* 14440 cm^{-1} can be assigned to the electronic transition ${}^2B_2 \rightarrow {}^2E$ ($d_{xy} \rightarrow d_{xz}, d_{yz}$), the second absorption band at *ca.* 17890 cm^{-1} due to ${}^2B_2 \rightarrow {}^2B_1$ ($d_{xy} \rightarrow d_{x^2-y^2}$) and the third absorption band at *ca.* 20710 cm^{-1} are due to ${}^2B_2 \rightarrow {}^2A_1$ ($d_{xy} \rightarrow d_z^2$). In all the complexes an intense band at *ca.* 24940 cm^{-1} is assignable to the phenolic oxygen $\rightarrow V_{(d\pi)}$ ligand to metal charge transfer (LMCT) band [13]. Two additional bands appearing in the UV region are due to intraligand transitions. The band due to LMCT may have merged with the third band in all the complexes.

Table 7.3. Electronic spectral assignments (cm^{-1}) of oxovanadium(IV) complexes

Compound	${}^2B_2 \rightarrow {}^2E$	${}^2B_2 \rightarrow {}^2B_1$	${}^2B_2 \rightarrow {}^2A_1$	LMCT	$n - \pi^*$	$\pi - \pi^*$
[VOL ¹ bipy]	14340	17790	21390	25570	30580	35080
[VOL ¹ phen] $\cdot \frac{1}{2}H_2O$	14850	18140	20870	23980	30480	35330
[VOL ¹ dmbipy]	15120	17330	20660	24150	30760	35410
[VOL ³ bipy]	13960	17510	20490	25250	34120	38020
[VOL ³ phen]	14100	18310	20440	25310	34480	37870
[VOL ³ dmbipy] $\cdot \frac{1}{2}H_2O$	14260	18240	20400	25380	34720	38160

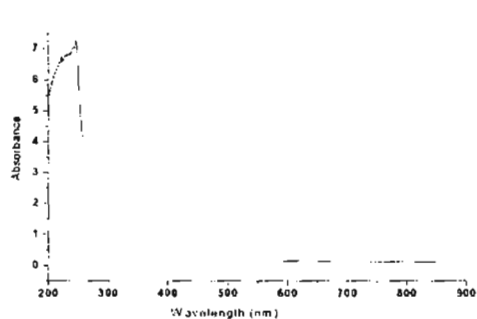
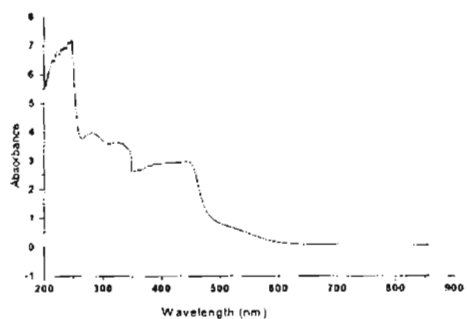
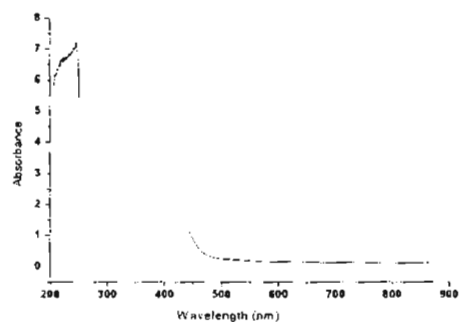
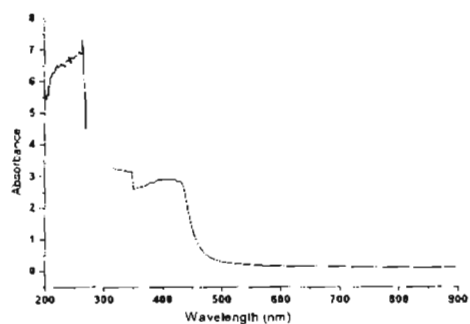
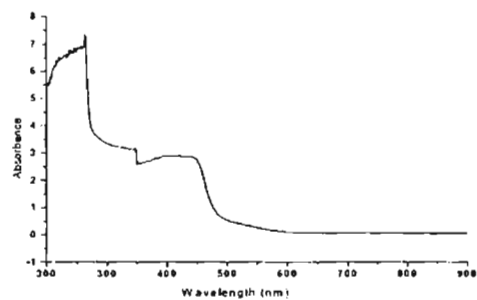
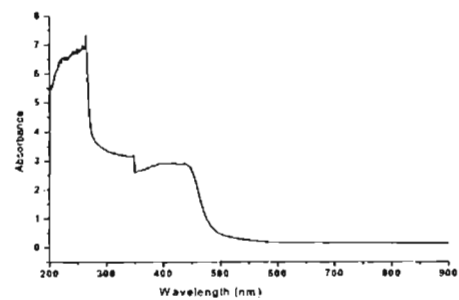
[VOL¹bipy] (25)[VOL¹phen]·½H₂O (26)[VOL¹dmbipy] (27)[VOL³bipy] (28)[VOL³phen] (29)[VOL³dmbipy]·½H₂O (30)

Figure 7.2. Electronic spectra of the compounds 25–30

7.3.4. EPR spectra

The EPR spectra of all the complexes were recorded in polycrystalline state at 298 K and in frozen DMF solution at 77 K. The EPR parameters of the complexes **25-30** are presented in Table 7.4.

The EPR spectra of all the compounds in polycrystalline state of 298 K have essentially identical features. The complexes **26-30** showed an isotropic signal centered at $g = 1.987$ corresponding to $\Delta M_S = \pm 1$. The EPR spectrum of the compound **25** in polycrystalline state of 298 K is not good and its interpretation is difficult.

In frozen DMF solution at 77 K, normal eight line spectra showing hyperfine splitting for the ^{51}V nucleus ($I = 7/2$) are obtained in all the cases. All the compounds show well-resolved axial anisotropy with two sets of eight line pattern with $g_{\parallel} < g_{\perp}$ and $A_{\parallel} \gg A_{\perp}$ relationship characteristic of an axially compressed d^1_{xy} configuration [14]. Ligand nitrogen or hydrogen superhyperfine splittings are not observed on the vanadium line. This indicates that the unpaired electron to be in b_{2g} (d_{xy} , 2B_2 ground state) orbital localized on metal, thus excluding the possibility of its direct interaction with the ligand [15, 16].

The EPR spectra show signals characteristic of mononuclear VO^{2+} species. The isotropic parameters are calculated using the equations $g_{\text{iso}} = 1/3(g_{\parallel} + 2g_{\perp})$ and $A_{\text{iso}} = 1/3(A_{\parallel} + 2A_{\perp})$ respectively. In the above complexes, the isotropic parameters g_{iso} and A_{iso} are ~ 1.976 and 95.6 G respectively. These values are in range for typical distorted octahedral VO^{2+} complexes [17,18].

The molecular orbital coefficients α^2 and β^2 were also calculated for the complexes by using the following equations:

$$\alpha^2 = (2.00277 - g_{\parallel}) \Delta E_{d-d} / 8\lambda\beta^2$$

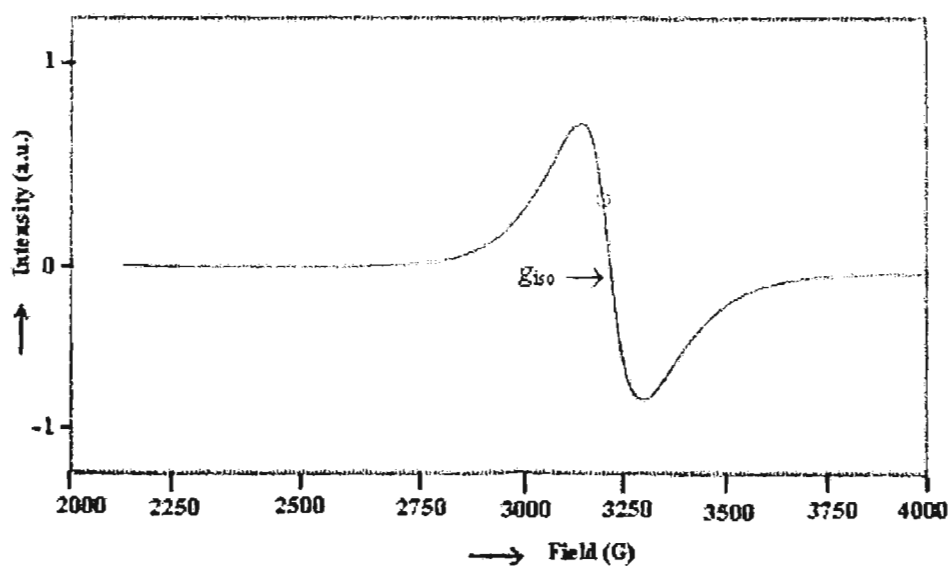
$$\beta^2 = 7/6 [(-A_{\parallel}/P) + (A_{\perp}/P) + (g_{\parallel} - 5/14 g_{\perp}) - 9/14 g_e]$$

where, $P = 128 \times 10^4 \text{ cm}^{-1}$, $\lambda = 135 \text{ cm}^{-1}$ and E is the electronic transition energy of ${}^2B_2 \rightarrow {}^2E$. The lower values for α^2 compared to β^2 indicate that in-plane σ bonding is more covalent than in-plane π bonding [19]. The in-plane π bonding parameter β^2 observed are consistent with those observed for McGarvey and Kivelson for vanadyl complexes of acetylacetonone [20,16].

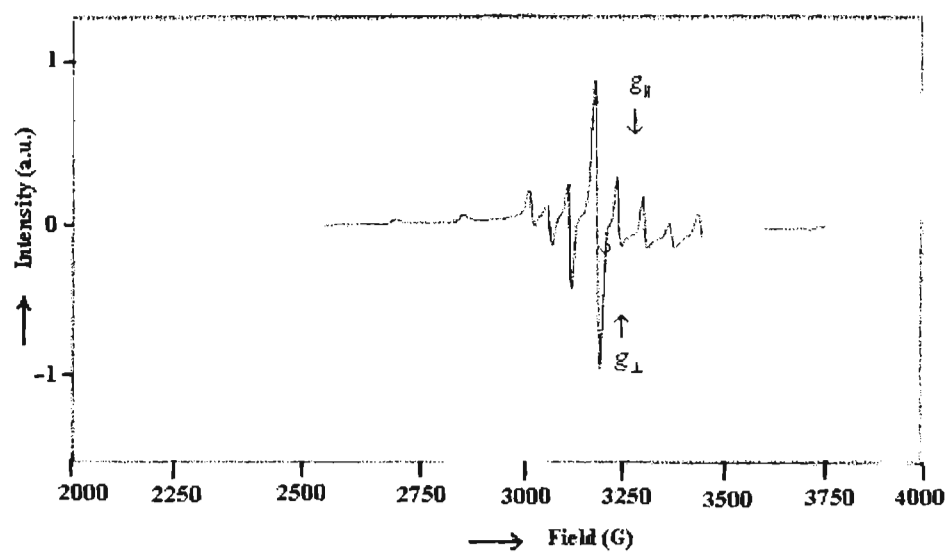
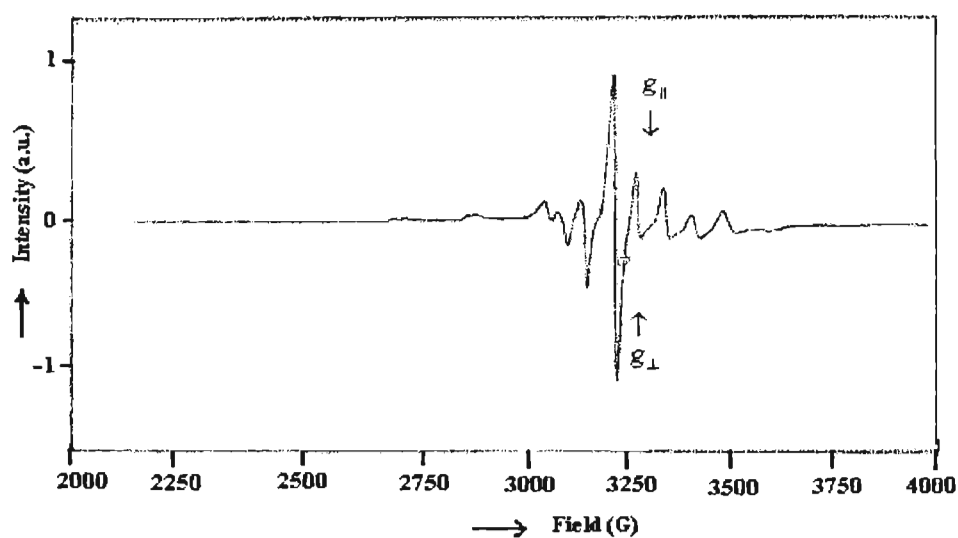
Table 7.4. EPR spectral assignments for oxovanadium(IV) complexes in polycrystalline state at (298 K) and frozen DMF solution at (77 K)

Compound	Polycrystalline state (298 K) (g_{iso})	DMF solution (77 K)					
		g_{\parallel}	g_{\perp}	A_{\parallel}^a	A_{\perp}	α^2	β^2
[VOL ¹ bipy]		1.963	1.981	185.5	57.3	0.53	0.99
[VOL ¹ phen] $\cdot\frac{1}{2}$ H ₂ O	1.984	1.956	1.982	182.2	60.9	0.66	0.96
[VOL ¹ dmbipy]	1.993	1.964	1.981	186.1	54.1	0.52	1.04
[VOL ³ bipy]	1.990	1.972	1.987	183.0	53.9	0.57	1.01
[VOL ³ phen]	1.984	1.965	1.985	178.2	56.1	0.52	0.96
[VOL ³ dmbipy] $\cdot\frac{1}{2}$ H ₂ O	1.989	1.962	1.984	149.7	46.3	0.54	0.98

^a Expressed in units of cm^{-1} multiplied by a factor of 10^{-4}



(i) [VOL³dmbipy] $\cdot\frac{1}{2}$ H₂O (30)

(ii) $[\text{VOL}^1\text{phen}]^{1/2}\text{H}_2\text{O}$ (26)(ii) $[\text{VOL}^3\text{bipy}]$ (28)**Figure 7.3.** EPR spectra of the compounds 26, 28 and 30

(i) Compound 30 in the polycrystalline state at 298 K

(ii) Compounds 26 and 28 in DMF solution at 77 K

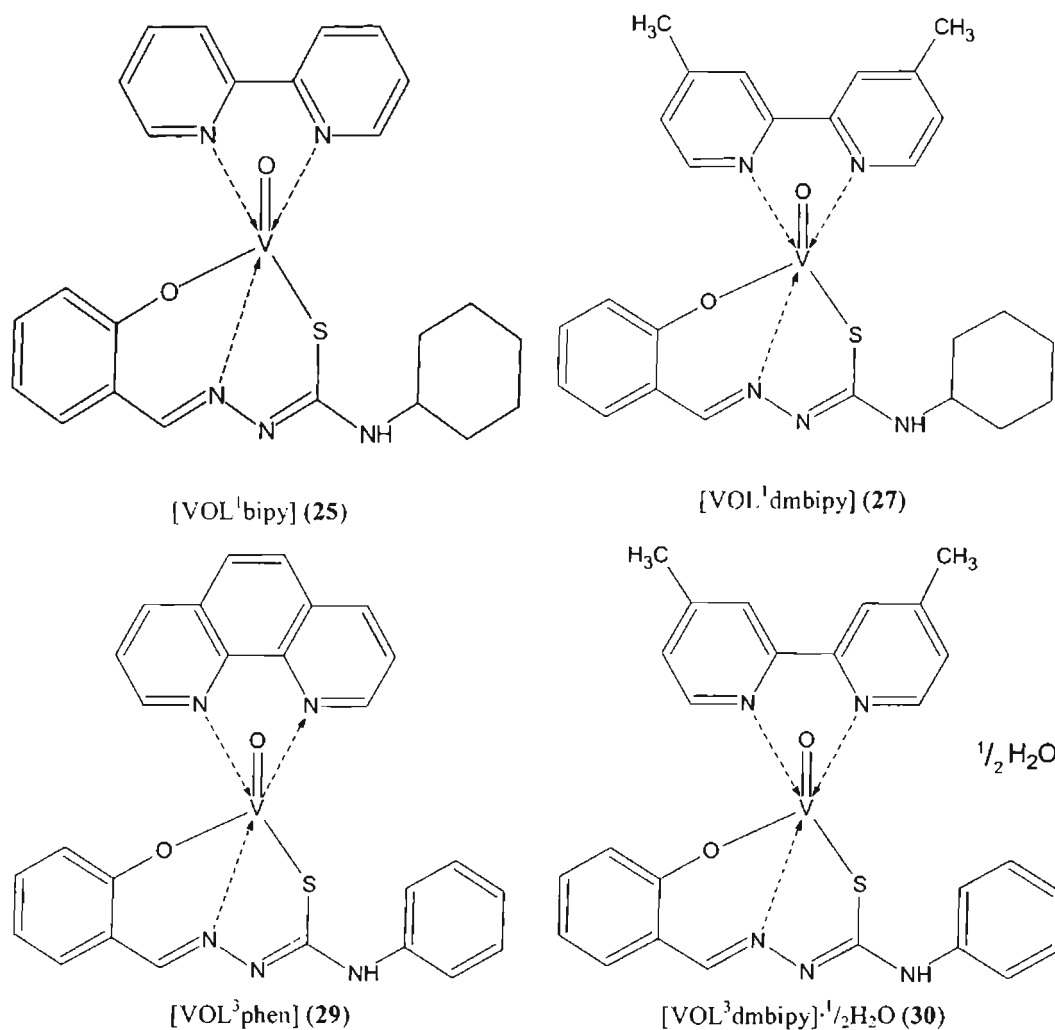


Figure 7.4. Tentative structure of the compounds 25, 27, 29 and 30.

References

1. E.M. Armstrong, R.L. Beddoes, L.J. Calviou, J.M. Charnock, D. Collison, N. Ertok, J.H. Naismith, C.D. Garner, *J. Am. Chem. Soc.* 115 (1993) 807.
2. A. Butler, C.J. Carrano, *Coord. Chem. Rev.* 109 (1991) 61.
3. A.P. Sinsberg, E. Roubek, H.J. Williams, *Inorg. Chem.* 5 (1966) 1656.

4. S.N. Rao, D.D. Mishra, R.C. Maurya, N.N. Rao, *Polyhedron* 16 (1997) 1825.
5. B.N. Figgis, J. Lewis, *Prog. Inorg. Chem.* 6 (1964) 37.
6. S.P. Rath, S. Mondal, T. Ghosh, *Trans. Met. Chem.* 21 (1996) 309.
7. P.B. Sreeja, M.R. P. Kurup, *Spectrochim. Acta* 61A (2004) 331.
8. M. Chatterjee, S. Ghosh, *Trans. Met. Chem.* 23 (1998) 355.
9. M. Chatterjee, S. Ghosh, Bo-Mu Wu, T.C.W. Mak, *Polyhedron* 17 (1998) 1369.
10. T. Ma, T. Kojima, Y. Matsuda, *Polyhedron* 19 (2000) 1167.
11. J. Selbin, *Chem. Rev.* 65 (1965) 153.
12. K.B. Pandeya, O. Prakash, R.P. Singh, *J. Indian Chem. Soc.* LX (1983) 531.
13. M.R. Maurya, S. Khurana, Shailendra, A. Azam, W. Zhang, D. Rehder, *Eur. J. Inorg. Chem.* (2003) 1966.
14. S. Bhattacharya, T. Ghosh, *Indian J. Chem.* 38A (1999) 601.
15. H. Kon, E. Sharpless, *J. Chem. Phys.* 42 (1965) 906.
16. D. Kivelson, S.K. Lee, *J. Chem. Phys.* 41 (1964) 1896.
17. Y. Dong, R.K. Narla, E. Sudbeck, F.M. Uckun, *J. Inorg. Biochem.* 78 (2000) 321.
18. J.G. Reynolds, S.C. Sendlinger, A.M. Murray, J.C. Huffman, G. Christou, *Inorg. Chem.* 34 (1995) 5745.
19. N. Raman, Y.P. Raja, A. Kulandaisamy, *Proc. Indian Acad. Sci. (Chem. Sci.)* 113 (2001) 183.
20. B.R. McGarvey, *J. Phys. Chem.* 71 (1967) 51.

CHAPTER 8

**SYNTHESIS, SPECTRAL AND STRUCTURAL STUDIES OF
DIOXOMOLYBDENUM(VI) COMPLEXES OF
2-HYDROXYACETOPHENONE N(4)-SUBSTITUTED
THIOSEMICARBAZONES**

8.1. Introduction

Molybdenum is a biologically important trace element that occurs in the redox-active sites of molybdoenzymes involved in nitrogen, sulfur or carbon metabolism [1]. The 'oxo-type' molybdoenzymes, which possess a common molybdenum cofactor, catalyze biological two electron reactions that involve a change in the number of oxygen atoms in the substrate [2]. The mononuclear molybdoenzymes contained terminal oxo-group(s), believed to be obligatory for the oxotransferase activity of these enzymes.

Molybdenum is a versatile transition element because it possesses a large number of stable and accessible oxidation states as well as coordination numbers. The formal oxidation state of molybdenum fluctuates between +6 and +4 *via* +5 intermediate during turnover [3]. Complexes containing the molybdenum-oxo group dominate the higher oxidation state of molybdenum. Most simple dioxomolybdenum(VI) coordination complexes contain the cis-MoO_2^{2+} cation.

Thiosemicarbazones obtained by condensing ring substituted aromatic thiosemicarbazides with *o*-hydroxy carbonyl compounds like salicylaldehyde and *o*-hydroxyacetophenone have rarely been used in molybdenum chemistry. The ligands are of particular interest because their complexes of the type MoO_2L or Mo(OL) possess one or two "open" coordination sites that can be utilized for substrate binding. This chapter describes synthesis and spectral characterization of dioxomolybdenum(VI) complexes of N(4)-substituted ONS donor ligands. It also

describes single crystal X-ray diffraction studies of three of the synthesized complexes.

8.2. Experimental

8.2.1. Materials

The reagents used for the synthesis of the ligands (H_2L^2 and H_2L^4) are discussed in Chapter 2. $MoO_2(acac)_2$ (Sigma aldrich) and pyridine (S.D.Fine Chemicals) were analar grade and used without further purification. The ligands were recrystallized from ethanol / methanol and dried *in vacuo* before complexation.

8.2.2. Synthesis of the complexes

$[(MoO_2L^2)_2]$ (31)

To a hot methanolic solution of the ligand H_2L^2 (2 mmol, 0.582 g), added methanolic solution of $MoO_2(acac)_2$ (2 mmol, 0.652 g) with constant stirring. The above orange solution was refluxed for about 3 h and allowed to cool. The orange crystals formed were separated and dried.

$[MoO_2L^2py]$ (32)

To a hot methanolic solution of complex 31 (0.5 mmol, 0.417 g), added 2 mL of pyridine and the mixture was heated until a clear deep yellow solution was produced. The above solution was refluxed for about 3 h and allowed to cool. Slow evaporation of the reaction mixture over 3 days produced yellow crystals.

$[MoO_2L^4]$ (33)

To a hot ethanolic solution of the ligand H_2L^4 (1.5 mmol, 0.428 g), added ethanolic solution of $MoO_2(acac)_2$ (1.5 mmol, 0.489 g) with constant stirring. The above orange solution was refluxed for about 3 h and the orange compound formed was filtered, washed with ethanol and ether and dried *in vacuo* over P_4O_{10} .

[MoO₂L⁴py] (34)

To a hot ethanolic solution of complex **33** (0.5 mmol, 0.205 g), added 2 mL of pyridine and the mixture was heated until a clear deep yellow solution was produced. The above solution was refluxed for about 3 h and allowed to cool. Slow evaporation of the reaction mixture over 5 days produced yellow crystals.

8.3. Results and discussion

8.3.1. Synthesis

The colors, partial elemental analyses and magnetic moments of the complexes (**31-34**) are presented in Table 8.1.

Table 8.1. Analytical data

Compound	Color	Found (Calculated) %			μ (B.M.)
		C	H	N	
[(MoO ₂ L ²) ₂] (31)	Orange	43.05(43.17)	4.52(4.59)	10.04(10.07)	Diamagnetic
[MoO ₂ L ² py] (32)	Yellow	48.16(48.39)	4.70(4.87)	11.12(11.29)	Diamagnetic
[MoO ₂ L ⁴] (33)	Orange	43.69(43.80)	3.02(3.19)	10.13(10.22)	Diamagnetic
[MoO ₂ L ⁴ py] (34)	Yellow	48.82(48.98)	3.65(3.70)	11.24(11.43)	Diamagnetic

For the preparation of complexes (**31-34**), the ligands H₂L² and H₂L⁴ (as described in Chapter 2) were used. The stoichiometric reaction of bis(acetylacetonato)dioxomolybdenum(VI) with H₂L in refluxing methanol / ethanol afforded the orange six and five-coordinate complexes of the type [(MoO₂L)₂] and [MoO₂L] (**31** and **33**) in excellent yield. The [MoO₂L(B)] complexes (**32** and **34**) were prepared by reaction of [(MoO₂L²)₂] (for **32**) and MoO₂L⁴ (for **34**) with

heterocyclic base {B = pyridine (py)} in methanol / ethanol. All these complexes are diamagnetic, indicating the presence of molybdenum in the +6 oxidation state. These complexes are soluble in DMF and DMSO.

8.3.2. Spectral studies

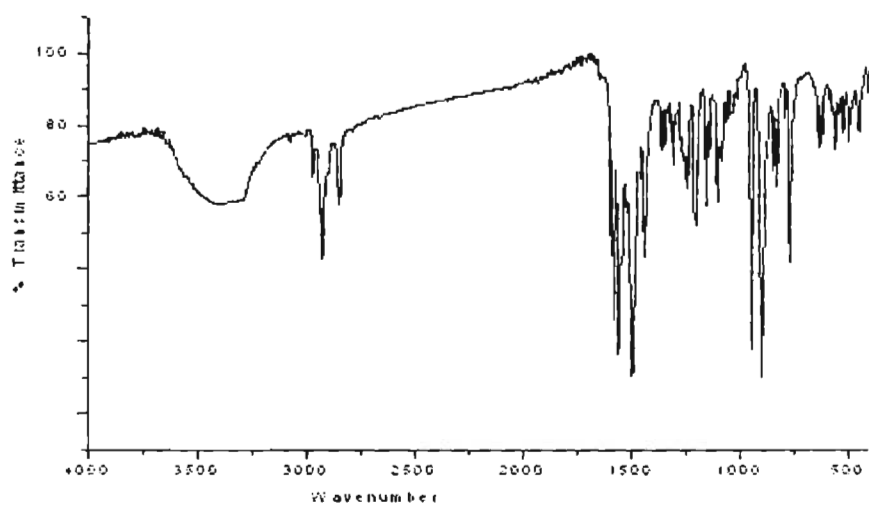
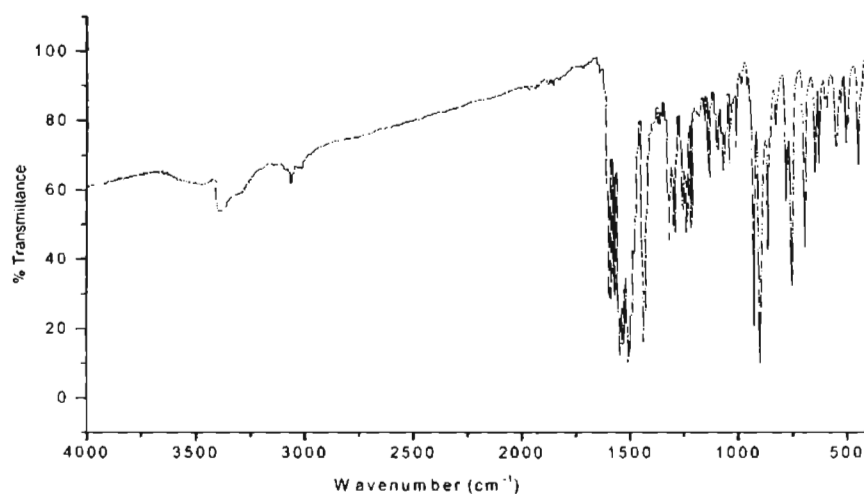
Selected spectroscopic data of the complexes are summarized in Tables 8.2 and 8.3. Table 8.2 lists the tentative assignments of main IR bands of dioxomolybdenum(VI) complexes for the ligands H_2L^2 and H_2L^4 in 4000-50 cm^{-1} region. The free ligands H_2L^2 and H_2L^4 show bands at *ca.* 3374 and 3060 cm^{-1} , which are due to -OH stretching mode and -NH groups respectively. These bands are absent in complexes, which suggests deprotonation of the phenolic group indicating the coordination through phenolic oxygen and enolization of the thione sulfur followed by deprotonation. On coordination of azomethine nitrogen, $\nu(C=N)$ shifts to lower wavenumbers by 10-20 cm^{-1} as the band shifts from *ca.* 1608 to 1592 cm^{-1} in the spectra of the four dioxomolybdenum(VI) complexes. The $\nu(N-N)$ of the thiosemicarbazone is found at *ca.* 1118 cm^{-1} . The increase in the frequency of this band in the spectra of the complexes, due to the increase in the bond strength, again confirms the coordination *via* the azomethine nitrogen [4].

The decrease in the stretching frequency of $\nu(CS)$ band from *ca.* 841 cm^{-1} in the thiosemicarbazones by 80-90 cm^{-1} upon complexation indicates coordination *via* the thiolato sulfur [5]. IR spectra of the complexes 31-34 show sharp bands at *ca.* 1540 cm^{-1} due to newly formed $\nu(N=C)$ bond indicating the coordination of sulfur in the enolate form rather than as keto form [6]. In all the complexes, phenolic oxygen is coordinated to molybdenum by loss of the OH proton. The ligands having band at *ca.* 1279 cm^{-1} , which is due to $\nu(C-O)$. This band is shifted to *ca.* 1244 cm^{-1} in the complexes, indicating the coordination of O^- [7]. It was reported that structurally characterized polymeric dioxomolybdenum(VI)-tridentate complexes have sharp

bands in 810-820 cm^{-1} region [8]. Here, in the complexes **31** and **33**, a strong band is observed at 821 and 810 cm^{-1} respectively, suggesting the presence of Mo=O...Mo bridging in their structures [9]. All complexes (**31-34**) exhibit two bands at *ca.* 891 and 927 cm^{-1} , assigned to symmetric and antisymmetric vibrations respectively, of the *cis*-MoO₂²⁺ core [10,11]. Representative IR spectra of the complexes **31** and **34** are presented in Figure 8.1.

Table 8.2. Selected IR bands (cm^{-1}) with tentative assignments of dioxomolybdenum(VI) complexes

Compound	$\nu(\text{C}=\text{N})$	$\nu(\text{N}=\text{C})$	$\nu(\text{N}-\text{N})$	$\nu(\text{C}-\text{S})$	$\nu(\text{C}-\text{O})$	$\nu(\text{Mo}=\text{O})$
H ₂ L	1613		1111	1358,846	1263	
[(MoO ₂ L ³) ₂]	1585	1549	1142	1352,768	1240	897,943
[MoO ₂ L ² py]	1596	1543	1136	1357,757	1252	886,926
H ₂ L ⁴	1603		1160	1362,835	1295	
[MoO ₂ L ⁴]	1590	1538	1136	1311,751	1246	886,914
[MoO ₂ L ⁴ py]	1597	1532	1130	1316,751	1240	898,926

 $[(\text{MoO}_2\text{L}^2)_2]$ (31) $[\text{MoO}_2\text{L}^4\text{py}]$ (34)**Figure 8.1.** IR spectra of the compounds 31 and 34

The electronic absorption bands of the dioxomolybdenum(VI) complexes recorded in DMF solution, are given in Table 8.3 and their representative spectra are in Figure 8.2. The thiosemicarbazones (H_2L^2 and H_2L^4) have ring $\pi \rightarrow \pi^*$ band at *ca.* 36690 cm^{-1} and a band at *ca.* 31050 cm^{-1} due to $n \rightarrow \pi^*$ transitions associated with the azomethine linkage (described in Chapter 2). These bands suffer marginal shifts on complexation. The complexes (31-34) display a shoulder in the $25000 - 23250\text{ cm}^{-1}$ region and two strong absorptions are located in the $30300 - 27020$ and $35710-33890\text{ cm}^{-1}$ regions, which are assignable to $L \rightarrow Mo(d\pi)$ LMCT and intraligand transitions respectively [12,13].

Table 8.3. Electronic spectral assignments (cm^{-1}) of the dioxomolybdenum(VI) complexes

Compound	$[(MoO_2L^2)_2]$ (31)	$[MoO_2L^2py]$ (32)	$[MoO_2L^4]$ (33)	$[MoO_2L^4py]$ (34)
L→Mo LMCT	34240	33890	34360	34120
	27020	28010	29940	28320
	23310	23750	24270	24150

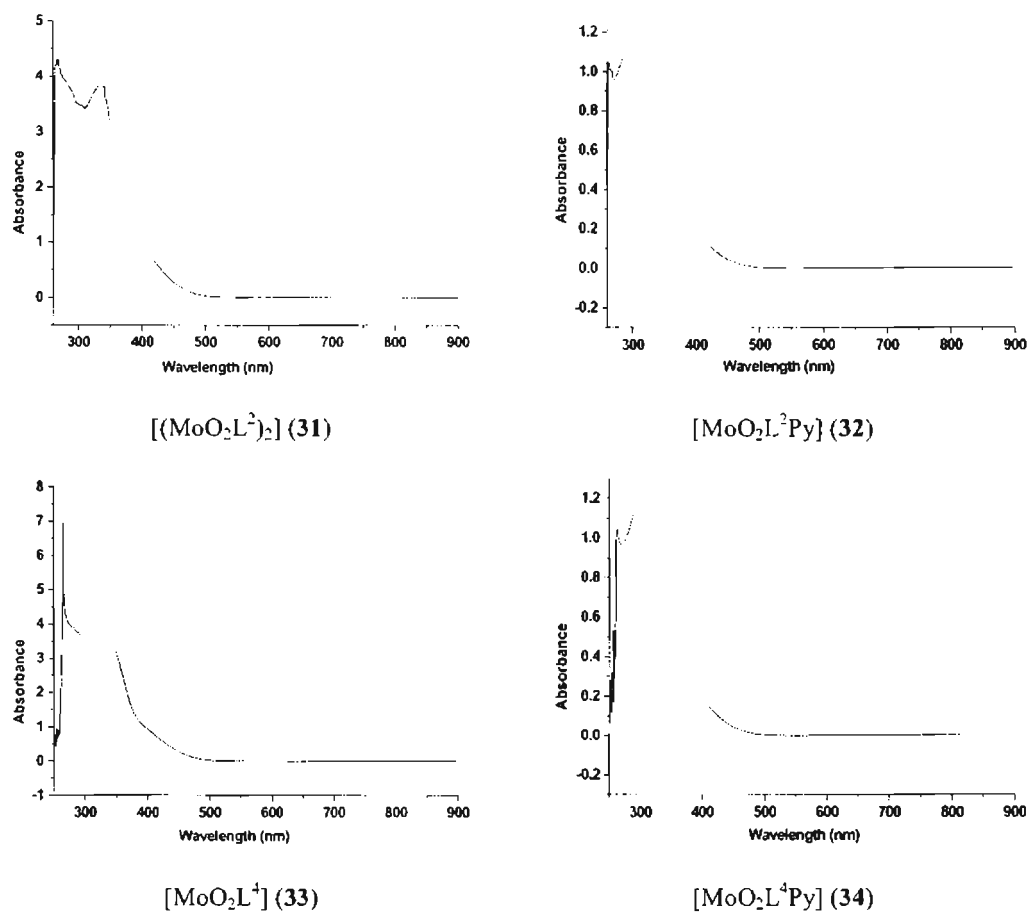


Figure 8.2. Electronic spectra of the compounds 31-34

8.3.3. Description of the crystal structures of the compounds $[(\text{MoO}_2\text{L}^2)_2]$ (31), $[\text{MoO}_2\text{L}^2\text{py}]$ (32) and $[\text{MoO}_2\text{L}^4\text{py}]$ (34)

An orange block crystal of the compound 31 crystallizes into a monoclinic lattice with space group $P2_1/c$. The single crystals of 32 and 34, are golden yellow and yellow in color respectively, crystallizes into triclinic lattice with space group $P\bar{1}$ in both cases. The crystallographic data and structure refinement parameters for the complexes at 293(2) K are given in Table 8.4.

Table 8.4. Crystal data and structure refinement parameters for $[(\text{MoO}_2\text{L}^2)_2]$ (31), $[\text{MoO}_2\text{L}^2\text{py}]$ (32) and $[\text{MoO}_2\text{L}^4\text{py}]$ (34).

	(31)	(32)	(34)
Empirical formula	$\text{C}_{30}\text{H}_{58}\text{Mo}_2\text{N}_6\text{O}_6\text{S}_2$	$\text{C}_{20}\text{H}_{24}\text{MoN}_4\text{O}_3\text{S}$	$\text{C}_{20}\text{H}_{18}\text{MoN}_4\text{O}_3\text{S}$
Formula weight	834.68	496.43	490.38
Temperature	293(2) K	293(2) K	293(2) K
Wavelength	0.71073 Å	0.71073 Å	0.71073 Å
Crystal system	Monoclinic	Triclinic	Triclinic
Space group	$P2_1/c$	$P\bar{1}$	$P\bar{1}$
Unit cell dimensions	a = 9.499(2) Å b = 12.3649(7) Å c = 14.488(2) Å $\alpha = 90^\circ$ $\beta = 96.506(15)^\circ$ $\gamma = 90^\circ$	a = 8.9127(7) Å b = 10.424(3) Å c = 11.726(3) Å $\alpha = 75.15(2)^\circ$ $\beta = 87.531(11)^\circ$ $\gamma = 86.643(12)^\circ$	a = 8.7464(16) Å b = 10.879(3) Å c = 11.098(2) Å $\alpha = 95.178(19)^\circ$ $\beta = 100.563(16)^\circ$ $\gamma = 103.999(19)^\circ$
Volume	1690.8(5) Å ³	1050.7(4) Å ³	997.2(4) Å ³
Z	4	2	2
Density (calculated)	1.639 Mg/m ³	1.569 Mg/m ³	1.633 Mg/m ³
Absorption coefficient	0.916 mm ⁻¹	0.752 mm ⁻¹	0.792 mm ⁻¹
F(000)	848	508	496
Crystal size	0.25 x 0.20 x 0.20 mm	0.30 x 0.25 x 0.20 mm	0.33 x 0.21 x 0.17 mm
θ range for data collection	3.17 to 30.09°	2.95 to 25.00°	3.15 to 25.00°
Index ranges	-13 ≤ h ≤ 11, -15 ≤ k ≤ 17, -20 ≤ l ≤ 19	-10 ≤ h ≤ 10, -12 ≤ k ≤ 12, -13 ≤ l ≤ 13	-10 ≤ h ≤ 10, -12 ≤ k ≤ 12, -13 ≤ l ≤ 13
Reflections collected	15752	8911	10402
Independent reflections	4891 [R(int) = 0.0207]	3670 [R(int) = 0.0142]	3511 [R(int) = 0.0212]
Refinement method	Full-matrix on F ²	Full-matrix on F ²	Full-matrix on F ²
Data / restraints/parameters	4891 / 0 / 217	3670 / 0 / 266	3511 / 0 / 267
Goodness-of-fit on F ²	1.071	1.063	1.073
Final R indices [$I > 2\sigma(I)$]	R ₁ = 0.0229, wR ₂ = 0.0558	R ₁ = 0.0388, wR ₂ = 0.1099	R ₁ = 0.0228, wR ₂ = 0.0505
R indices (all data)	R ₁ = 0.0297, wR ₂ = 0.0579	R ₁ = 0.0429, wR ₂ = 0.1132	R ₁ = 0.0271, wR ₂ = 0.0514
Largest diff. peak and hole	0.428 and -0.452 e.Å ⁻³	1.864 and -0.627 e.Å ⁻³	0.348 and -0.331 e.Å ⁻³

The X-ray diffraction data were measured at 293(2) K, data acquisition and cell refinement were done using the Argus (Nonius, MACH3 software) [14]. The Maxus software package (Nonius) was used for data reduction [15]. The structure was solved by direct methods and full-matrix least-squares refinement using SHELXL97 [16] package. The positions of all the non-hydrogen atoms were included in the full-matrix least-squares refinement using SHELXL97 program and all the hydrogen atoms were fixed in calculated positions. The structures of the compounds **31**, **32** and **34** were plotted using the program Diamond Version 3.0 [17].

The molecular structure and the atom numbering scheme for complexes **31**, **32** and **34** are shown in Figures 8.3-8.5, respectively with relevant bond distances and angles are presented in Tables 8.5 and 8.6. The coordination geometry around molybdenum can be described as distorted octahedral in the three dioxomolybdenum(VI) complexes (**31**, **32** and **34**), the ligands H_2L^2 (for complexes **31** and **32**) and H_2L^4 (for complex **34**) acting in a planar tridentate manner forming six membered metallocycle involving the MoO_2^{2+} moiety. In complex **31**, the ligand H_2L^2 is bonded to *cis*- MoO_2^{2+} in a planar fashion, coordinating through one nitrogen, one sulfur and four oxygen atoms.

The compound **31** is a binuclear dioxomolybdenum(VI) complex, in which the structure evidence for the achievement of hexacoordination through $Mo=O...Mo$ bridging is observed. Three atoms O(1), N(1) and S(1) (from the H_2L^2 ligand) and one terminal oxo atom, O(3), occupying the meridional plane and lie at 0.0599, 0.0983, 0.0105 and 0.0720 Å respectively out of the least squares plane through them and the Mo atom lies 0.4164 Å out of this plane in the direction of the O(2) atom, the other terminal oxygen. Both oxygen atoms O(2) and O(1') occupy the axial positions and form an O(2)–Mo(1)–O(1') angle of 166.97(5)°. The Mo(1)–O(1') bond [2.4241(12) Å] is significantly longer than the other Mo–O bonds [Mo(1)–O(2), 1.6845(13) Å; Mo(1)–O(3), 1.7075(12) Å; Mo(1)–O(1), 1.9977(11) Å] indicates that

the O(1') is weakly bonded to the Mo(1)–O₂²⁺ moiety. The Mo(1)–O(2) and Mo(1)–O(3) bond distances of the MoO₂²⁺ group are unexceptional and almost equal [Mo(1)–O(2), 1.6845(13) Å; Mo(1)–O(3), 1.7075(12) Å]. Similar trend is observed in the second molybdenum atom (Mo1') and its coordinated atoms of the same compound.

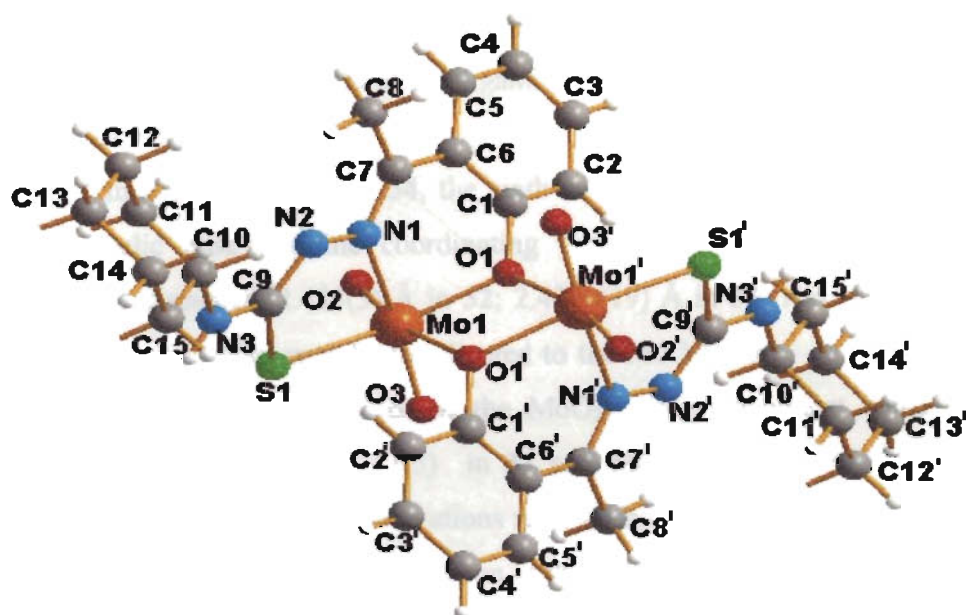


Figure 8.3. Structure and labeling diagram of the compound 31

From comparison of the bond distances and angles of the ligand (H₂L²⁻) and compound 31, it is clear that the ligand coordinates to the MoO₂²⁺ core in the deprotonated thiolate form because in compound 31, the C–S bond distance [C(9)–S(1)] exhibits the value of 1.7632(16) Å and is nearer to a C–S single bond [1.81 Å] than to a C–S double bond distance [1.60 Å] [18]. However, it falls short of the pure C–S single bond distance. The reason for such shortening may be attributed

to electron delocalization in the coordinated ligand [19]. The adjacent C(9)–N(2) bond now display a typical double bond distance [1.299(2) Å] and the N(1)–N(2) bond distance of 1.3851(19) Å are also apparent for the compound **31**. But in the uncomplexed H₂L² ligand, the similar bonds C(8)–N(2) and N(1)–N(2) are 1.351(2) Å and 1.392(2) Å respectively. The C(7)–N(1) bond distance in compound **31** is close to the usual C=N bond length [C(7)–N(1), 1.3078(19) Å]. The N–N–C bond angle of the ligand (H₂L²) [N(1)–N(2)–C(8), 119.95(17)°] is reduced by few degrees [N(1)–N(2)–C(9), 113.28(13)° in **31**] on complex formation. These changes are directly due to coordination of the ligand to the MoO₂²⁺ moiety when it becomes a delocalized system [20].

In complexes **32** and **34**, the sixth coordination position is occupied by the heterocyclic base pyridine coordinating through its nitrogen N(4). The large Mo–N(4) distances [2.433(3) Å in **32**; 2.4380(19) Å in **34**] reveal that the pyridine moiety is also rather weakly coordinated to the MoO₂²⁺ core. In complexes **32** and **34**, the Mo–O bond distances of the MoO₂²⁺ core are almost equal [Mo–O(2), 1.688(3) and Mo–O(3), 1.713(3) in **32** and Mo–O(2), 1.7070(15) and Mo–O(1), 1.7121(15) in **34**]. These observations raise an interesting point about the suspected inherent weakness of the sixth position in the coordination octahedron of the MoO₂²⁺ core, trans to the Mo=O(2) bond [21,22].

By comparing the bond distances and angles of ligands (H₂L² and H₂L⁴) with their respective complexes **32** and **34**, it is clear that the ligands coordinate to the MoO₂²⁺ core in the deprotonated enol form [C(8)–S(1), 1.688(2) Å in H₂L² and 1.6653(17) Å in H₂L⁴; C(9)–S(1), 1.746(4) Å in **32** and 1.766(2) Å in **34**; C(8)–N(2), 1.351(2) Å in H₂L² and 1.363(2) Å in H₂L⁴; C(9)–N(2), 1.299(5) Å in **32** and 1.304(3) Å in **34**; N(1)–N(2)–C(8), 119.95(17)° in H₂L² and 118.60(15)° in H₂L⁴; N(1)–N(2)–C(9), 113.4(3)° in **32** and 113.35(16)° in **34**].

Table 8.5. Selected bond lengths (Å) for the compounds **31**, **32** and **34**.

<i>Bond lengths</i>	(31)	(32)	(34)		
Mo(1)–O(2)	1.6845(13)	Mo(1)–O(2)	1.688(3)	Mo(1)–O(2)	1.7070(15)
Mo(1)–O(3)	1.7075(12)	Mo(1)–O(3)	1.713(3)	Mo(1)–O(1)	1.7121(15)
Mo(1)–O(1)	1.9977(11)	Mo(1)–O(1)	1.939(3)	Mo(1)–O(3)	1.9479(15)
Mo(1)–N(1)	2.2801(13)	Mo(1)–N(1)	2.294(3)	Mo(1)–N(1)	2.3094(17)
Mo(1)–S(1)	2.4090(5)	Mo(1)–S(1)	2.4258(12)	Mo(1)–S(1)	2.4257(8)
Mo(1)–O(1')	2.4241(12)	Mo(1)–N(4)	2.433(3)	Mo(1)–N(4)	2.4380(19)
S(1)–C(9)	1.7632(16)	S(1)–C(9)	1.746(4)	S(1)–C(9)	1.766(2)
N(1)–C(7)	1.3078(19)	N(1)–C(7)	1.300(5)	N(1)–C(7)	1.312(3)
N(1)–N(2)	1.3851(19)	N(1)–N(2)	1.387(4)	N(1)–N(2)	1.397(2)
N(2)–C(9)	1.299(2)	N(2)–C(9)	1.299(5)	N(2)–C(9)	1.304(3)
O(1)–C(1)	1.3841(17)	N(3)–C(9)	1.344(5)	N(3)–C(9)	1.356(3)
O(1)–Mo(1')	2.4241(12)				

Table 8.6. Selected bond angles (°) for the compounds **31**, **32** and **34**.

<i>Bond angles</i>	(31)	(32)	(34)		
O(2)–Mo(1)–O(3)	105.45(6)	O(2)–Mo(1)–O(3)	105.79(15)	O(2)–Mo(1)–O(1)	106.05(7)
O(2)–Mo(1)–O(1)	99.41(6)	O(2)–Mo(1)–O(1)	96.23(13)	O(2)–Mo(1)–O(3)	96.63(7)
O(3)–Mo(1)–O(1)	105.79(5)	O(3)–Mo(1)–O(1)	107.72(13)	O(1)–Mo(1)–O(3)	107.45(7)
O(2)–Mo(1)–N(1)	94.74(6)	O(2)–Mo(1)–N(1)	92.25(13)	O(2)–Mo(1)–N(1)	91.11(7)
O(3)–Mo(1)–N(1)	158.27(5)	O(3)–Mo(1)–N(1)	159.03(13)	O(1)–Mo(1)–N(1)	160.00(7)
O(1)–Mo(1)–N(1)	78.10(5)	O(1)–Mo(1)–N(1)	80.20(10)	O(3)–Mo(1)–N(1)	80.02(6)
O(2)–Mo(1)–S(1)	103.18(5)	O(2)–Mo(1)–S(1)	99.85(11)	O(2)–Mo(1)–S(1)	100.86(6)
O(3)–Mo(1)–S(1)	91.75(4)	O(3)–Mo(1)–S(1)	90.94(11)	O(1)–Mo(1)–S(1)	90.64(6)
O(1)–Mo(1)–S(1)	146.45(4)	O(1)–Mo(1)–S(1)	150.99(8)	O(3)–Mo(1)–S(1)	150.25(5)
N(1)–Mo(1)–S(1)	75.62(3)	N(1)–Mo(1)–S(1)	75.22(8)	N(1)–Mo(1)–S(1)	75.79(5)
O(2)–Mo(1)–O(1')	166.97(5)	O(2)–Mo(1)–N(4)	169.42(13)	O(2)–Mo(1)–N(4)	168.87(6)
O(3)–Mo(1)–O(1')	84.55(5)	O(3)–Mo(1)–N(4)	84.18(13)	O(1)–Mo(1)–N(4)	84.30(7)
O(1)–Mo(1)–O(1')	69.39(5)	O(1)–Mo(1)–N(4)	77.02(11)	O(3)–Mo(1)–N(4)	75.96(6)
N(1)–Mo(1)–O(1')	76.79(4)	N(1)–Mo(1)–N(4)	78.68(10)	N(1)–Mo(1)–N(4)	79.53(6)
S(1)–Mo(1)–O(1')	84.50(3)	S(1)–Mo(1)–N(4)	83.21(8)	S(1)–Mo(1)–N(4)	82.78(5)
C(9)–S(1)–Mo(1)	100.04(5)	C(9)–S(1)–Mo(1)	100.57(12)	C(9)–S(1)–Mo(1)	100.63(8)
C(7)–N(1)–N(2)	114.74(13)	C(7)–N(1)–N(2)	114.4(3)	C(7)–N(1)–N(2)	115.17(16)
C(7)–N(1)–Mo(1)	123.09(11)	C(7)–N(1)–Mo(1)	123.5(2)	C(7)–N(1)–Mo(1)	122.68(14)
N(2)–N(1)–Mo(1)	122.16(9)	N(2)–N(1)–Mo(1)	122.0(2)	N(2)–N(1)–Mo(1)	122.06(12)
C(9)–N(2)–N(1)	113.28(13)	C(9)–N(2)–N(1)	113.4(3)	C(9)–N(2)–N(1)	113.35(16)

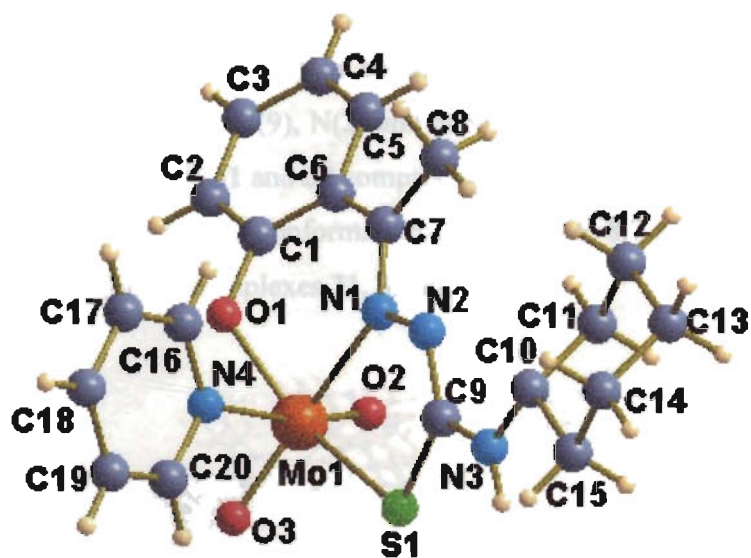


Figure 8.4. Structure and labeling diagram of the compound 32

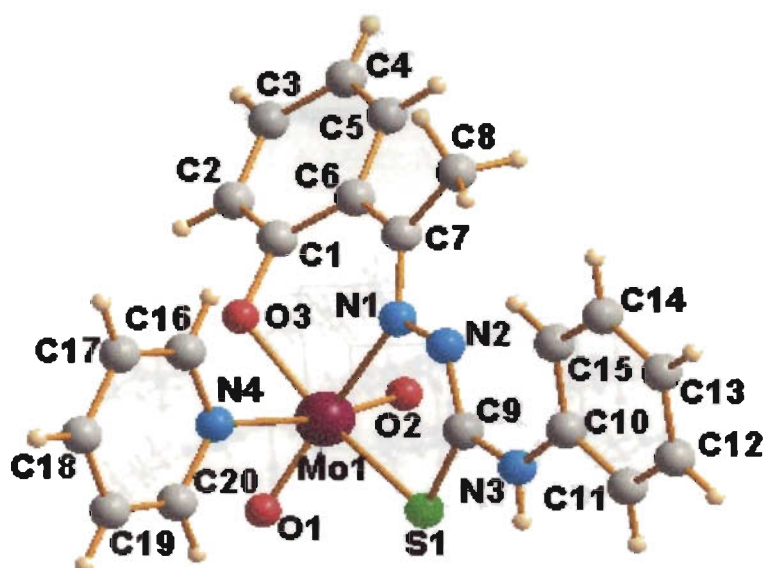


Figure 8.5. Structure and labeling diagram of the compound 34

Ring puckering analyses and least-square plane calculations shows that the rings Cg(2) in complex **31** and Cg(1) in complex **32** and Cg(1) in complex **34** comprising of atoms Mo(1), S(1), C(9), N(2) and N(1) adopts an envelope on Mo(1) and the ring Cg(5) in complexes **31** and **32** comprising of atoms C(10), C(11), C(12), C(13), C(14) and C(15) adopt chair conformations. Figure 8.6, 8.7 and 8.8 show the contents of the unit cell for the complexes **31**, **32** and **34**.

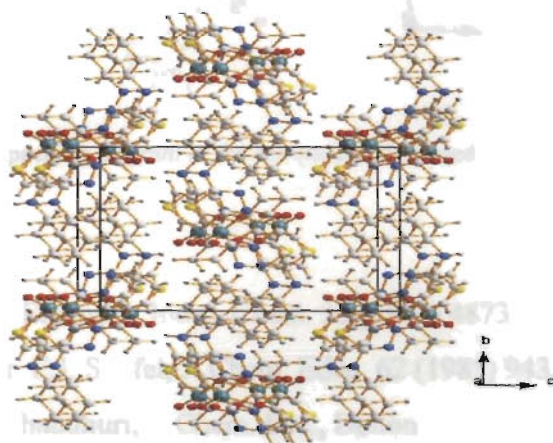


Figure 8.6. Unit cell packing diagram of the compound **31** viewed along the *a* axis

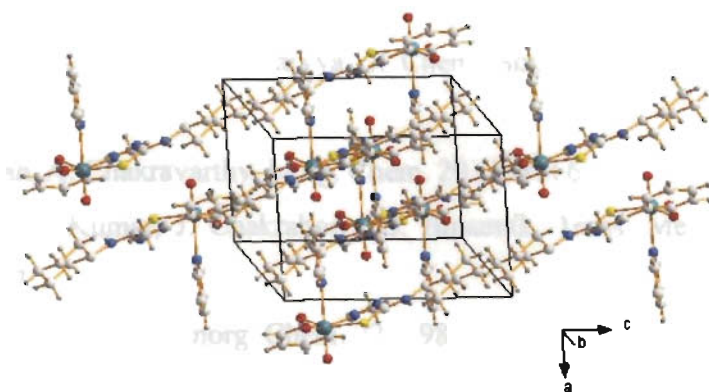


Figure 8.7. Unit cell packing diagram of the compound **32** viewed along the *b* axis

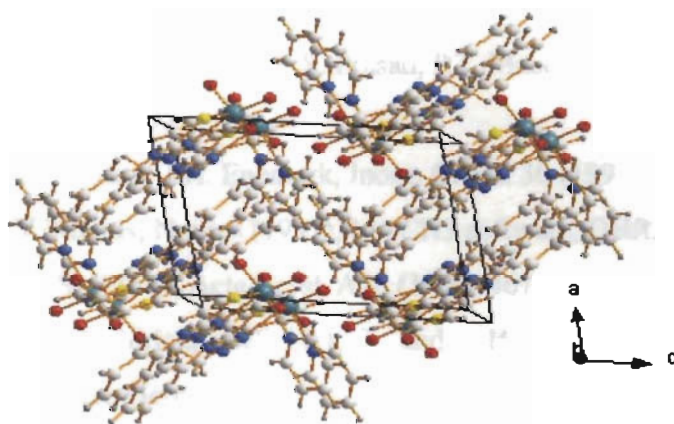


Figure 8.8. Unit cell packing diagram of the compound 34 viewed along the *b* axis

References

1. I.K. Dhavan, J.H. Enemark, *Inorg. Chem.* 35 (1996) 4873.
2. S.J.N. Burgmayer, E.I. Stiefel, *J. Chem. Educ.* 62 (1985) 943.
3. S.B. Kumar, M. Chaudhuri, *J. Chem. Soc., Dalton Trans.* (1992) 269.
4. A. Syamal, K.S. Kale, *Inorg. Chem.* 4 (1965) 867.
5. L.J. Willis, J.M. Loehr, K.F. Miller, A.E. Bruce, E.I. Stiefel, *Inorg. Chem.* 25 (1986) 4289.
6. S. Bhattacharjee, R. Bhattacharyya, *J. Chem. Soc., Dalton Trans.* (1993) 1151.
7. O.A. Rajan, A. Chakravarthy, *Inorg. Chem.* 20 (1981) 660.
8. R.A. Lal, A. Kumar, J. Chakraborty, S. Bhaumik, *Trans. Met. Chem.* 26 (2001) 557.
9. J.M. Berg, R.H. Holm, *Inorg. Chem.* 22 (1983) 1768.
10. F.J. Arnaiz, R. Aguado, M.R. Podrosa, A.D. Cian, J. Fischer, *Polyhedron* 19 (2000) 2141.

SUMMARY AND CONCLUSION

The thesis deals with synthesis, spectral and structural studies of mono- and binuclear transition metal complexes of N(4)-substituted thiosemicarbazones derived from salicylaldehyde and 2-hydroxyacetophenone. The entire thesis is divided into eight chapters.

Chapter 1 embodies a brief introduction of thiosemicarbazones and their transition metal complexes. It includes bonding, stereochemistries, oxidation states and biological applications of metal complexes of thiosemicarbazones, various instrumental techniques adopted in the characterization process and also objective and scope of the present work outlined in this thesis.

Chapter 2 describes synthesis, spectral and structural studies of various N(4)-substituted ONS donor ligands. It includes salicylaldehyde N(4)-cyclohexyl/phenyl thiosemicarbazones and 2-hydroxyacetophenone N(4)-cyclohexyl/phenyl thiosemicarbazones. Out of the four ligands, single crystals of three of them were obtained. Structural studies of these three ligands were done using X-ray diffraction techniques. It also deals with spectral characterization of the above four thiosemicarbazone ligands using IR, electronic and ^1H NMR spectroscopy. Single crystal X-ray diffraction study of an unusual compound 2-[5-(cyclohexylamino)-1,3,4-thiadiazol-2-yl]phenol was also reported in this chapter.

Chapter 3 describes the synthesis, spectral and structural studies of Cu(II) complexes of N(4)-substituted thiosemicarbazones of salicylaldehyde and 2-hydroxyacetophenone. Fourteen Cu(II) complexes were synthesized. It includes mononuclear as well as binuclear complexes. Some of the mononuclear complexes

are heterocyclic base adduct complexes, while others are monoanionic complexes. Characterizations were done using elemental analyses, magnetic susceptibility measurements, IR, electronic and EPR studies. The EPR spectra of all the compounds in polycrystalline state at 298 K and in DMF solution at 77 K were recorded. The information obtained from the spectra were used for calculating the EPR bonding parameters of the compounds. Single crystals of two of the Cu(II) complexes were obtained. One was mononuclear five coordinated heterocyclic base adduct complex and the other was binuclear Cu(II) complex with each copper atom is four coordinated.

Chapter 4 describes synthesis and spectral studies of Ni(II) complexes of 2-hydroxyacetophenone N(4)-cyclohexylthiosemicarbazone. Three Ni(II) complexes were synthesized and their structural characterizations were done using elemental analyses, magnetic susceptibility measurements, IR and electronic spectral studies. The magnetic moment values for these three compounds are in the range 2.00-2.75 B.M., which is closer to the magnetic moment value for the five coordinated high spin Ni(II) complexes.

Chapter 5 deals with the synthesis and spectral studies of Mn(II) complexes of N(4)-substituted ONS donor ligands. Two Mn(II) complexes were synthesized and their structural characterizations were done using elemental analyses, magnetic susceptibility measurements, IR, electronic and EPR spectral studies. The magnetic moment values for these two compounds are in the range 5.65-5.95 B.M., which is in agreement with the magnetic moment value for the high spin Mn(II) compounds with d^5 configuration. Electronic spectral bands observed for these two Mn(II) complexes fit the Tanabe-Sugano diagram for octahedral Mn(II) complexes with d^5 configuration and comparing with this, the ligand field parameters for Mn(II) complexes were calculated. The EPR spectra of the two Mn(II) compounds in polycrystalline state at

RT and in frozen DMF solution at 77 K are isotropic. Both the spectra in polycrystalline state at RT gave broad signals, while in DMF solution at 77 K exhibit six-line hyperfine splitting for ^{55}Mn ($I = 5/2$).

Chapter 6 describes the synthesis, spectral and structural studies of Zn(II) complexes of salicylaldehyde N(4)-phenylthiosemicarbazone. Five Zn(II) complexes were synthesized and their structural characterizations were done using elemental analyses, magnetic susceptibility measurements, IR, electronic and ^1H NMR spectral studies. Single crystals of one of the compound was obtained by X-ray diffraction studies and that was a five coordinated heterocyclic base adduct complex having approximately trigonal bipyramidal geometry with distortion from the square based pyramidal geometry.

Chapter 7 deals with the synthesis and spectral studies of oxovanadium(IV) complexes of N(4)-substituted thiosemicarbazone ligands. Six oxovanadium(IV) complexes were synthesized and their structural characterizations were done using elemental analyses, magnetic susceptibility measurements, IR, electronic and EPR spectral studies. The magnetic moment values for these compounds are in the range 1.58-1.83 B.M. These values correspond to the spin only value of the systems having one electron. The EPR spectra of all the compounds in polycrystalline state at RT showed isotropic spectra and in frozen DMF solution at 77 K, all the six compounds showed axial spectra *ie*, normal eight line spectra with hyperfine splitting for the ^{51}V nucleus ($I = 7/2$) and these EPR signals are characteristic of mononuclear VO^{2+} species.

Chapter 8 describes the synthesis, spectral and structural studies of dioxomolybdenum(VI) complexes of 2-hydroxyacetophenone N(4)-substituted thiosemicarbazones. Four dioxomolybdenum(VI) complexes were synthesized and their structural characterizations were done using elemental analyses, magnetic

susceptibility measurements, IR and electronic spectral studies. All the four dioxomolybdenum(VI) complexes are diamagnetic. Out of the four complexes, single crystals of three of the complexes were obtained by X-ray diffraction studies.

Curriculum vitae

Personal details

Name	SEENA E.B.
Date of Birth	3 rd May 1979
Permanant address	Namitha House, Parambithara Cross Road, Panampilly Nagar P.O., Cochin - 682 036, Kerala, India
Marital Status	Married
Contact Phone number	0484-2312447
E-mail	<u>seena-eb@cusat.ac.in</u> , <u>seenaeb@rediffmail.com</u>

Education

1994	S.S.L.C., St. Sebastian's C.G.H.School, Thrissur (84.6%)
1994-1996	Pre-Degree, St. Mary's College, Thrissur (63.5%)
1996-1999	B.Sc. Chemistry, Vimala College, Thrissur (87.3%)
1999-2001	M.Sc. Chemistry, Christ College, Irinjalakuda, Thrissur (69.3%)
2001-2002	B.Ed. Physical science, I.A.S.E., Thrissur (58.6%)

Career objective

A motivated chemist seeking a post-doctoral position in research and development. Able to work individually and interested to work in teams with colleagues. Keenly interested in pursuing career as a teacher without compromising my research objectives.

Teaching experience

Worked as Guest Lecturer in V.H.S.E. Ramavarmapuram, Thrissur from 13th August 2002 to 11th October 2002.

Research experience

More than 3 years research experience in the field of Coordination chemistry.

Computer skills

Certificate in Office Automation from CDAC, GIST, Irinjalakuda, Thrissur.

Windows, MS Office, Adobe Photoshop, Chems sketch, Chem Draw, ISIS Draw, ORIGIN, ORTEP, PLATON, DIAMOND, EPR Simulation etc.

Research Publications/Presentations

1. A crystallographic study of 2-hydroxyacetophenone N(4)-cyclohexyl thiosemicarbazone, E.B. Seena, B.N. Bessy Raj, M.R.P. Kurup, E. Suresh, J. Chem. Cryst., in press.
2. 2-Hydroxyacetophenone N(4)-phenylthiosemicarbazone, E.B. Seena, E. Manoj, M.R.P. Kurup, Acta Cryst. C62 (2006) o486-o488.
3. Spectral and structural studies of mono- and binuclear copper(II) complexes of salicylaldehyde N(4)-substituted thiosemicarbazones, E.B. Seena, M.R.P. Kurup, Polyhedron, under revision.
4. Investigations of oxovanadium(IV) heterochelate complexes, National seminar on Frontiers in Inorganic Chemistry, CUSAT, March 24-25, 2006.
